Uncovering the roles of G protein-coupled kinase 2 in the *Drosophila* Hedgehog signaling pathway.

An evolutionarily ancient regulator of Smoothened and general modulator of the Hedgehog response in flies.

Dominic Maier

Doctor of Philosophy

Faculty of Medicine

Department of Anatomy and Cell Biology

McGill University, Montreal

A thesis submitted to McGill University in partial fulfillment of the requirements of the degree of Doctor of Philosophy

Montreal, Quebec, Canada

March 2015

To Shuofei, Johannes and Lily

Acknowledgments

First and foremost, I would like to thank my supervisor Dr David Hipfner for his support through all these years. Going back in time, I think I was not exactly the grad student David might have looked for. I essentially ended up in the lab because I followed my then girlfriend, later wife, Shoufei Cheng to Montreal. We had met in Germany, but she had already committed to a PhD in David's lab overseas. So I joined the lab and introduced myself as a microbiologist with limited interests in fly genetics or developmental biology. For some reason, David accepted my somewhat questionable attitude towards his main research focus and here I am now, finishing up my PhD after six years in his lab. To be fair, I still cannot claim to be a fly geneticist. Shuofei and David did pretty much all the flywork for my thesis and I worked the project mainly from a biochemical angle. But soon after I joined David's group, I started to appreciate the *Drosophila* model more and more and I think I can introduce myself now as a developmental biologist. Thank you David for taking a chance and for patiently teaching me all I needed to know about flies and developmental biology.

I would also like to thank the members of my scientific committee: Dr. Audrey Claing, Dr. Jean-François Côté, Dr. Marko Horb and Dr. Isabelle Roullier, who is also my mentor in the Department of Anatomy and Cell Biology at McGill. Thanks to you all for providing a fresh perspective and constructive feedback for my work.

Thanks to the Department of Anatomy and Cell Biology at McGill and to the academic affairs department of the IRCM for all the administrative help during my PhD studies.

I would also like to mention the proteomics core facility at the IRCM for all their help with the Mass-spec analysis. Thanks to Dr. Denis Faubert for all the tedious quantifications of peptide peaks.

Thanks to all the current and past lab members. To me it always felt quite like family, a comfortable place, were you can share all the joys but also sorrows of live. Special thanks to Karen, who executed a lot of my clonings, especially at the end of the project. Thanks also to Aurore and Greta, two incredible talented and motivated summer students, who helped establishing the *ptc-luc* reporter and BRET assays.

Work at the IRCM would not have been the same without the friendships forming over the years. You guys made the IRCM fun and there was always something ongoing, 5 à 7s, softball, badminton, skating, watching a movie... . Thanks to Chris, for all the delicious backyard BBQs and special thanks to Mathieu and Ariane who not only kept me updated with the latest news and stories at the institute but were also present at the significant events in my live, such as my wedding or the birth of my children. In addition, Mat proof-read the whole thesis and gave many helpful tips to improve my German-influenced writing. Ariane translated the abstract into French. Thanks for that as well.

Ich möchte mich bei meiner Familie in Deutschland bedanken. Ich weiß, einige von euch hatte Zweifel, aber ich bin jetzt wirklich fast fertig! Ganz lieben Dank an meine Eltern für all eure Unterstützung. Danke lieber Papa, dass Du mich immer auf dem Laufenden gehalten hast. Trotz der Entfernung von knapp 6000 km war ein Teil von mir immer auf dem Hof.

Finally, I would like to thank the three people who matter most to me, my wife Shuofei and my to children Johannes and Lily. Johannes and Lily, you have no idea what I am doing during the day. But the arrival of you two changed everything. I am more efficient and focussed, because I want to spent time in the evening with you and not with my western blot. But more importantly, you put everything in perspective. Lab work and research is good and important, but nothing beats hearing you guys laugh and sing!

Shoufei, you lured me into the adventure of studying abroad, something I would have never thought possible. We explored Montreal and Canada and climbed our way up together, starting from that tiny apartment near Parc Lafontaine. We worked side by side in the lab and I enjoyed every day of it. You had my back every step of the way and in the midst of your own PhD studies you gave birth to our first son Johannes. Having you on my side, could I ask for anything more? Lieb' Dich, quack, quack, quack!

Montreal, Canada, November 2014

Preface & Contribution of Authors

My PhD thesis is written in the classical format. However, the presented worked contributed to the following peer-reviewed publications:

- **Maier, D.**, Cheng, S., Faubert, D., Hipfner, D.R., 2014. A broadly conserved G-protein-coupled receptor kinase phosphorylation mechanism controls *Drosophila* Smoothened activity. PLoS genetics 10, e1004399.
- **Maier, D.**, Cheng, S., Hipfner, D.R., 2012. The complexities of G-protein-coupled receptor kinase function in Hedgehog signaling. Fly 6, 135-141.
- Cheng, S.*, **Maier, D.***, Hipfner, D.R., 2012. *Drosophila* G-protein-coupled receptor kinase 2 regulates cAMP-dependent Hedgehog signaling. Development 139, 85-94.

  ***equal contribution**
- Cheng, S., **Maier, D**., Neubueser, D., Hipfner, D.R., 2010. Regulation of Smoothened by *Drosophila* G-protein-coupled receptor kinases. Developmental biology 337, 99-109.

My PhD thesis represent a collective effort and I would like to acknowledge the contribution of all the people involved:

- **Shuofei Cheng** performed all fly-related experiments (crosses, microdissections, immuno-stainings, microscopy and wing measurements) in Chapter 3 and 4. Some of the transgenic animals used in Chapter 5 were generated by her as well.
- **Dr. David Hipfner** took over all the fly work (crosses, microdissections, immuno-stainings, microscopy and wing measurements) in Chapter 5. He also did the sequence analysis of Smo C-terminal domains and helped with the quantification of the Mass-spec data. As my supervisor he oversaw all the experimental design of this thesis.
- **Dr. Denis Faubert** is the head of the IRCM proteomic core facility, which processed my protein samples for LC-MS/MS analysis. He identified and quantified all phospho-petides presented in this study.

- **Dr. Dagmar Neubüser** generated the *gprk2* mutant alleles and started the initial characterization of the mutants.
- **I myself** did all the remaining experiments. Specifically, I executed and analyzed all western blot and tissue culture experiments. I cloned most of the constructs used for protein expression or to generate transgenic animals. I purified the Gprk2 and Smo antigens used to raise the respective antisera in guinea pigs. I characterized both antibodies and affinity purified the Gprk2 antiserum for the use in immunostaings. Under the supervision of Dr. Hipfner, I conceived and designed all experiments.

Abstract

The Hedgehog (Hh) signaling pathway plays crucial roles in the control of tissue growth and patterning during embryonic development and adult tissue homeostasis of most bilaterian animals. Misregulation of this pathway has been linked to numerous human disorders including cancer. Intracellular Hh signaling is initiated by Smoothened (Smo), a seven-pass transmembrane protein and distant member of the G protein-coupled receptor (GPCR) protein family. Smo itself is activated by multisite phosphorylation involving several kinases. In *Drosophila* and probably other arthropods, cAMP-dependent Protein kinase A (PKA) is indispensable for this step. However, there is no evidence that PKA regulates mammalian Smo orthologs. In recent years GRKs have emerged as new components of the Hh pathway. GRKs are required for efficient Hh target gene expression in several organisms suggesting they have an evolutionarily conserved function in the pathway.

My work focused on G protein-coupled receptor kinase 2 (Gprk2), a GRK in *Drosophila*. We demonstrated that Hh target gene expression is strongly impaired in *gprk2* mutant flies, indicating that Gprk2 positively regulates Hh signaling. We identified two roles of Gprk2 in the Hh pathway, one direct and the other indirect.

The indirect role is based on the observation that loss of Gprk2 results in a decrease in cellular cAMP concentrations to a level that is limiting for Hh target gene activation. Normal expression of target genes was restored in *gprk2* mutants by stimulating cAMP production or by mimicking PKA phosphorylation at the level of Smo. Our results suggest that Gprk2 is important for normal cAMP regulation, and thus has an indirect effect on the activity of PKA-regulated components of the Hh pathway, including Smo itself.

To investigate the effect of direct phosphorylation of Smo by Gprk2, we mapped four phosphorylation site clusters located in the membrane-proximal cytoplasmic C-terminal tail of Smo. Although phosphorylation at these sites is required for maximal Smo activation both *in vitro* and *in vivo*, mutation of the sites to Ala does not fully recapitulate the phenotype of *gprk2* mutants *in vivo*. This is consistent with a minor role of Gprk2 in the activation of Smo while the major activating kinase for Smo in flies is PKA. Taken together, our results suggest that the main

function of Gprk2 in the *Drosophila* Hh pathway is to keep cellular cAMP levels and PKA activity in a permissive range for Hh target gene expression.

Interestingly, our mapped Gprk2 clusters overlap with regulatory GRK phosphorylation sites in mouse Smo, and are highly conserved throughout the bilaterian lineages. A truncated form of *Drosophila* Smo (Smo^{core}) consisting of just the evolutionarily conserved core, including Gprk2 regulatory sites, can recruit the downstream effector Costal-2 (Cos2) to a newly identified binding site. Furthermore, Smo^{core} activates target gene expression in a Gprk2-dependent manner. These results indicate that GRK phosphorylation in the membrane-proximal C-terminus is an evolutionarily ancient mechanism of Smo regulation. The fact that Smo^{core} lacks PKA phosphorylation sites and is only regulated by Gprk2 points point to a higher degree of similarity in the regulation and signaling mechanism of bilaterian Smo proteins than has previously been recognized. We speculate that the regulation of Smo by PKA was specifically acquired during the evolution of Smo proteins within the arthropod lineage.

Résumé

La voie de signalisation de Hedgehog (Hh) joue un rôle crucial dans le contrôle de la croissance tissulaire, dans le modellage des tissus embryonnaires et le maintien de l'homéostasie des tissus adultes chez la majorité des animaux bilatériens. Il a été démontré que la dérégulation de cette voie de signalisation est associée à de nombreuses maladies chez l'humain, dont le cancer. La signalisation intracellulaire de Hh est initiée par Smoothened (Smo), une protéine transmembranaire et un membre éloigné de la famille de récepteurs couplés aux protéines G. La protéine Smo est acitvée grâce à de multiple sites de phosphorylation qui sont la cible de plusieurs kinases. Chez la drosophile, et probablement chez plusieurs autres arthropodes, la protéine "cAMP-dependent Protein kinase A" (PKA) est indispensable pour cette étape d'activation. Toutefois, il n'y a aucune évidence qui démontre que PKA régule les orthologues de Smo chez les mammifères. Au cours des dernières années, il a été démontré que les protéines de la famille GRK sont des composantes de la voie de signalisation Hh. Les GRK sont requises pour une activation complète des gènes cibles de la voie Hh chez de nombreux organismes, suggèrant donc que leur fonction a été conservée au fil de l'évolution.

Mon travail a porté principalement sur l'étude d'une GRK, la protéine "G protein-coupled receptor kinase 2" (Gprk2), chez la drosophile. Nous avons démontré que l'expression des gènes cibles de Hh est grandement inhibée chez des mouches mutantes pour *gprk2*, ce qui indique que Gprk2 régule de façon positive la voie Hh. Nous avons identifé deux rôles de Gprk2 dans cette voie de signalisation, un rôle direct et un indirect.

Le rôle indirect est basé sur l'observation que la perte de Gprk2 diminue les concentrations intracellulaires d'AMPc à un niveau qui est limitant pour l'activation des génes cibles de Hh. L'expression de ces gènes chez des mutants de gprk2 est rétablie lorsqu'on stimule la production d'AMPc ou lorsque nous simulons la phosphorylation de PKA sur Smo. Nos réusltats suggèrent que Gprk2 est importante pour la régulation normale de l'AMPc, et joue donc un rôle indirect sur l'activité des composantes de la voie de signalisation Hh qui sont régulées par PKA, dont Smo fait partie.

Pour étudier l'effet de la phosphorylation directe de Smo par Gprk2, nous avons identifé quatre groupes de sites de phosphorylation localisés dans la partie proximale de la membrane

cytoplasmique de la queue C-terminale de Smo. Bien que la phosphorylation de ces sites soit requise pour une activation maximale de Smo *in vitro* et *in vivo*, la mutation de ces sites pour des Ala ne récapitule pas pleinement le phénotype obersvé chez les mutants de *gprk2 in vivo*. Ceci est cohérent avec le fait que Gprk2 joue un rôle mineur dans l'activation de Smo chez la drosophile, où la kinase activatrice principale est PKA. Ainsi, nos résultats suggèrent que la fonction principale de Gprk2 dans la voie de signalisation Hh de la drosophile est de maintenir des niveaux intracellulaires d'AMPc et un niveau d'activité de PKA qui sont dans un intervalle permissive pour permettre l'expression des gènes cibles de Hh.

Il est intéressant de noter que les groupes de sites de phosphorylation que nous avons identifiés chevauchent des sites de phosphorylation régulateurs chez la protéine Smo de souris. De plus, ces sites sont conservés à travers les espèces bilatériennes. Une forme tronquée de Smo (Smo^{core}) qui est constituée uniquement de la portion conservée, incluant les sites de régulation de Gprk2, peut recruter l'effecteur Costal-2 (Cos2) à un site de liaison nouvellement identifié. De plus, Smo^{core} active l'expression des gènes cibles de Hh et ceci est dépendant de Gprk2. Ces résultats nous indiquent que la phosphorylation par les GRK de la portion proximale à la membrane de la queue C-terminale est un ancien mécanisme de régulation de Smo qui a été conservé à travers l'évolution. Le fait que Smo^{core} n'a pas de site de phosphorylation par PKA et est uniquement régulée par Gprk2 nous indique que le taux de conservation dans les mécanismes de régulation et de signalisation des protéines Smo chez les animaux bilatériens est plus élevé que ce que les scientifiques croyaient précédemment. Nous spéculons que la régulation des protéines Smo par PKA a été acquise au fil de l'évolution des arthropodes.

Table of contents

Table of figures

List of tables

Chapter 1: Introduction

1.1. The Hedgehog (Hh) pathway is a conserved signaling cascade crucial for embryonic development and tissue maintenance of metazoans.

Multicellular organisms require cell-to-cell communication, co-ordinated cell division and specification in order to develop and maintain a complex body with its various organs, tissues and cell-types. Evolutionary processes have lead to the creation a huge number of highly diverse metazoan species. Perhaps surprisingly, this diversity is generated by only a handful of highly conserved molecular signaling cascades, co-ordinating growth and shape of the organism at a cellular level. Signaling is often initiated by a morphogen, a secreted protein forming a diffusion gradient around its source and directing tissue patterning in a concentration-dependent manner. The Hh protein is such a morphogen and it initiates a conserved signaling pathway baptized in its name. The *hh* gene and most pathway components were initially discovered in the arthropod *Drosophila melanogaster*, but soon orthologous genes were identified in many more metazoan phyla including chordates (Ingham and McMahon, 2001). The ever growing list of complete genome sequences suggests that a functional Hh pathway is most likely present in most bilaterian species and its origin might even be further back in metazoan evolution (Ingham et al., 2011). This remarkable conservation of the Hh pathway over hundreds of million of years highlights its functional importance in the development and adult life of most bilateria.

1.1.1. Disturbance of the Hh pathway causes birth defects and several forms of cancer in humans.

Hh signaling plays multiple roles throughout human embryogenesis starting at the earliest stages. Not surprisingly, misregulation of the pathway causes severe congenital defects. An example is holoprosencephaly, a cranial defect, caused by incomplete separation of midline structures in the brain and face. In its most extreme form, holoprosencephaly is most prominently characterized by the failure to separate the brain hemispheres and by cyclopia, which describes the presence of only a single eye. The cause for holoprosencephaly is loss of Hh pathway activity either due to gene mutations or to teratogenic drugs affecting Hh pathway proteins. Conversely, mutations resulting in abnormal pathway activation are also known. An example for this condition is Gorlin syndrome, which is characterized by skeletal defects, large body size and broad facial features

(McMahon et al., 2003). Gorlin syndrom patients are also prone to develop certain types of cancers later in life, most often medullablastoma, a brain cancer, or basal cell carcinoma in the skin. This illustrates that Hh signaling not only affects embryogenesis but also the adult organism. Not surprisingly, the same mutations causing Gorlin syndrome can also occur spontaneously in healthy individuals after birth leading to the same types of cancers. Furthermore, because Hh signaling regulates cell proliferation, up-regulation of Hh signaling might be a more general factor in cancer biology (Beachy et al., 2004).

1.1.2. Hh signaling was discovered in genetic model organisms.

The fruit fly has been studied by biologists for over hundred years, but it was the groundbreaking work of two geneticists, Christiane Nüsslein-Volhard and Eric Wieschaus that established *Drosophila melanogaster* as a tool for the systematic study of embryonic development. By conducting large scale mutagenesis screens they identified genes essential for proper *Drosophila* development. Phenotypic characterizations and genetic analyses eventually revealed groups of genes that form signaling pathways. This approach led to the discovery of several important signaling cascades including the Hh pathway (Nusslein-Volhard and Wieschaus, 1980) and led to the awarding of the 1995 Nobel prize in medicine (Raju, 2000).

As previously mentioned, Hh signaling is highly conserved throughout the animal kingdom and has also been extensively studied in other model organisms such as mouse, chicken, zebrafish, and the frog *Xenopus laevis* (Ingham and McMahon, 2001). Many tissues patterned by Hh have been identified and striking parallels can been drawn across species. For instance Hh patterning in the vertebrate neural tube and in the *Drosophila* wing disc are similar in many ways (Hooper and Scott, 2005). The wing disc develops into the adult fly wing and I will introduce Hh patterning of the wing disc in the next section.

1.1.3. Hh pattens the *Drosophila* wing disc.

The wing imaginal disc is an epithelial tissue present in *Drosophila* embryos and larvae. Based on gene expression profiles and cellular characteristics, it can be divided into four distinct compartments: dorsal (D), ventral (V), anterior (A) and posterior (P) (Figure 1.1A). Hh signaling

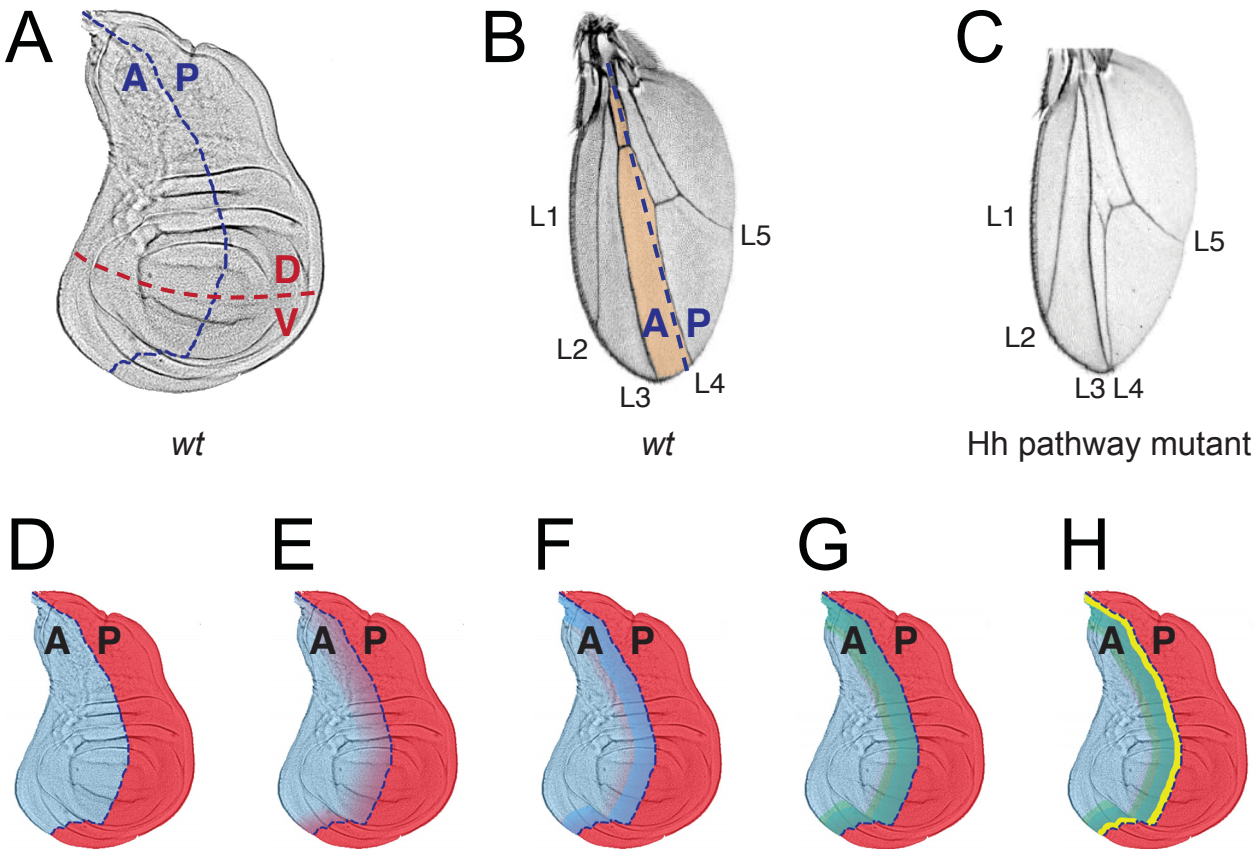

Figure 1.1. Patterning of the *Drosophila* wing disc and adult wing.

(A) Micrograph of a *wt Drosophila* wing disc. Dotted lines indicate the boundaries of the four compartments: anterior A, posterior P, dorsal D, ventral V. **(B, C)** Adult fly wings. The A/P compartment border (dotted line) and the region patterned by Hh are indicated (yellow shade) in **(B)**. The Hh responsive zone between longitudinal veins 3 (L3) and 4 (L4) is reduced in Hh pathway mutants **(C)**. **(D-H)** Schematics of wing disc illustrating protein expression patterns of pathway components. **(D)** A compartment cells express the transcription factor Ci (blue shade) whereas Hh (red) is produced in the P compartment. **(E)** Hh diffuses into the A compartment forming a morphogen gradient (red shade). **(F)** Full-length Ci^{155} (blue) is stabilized in the presence of Hh. **(G)** Low threshold Hh target genes (e.g. *dpp*, green) are expressed anteriorly almost throughout the Hh diffusion zone. **(H)** High threshold Hh target genes (e.g. *en*, yellow) come in a narrow stripe of A cells where Hh concentrations are high. Images for **(B)** and **(C)** are adapted from (Bier, 2005).

takes place along the A/P boundary and is also required to maintain the A/P compartment boundary. As the name suggests, the wing disc gives rise to the adult fly wing and part of the body wall. Therefore, the wing disc compartments are corresponding to areas of the adult wing (Figure 1.1B). The longitudinal vein 4 (L4) marks the A/P boundary; the D/V border is reflected in the wing margin, due to folding of the wing during morphogenesis (Blair, 1995).

Hh forms a concentration gradient in the A compartment. The Hh protein is solely expressed in the P compartment of the fly wing disc. P cells are not responsive to Hh because they do not express the key transcription factor of the pathway (Figure 1.1D). Hh diffuses into the A compartment and forms a concentration gradient along the A/P boundary (Figure 1.1E). A cells close to the Hh source are exposed to high concentrations of Hh, whereas cells that are more distant from the A/P border receive only small amounts of Hh. The Hh diffusion range is limited and cells located in the far A compartment are not exposed to Hh (Strigini and Cohen, 1997; Tabata and Kornberg, 1994).

Hh drives expression of Hh-responsive genes (Hh target genes) in a stripe of wing disc cells. Hh target genes are roughly divided into three groups; high, medium and low threshold Hh target genes. Small amounts of Hh are sufficient to induce transcription of low threshold Hh target genes and as a result this subset of Hh target genes is expressed almost throughout the Hh diffusion zone. Consequently, low threshold target genes are transcribed in a wide stripe of A cells (Figure 1.1G). The most notable low threshold target gene is *decapentaplegic* (*dpp*), which is a morphogen itself and required for growth and additional pattering of the wing disc (Capdevila and Guerrero, 1994). High threshold Hh target genes require high concentrations of Hh and are therefore only induced in a few rows of cells in the A compartment adjacent to the A/P border (Figure 1.1H). Examples of high threshold Hh target genes are *collier* (*col*) and A *engrailed* (*en*). The latter requires the highest known Hh threshold and only a very narrow stripe of A cells are positive for En protein. It should be noted that En is also expressed in the P compartment; however, P *en* is not under the influence of Hh signaling. Lastly, *patched* (*ptc*) can be classified as a medium threshold Hh target gene, because its expression domain is narrower than that of *dpp* but substantially wider than that of *col* or A *en* (Phillips et al., 1990).

Hh signaling defects manifests themselves in patterning of the adult wing and the wing disc. Complete loss of Hh signaling in the wing disc results in the absence of an adult wing, while partial impairment leads to a smaller wing. Specifically the space between longitudinal veins L3 and L4 is reduced (Bier, 2005) (Figure 1.1C). Conversely, inappropriate pathway activity manifests itself in the overgrowth of the entire A wing compartment and the presence of ectopic veins (Tabata and Kornberg, 1994). The adult wing phenotypes are reflected in the seize of the

wing disc and can be visualized on a molecular level by probing for Hh target genes. Gain or loss-of-function of Hh signaling cause a widening or narrowing of the Hh-responsive zone, respectively.

To summarize, the *Drosophila* wing and the imaginal wing disc are a well studied and accessible tool for the *in vivo* study of Hh signaling.

1.2. Molecular biology of the Hh pathway in *Drosophila*.

One of the major questions regarding Hh biology is how the secreted Hh protein induces target gene expression in a concentration-dependent manner. Extensive research over the last 30 years has tried to answer this question by defining the Hh signaling cascade at the molecular level. The pathway is best understood in *Drosophila*, where most of the pathway components were initially discovered through genetic screens.

1.2.1. General pathway architecture.

The transcription factor Cubitus interruptus (Ci) controls transcription of Hh target genes. Hh target gene expression is mediated in flies by the bifunctional transcription factor Ci, which can act as transcriptional activator and repressor. In the absence of Hh, the 155kDa full-length Ci-protein (Ci^{155}) is proteolytically processed into a truncated version of about 75kDa molecular weight (Ci^{75}). Ci^{75} is capable of binding DNA via its zinc finger domain, but acts as a transcriptional repressor for at least some Hh target genes. For instance, *dpp* expression is blocked by Ci^{75} (Dominguez et al., 1996). In presence of Hh, the equilibrium between Ci^{75} and Ci^{155} shifts in favor of the full-length transcriptional activator because proteolytic processing of Ci is impaired (Figure 1.1F). Consequently, Ci^{155} accumulates in the Hh responsive zone of a of a *Drosophila* wing disc (Slusarski et al., 1995). However, in few rows of A cells, close to the A/P compartment border, Ci^{155} levels are surprisingly low (Ohlmeyer and Kalderon, 1998). Nevertheless, these cell express high threshold Hh target genes such as *col* and A *en*. This lead to the model that in these cells Ci^{155} is further activated but that this hyper-active form of Ci is unstable and labile (Kent et al., 2006). In addition to the role of Hh in controlling Ci^{155} levels, Hh also regulates translocation of Ci^{155} to the nucleus (Chen et al., 1999a).

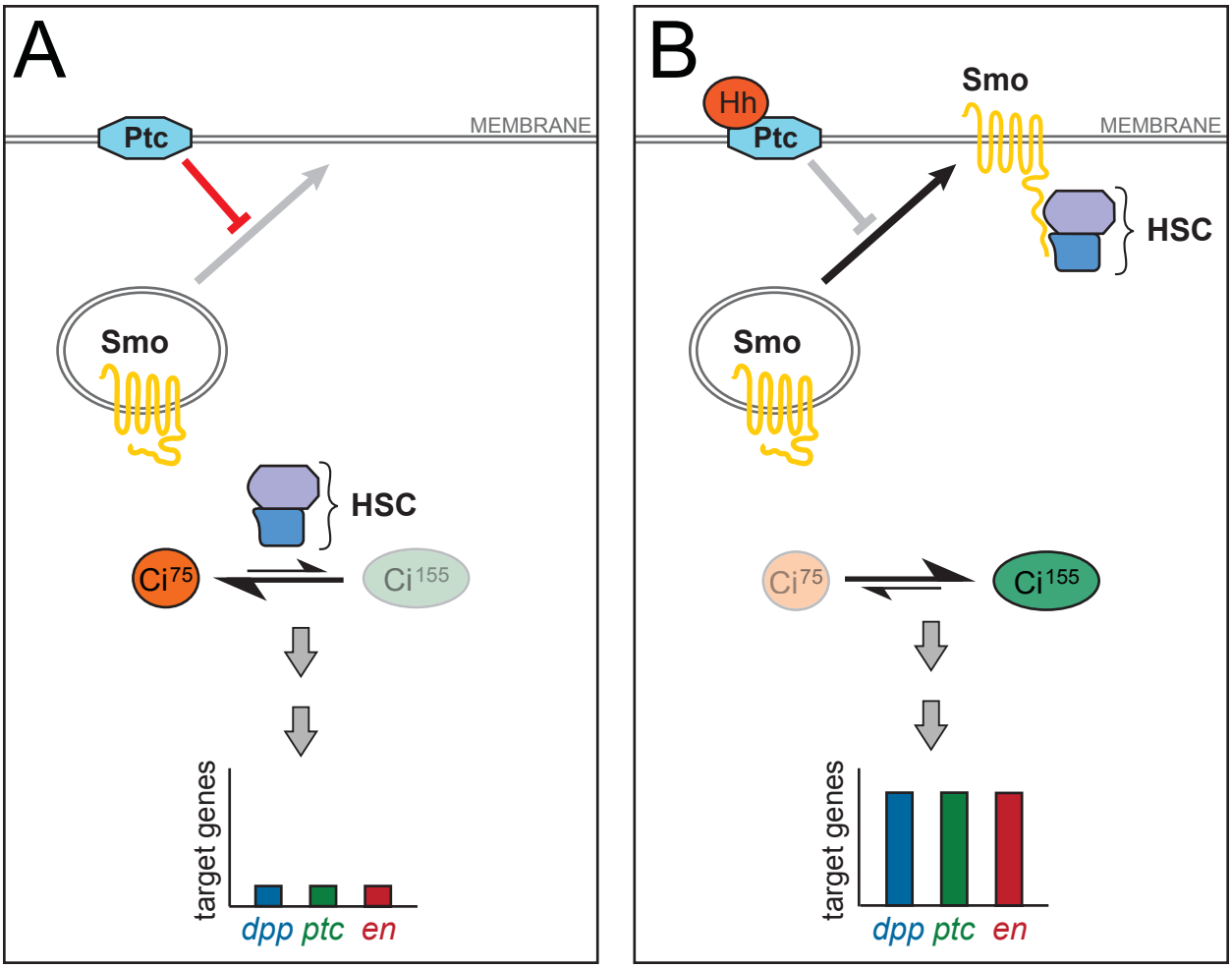

Figure 1.2. General architecture of the Hh signaling pathway in *Drosophila*.

(A) The Hh pathway is off in the absence of Hh. Ptc prevents Smo activation and membrane accumulation. The **H**edgehog **S**ignaling **C**omplex (HSC) shifts the equilibrium between the Ci isoforms (Ci^{75} and Ci^{155}) towards the repressor form Ci^{75}. Consequently, Hh target gene expression is off. **(B)** Hh turns the pathway on. Hh binds to Ptc and the inhibition of Ptc towards Smo is released. Smo accumulates at the plasma membrane in an active state and binds the HSC. The equilibrium of Ci is now in favor of the transcription factor Ci^{155} which turns on low (*dpp*), medium (*ptc*) and high (*en*) threshold Hh target genes.

In conclusion, Ci exists in at least three states; as transcriptional repressor Ci^{75}, as activator Ci^{155} and as hyper-active, unstable form of Ci^{155}. Hh controls the balance between these forms; high levels of Hh shift Ci into its hyper-active form, whereas no Hh results into Ci processing to Ci^{75} (Figure 1.2). The nature of the transcriptional response, that is whether low, medium or high threshold target genes are expressed, depends on the state of Ci. For instance, expression of A *en* in the wing disc requires hyper-active and labile Ci. Accumulation of Ci^{155} is sufficient to at least partially turn on medium threshold genes such as *ptc*. Finally, transcription

of the low threshold target gene *dpp* is already achieved by releasing the transcriptional inhibition of Ci^{75} and does not require activation by Ci^{155} (Hooper and Scott, 2005).

Members of the Hh signaling pathway connect Hh and Ci. The core components of the Hh pathway consists of two integral membrane proteins, Patched (Ptc) and Smoothened (Smo), and the cytosolic Hedgehog Signaling Complex (HSC; Figure 1.2). Functionally, Ptc is the Hh receptor and negatively regulates Smo activity. Smo is the central signal transducer of the Hh pathway. In the presence of Hh, Smo is stabilized at the plasma membrane and activated. The HSC consists of several proteins and controls Ci processing and activity. It also bridges the signaling gap between the membrane protein Smo and the cytosolic/nuclear transcription factor Ci (Briscoe and Therond, 2013).

To summarize, activation of the *Drosophila* Hh pathway occurs in three main steps: first, the Hh-dependent release of Smo inhibition by Ptc; second, stabilization and activation of Smo; and third, the role of the HSC in controlling Ci. I will discuss these three points in the following sections (Figure 1.2).

1.2.2. The Hh receptor Ptc and its relationship to Smo.

The function of Ptc is well characterized; it acts negatively on the Hh pathway (Hooper and Scott, 1989; Nakano et al., 1989) by constitutive repression of Smo (Ingham et al., 2000). Ptc prevents Smo membrane accumulation and activation and keeps Smo trapped in intracellular vesicles (Denef et al., 2000). Ptc is a Hh receptor and Hh binding to Ptc releases its inhibition of Smo (Chen and Struhl, 1996). Several other Hh receptors exist as well, but in contrast to Ptc, these receptors play a positive role in the Hh pathway and promote Hh signaling. Generally, these other receptors seem to act as scavengers and present Hh molecules to Ptc. Therefore, they ensure efficient inhibition of Ptc by Hh, explaining their positive role in the pathway (Beachy et al., 2010).

The molecular mechanisms behind Ptc-mediated Smo repression remain still unclear. Ptc is a multi-pass transmembrane and belongs to the superfamily of Resistance-Nodulation-Division (RND) transporters implicated in promoting the flux of specific chemical compounds across membranes (Tseng et al., 1999). A related protein, the Neimann-Pick disease type C1 protein

(NPC1) was found to mediate the efflux of lipid and cholesterol derivatives from the lysosome to other cellular sites (Peake and Vance, 2010). The recognition of sterols by NPC1 is mediated via its sterol-sensing domain (SSD) which directly binds some sterol-related compounds such as cholesterol and various oxysterols (Infante et al., 2008; Liu et al., 2009). The function of Ptc as a transporter and the Ptc SSD seem to be functionally relevant because mutation of the permease motif or the SSD abrogates its inhibition of Smo (Martin et al., 2001; Strutt et al., 2001). This finding led to the compelling speculation that Ptc transports and therefore controls the availability of an endogenous Smo ligand (Taipale et al., 2002). Smo is a member of the GPCR family and these receptors are often regulated by small molecule ligands. Furthermore, Ptc catalytically represses Smo with a stoichiometry of up to 1:50; arguing against a mechanism relying on direct Ptc-Smo interactions as initially thought (Taipale et al., 2002). The nature of an endogenous Smo ligand is still unknown, but tissue culture experiments with vertebrate Smo provide several lines of evidence that derivatives of sterol regulate Smo activity. For instance, oxysterols, originating from the oxidation of sterols, directly bind Smo and promote Hh signaling (Corcoran and Scott, 2006; Dwyer et al., 2007; Nachtergaele et al., 2012). On the other hand, pro-vitamin D3, another sterol-based compound, acts as a Smo antagonist to inhibit Hh signaling in tissue culture systems (Bijlsma et al., 2006). In conclusion, several natural occurring derivatives of sterol modulate Smo activity by acting either as agonists or antagonists. It is tempting to speculate that Ptc recognizes the Smo ligand via its SSD and transports it in a way that results in potent Smo inhibition. Hh binding blocks this transport and therefore leads to Smo activation. However, both the biological relevance of sterol metabolites in Smo regulation and whether Ptc is responsible for their transport are unknown.

Studies in *Drosophila* added another aspect of to the Ptc-Smo relationship. In flies, Ptc prevents Smo accumulation at the plasma membrane and instead keeps Smo trapped in endocytic vesicles (Denef et al., 2000). Smo trafficking to the membrane is also negatively influenced by lipoproteins called lipophorins in flies. Ptc was shown to bind internalized lipophorins, recruit them to Smo vesicles, and change the lipid composition of the vesicular membrane by incorporating lipophorin lipids (Callejo et al., 2008; Khaliullina et al., 2009). This steps seems to be responsible for sending Smo vesicles en route to degradation.

Taken together, in *Drosophila* Ptc regulates trafficking of Smo towards its degradation, and may also control cellular levels of an endogenous Smo ligand. Both processes might be related, as both depend on the Ptc SSD. Future research will be needed to clarify their relationship.

One additional aspect of Ptc biology is that it is at the center of a negative feedback loop limiting the global Hh response. In its function as Hh receptor, Ptc binds Hh and both receptor and ligand are internalized and degraded (Cheng et al., 2010). Through this function Ptc acts negatively on Hh protein levels and so shapes the Hh gradient. In addition, Ptc is also a transcriptional target of the pathway (Forbes et al., 1993), therefore, this role of Ptc is amplified in response to Hh itself. In conclusion, Hh negatively limits its distribution via up-regulation of Ptc.

1.2.3. Active Smo is a membrane localized, highly phosphorylated protein.

The inhibition of Ptc by Hh is crucial for translocation of Smo to the plasma membrane, but Smo itself is also post-translationally modified and stabilized in response to Hh. Like all GPCRs, Smo contains seven transmembrane domains, an extracellular N-terminus and a cytoplasmic C-terminal tail. The particularly long C-terminus of *Drosophila* Smo (~470 amino acids) is highly phosphorylated in response to Hh. Treatment of cells in tissue culture with Hh resulted in the phosphorylation of at least 26 Ser/Thr residues and several Smo kinases have been identified to account for these phosphorylation events (Zhang et al., 2004). Functionally, the most important kinase is Protein kinase A (PKA), which acts in conjunction with Casein kinase 1 (Ck1) (Jia et al., 2004). In addition, Casein kinase 2 (Ck2) and G protein-coupled receptor kinase 2 (Gprk2) are also known to phosphorylate Smo (Cheng et al., 2010; Jia et al., 2010). The role of Gprk2 in Smo regulation is at the center of this thesis. Smo phosphorylation is tightly controlled not only by kinases but also by phosphatases. Several phosphatases are known to de-phosphorylate Smo (Jia et al., 2009; Su et al., 2011). This suggests that the net phosphorylation state of Smo is determined by the interplay of several signaling cascades.

Smo phosphorylation and its membrane accumulation are tightly correlated and both processes can be used as read-outs for Smo activity. However, the subcellular localization of

Smo seems to be determined by the phosphorylation state of Smo. Mutation of the PKA and Ck1 sites in Smo strongly impacts Smo trafficking (Zhao et al., 2007). In the following section, I will summarize our understanding of Smo regulation by phosphorylation and its impact on Smo activity and the subcellular localization.

1.2.3.1. PKA and Ck1 control Smo stability and activity.

The identification of PKA as a Smo kinase was a milestone in the characterization of Smo biology (Apionishev et al., 2005; Jia et al., 2004; Zhang et al., 2004). PKA initiates Smo phosphorylation within three clusters of Ser residues, all located in the cytoplasmic tail of Smo. Each cluster harbors three Ser residues in the same sequence arrangement (RRxSxxSxxS). The first, most N-terminal Ser residues conform to the PKA consensus sequence whereas the two downstream serines are typical Ck1 sites. PKA controls Ck1 phosphorylation, because Ck1 requires a phosphorylated Ser/Thr residue at the upstream -2 position, which in this case is primed by PKA. Mutating all Ser residues within the three clusters to Asp (Smo^{SD}), thereby mimicking the charge of the phosphate groups, results in a constitutively active form of Smo. Transgenic expression of Smo^{SD} in *Drosophila* wing discs induces ectopic expression of Hh target genes in the far A compartment of the disc, independent of the Hh ligand. In *Drosophila* cell cultures, Smo^{SD} is highly expressed and localizes to the plasma membrane even in the absence of Hh. The behavior of Smo^{SD} differs from wild-type (wt) Smo, which is constitutively degraded and practically not present at the plasma membrane in the absence of Hh (Denef et al., 2000). However, co-expression of Hh or Hh treatment triggers stabilization and membrane accumulation of wt Smo to a comparable extent as observed for Smo^{SD}. Therefore, Smo^{SD} mimics the active state of wt Smo but in a Hh-independent manner. The opposite effects are observed when the PKA sites are mutated to Ala (Smo^{SA}), preventing the phosphorylation of the three PKA clusters. Smo^{SA} is functionally inactive and insensitive to Hh stimulation. Furthermore, the protein is poorly expressed in cells and does not accumulate at the membrane. Together, the Smo^{SA} and Smo^{SD} mutants highlight the key roles of PKA and Ck1 in the regulation of Smo activity and membrane recruitment (Jia et al., 2004).

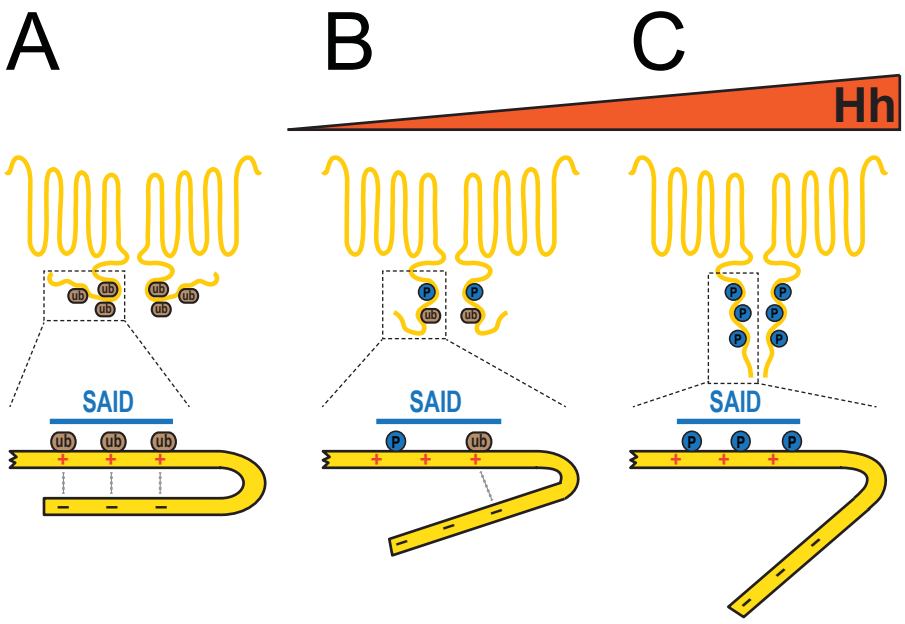

Smo localization:	internal vesicles	membrane	membrane
Smo stability:	degradation	accumulation	accumulation
Smo CT conformation:	closed	partially open	open
Dimerization of CTs:	n.a.	partial	full
Smo activation state:	inactive	partially active	fully active
Hh target genes:	none	low threshold e.g. *dpp*	low & high threshold e.g. *dpp*, *ptc*, *col*, *en* (A)

Figure 1.3. Smo activation states and conformations of the C-terminus in response to Hh.

(A) In the absence of Hh the C-terminal domain of Smo is in a closed conformation through electrostatic interactions between positive charged residues within the SAID and negative charged amino acids in the distal C-terminus. In this state, Smo is found mostly in internal vesicles and en route to ubiquitin-dependent degradation. **(B)** Low doses of Hh partly activate Smo and allow membrane accumulation. The conformation and dimerization state of the Smo C-terminal domains allow for expression of low threshold Hh target genes. **(C)** High doses of Hh shift Smo in a maximal active state. Phosphorylation within the SAID blocks Smo degradation and breaks the interaction with the distal Smo C-terminus. As a result, Smo adopts a fully open conformation and Smo C-termini are completely dimerized. Consequently, low and high threshold Hh target genes are turned on.

PKA and Ck1 phosphorylation antagonize the Smo autoinhibitory domain (SAID). The mechanisms behind the two effects, Smo stabilization and activation, has been elucidated over the last ten years. The region of the Smo C-terminus harboring the PKA clusters was identified as the Smo autoinhibitory domain (SAID; Figure 1.3) (Zhao et al., 2007). Deletion of this domain renders Smo constitutively active, suggesting that PKA-dependent phosphorylation counteracts the autoinhibition. The SAID domain encodes several stretches of Arg and Lys residues and these clusters of positive charges are adjacent to the three PKA clusters. The SAID acts on both levels, Smo activation and Smo stability. Smo protein levels are negatively controlled by endocytosis followed by proteasomal and lysosomal degradation. This Smo turnover depends on ubiquitination of multiple Lys residues, including the ones in the SAID. Hh-dependent phosphorylation of the PKA clusters prevents ubiquitination and therefore leads to Smo stabilization and membrane accumulation (Li et al., 2012). A Smo-specific E3 ubiquitin ligase has not yet been identified, making it unclear whether PKA/Ck1 phosphorylation prevents binding of that ligase. Alternatively, phosphorylation of the SAID could trigger the removal of ubiquitin modifications and prevent Smo degradation this way. Consistent with this, Ubiquitin-Specific Protease 8 (USP8) was identified as a Smo deubiquitinase and a positive role of USB8 in Smo regulation and the Hh pathway was confirmed (Xia et al., 2012).

The SAID also regulates Smo signaling activity by affecting its conformation (Zhao et al., 2007). Hh and PKA/Ck1-dependent phosphorylation triggers a conformational change in Smo. In the unphosphorylated state, Smo adopts a closed, inactive conformation (Figure 1.3A). This arrangement is mediated through electrostatic interactions between the positively charged Arg/Lys clusters in the SAID and negatively charged amino acids in the distal C-terminus. Phosphorylation within the SAID neutralizes the positive charges of the Arg/Lys clusters and disrupts the interaction with the distal C-terminus. Smo switches into an open conformation which allows dimerization of Smo C-terminal tails (Zhao et al., 2007) (Figure 1.3B, C). The open conformation of Smo is recognized by the HSC, the protein complex regulating the transcription factor Ci (see below). Binding of HSC proteins to active Smo impairs Ci processing and leads to the stabilization and activation of full-length Ci.

The Hh gradient is translated in distinct Smo activation states. The conformational switch model of Smo offers an elegant explanation of how the Hh gradient is translated into a graded pathway response. In brief, the Hh gradient is converted into distinct Smo activation states, corresponding to various signaling strengths, depending on the extent of PKA/Ck1 phosphorylation within the SAID. High levels of Hh result in complete phosphorylation of all three PKA/Ck1 clusters in Smo and high threshold target gene expression (Figure 1.3B, C). Lower levels of Hh only result in partial phosphorylation and signaling activity. At least three lines of compelling experimental evidence supports this model.

Mutation of PKA and Ck1 sites within Smo yielded the first clues for this model. Mimicking complete phosphorylation at all PKA/Ck1 sites by exchanging Ser residues with Asp (Smo^{SD}), renders Smo highly active in the absence of Hh. Furthermore, Hh treatment does not elevate Smo^{SD} signaling, suggesting that it already is maximally active. The conformation of Smo and dimerization of Smo cytoplasmic C-termini can be visualized by fluorescence resonance energy transfer (FRET) when Smo proteins tagged with various fluorescent proteins are expressed in cells. This technique was used to demonstrate that Smo^{SD} fully mimics the conformation and dimerization state of wt Smo in cells treated with high doses of Hh (Zhao et al., 2007). Mimicking partial PKA/Ck1 phosphorylation by substituting only a subset of the three phosphorylation clusters resulted in partially active and partially Hh-responsive forms of Smo. Compared to Smo^{SD}, these mutants had markedly reduced signaling activity in the absence of Hh but its presence increased signaling to the level of Smo^{SD} (Jia et al., 2004). The signaling capabilities of these mutants was well matched with their behavior in the FRET assays. They displayed intermediate levels of Smo conformation change and C-termini dimerization, shifting into fully active conformations upon Hh treatment (Zhao et al., 2007).

The second line of evidence for the graded activation of Smo was provided by FRET experiments *in vivo*. In *Drosophila* wing discs Smo is in an active conformation in the P compartment and at the A/P boundary and where Hh is present at high concentrations. The FRET analysis confirms that Smo adopts an inactive conformation in the far A compartment where Hh is absent (Zhao et al., 2007).

The third and most direct validation for the graded Smo activation came from studies using phospho-specific antisera. The antibodies targeted distinct PKA sites within the SAID and confirmed phosphorylation at these sites in a Hh dose-dependent manner (Fan et al., 2012; Su et al., 2011). It has even been suggested that the PKA/Ck1 clusters are phosphorylated in a specific sequence starting from the most N-terminal and ending with the most C-terminal cluster. This way, the phosphorylation acts like a zipper and locks Smo in its active conformation the more it moves towards the C-terminal PKA/Ck1 clusters (Fan et al., 2012).

To summarize, the existence of various Smo activation states corresponding to Hh concentrations seems well supported. The studies above imply that Smo adopts several distinct conformations representing distinct signaling strengths. Rather than a multi-conformation hypothesis, a binary model of Smo activity could also be true. In this scenario, Smo constantly switches between an active and inactive state. Phosphorylation could effect the equilibrium between the two states and full PKA/Ck1 phosphorylation would strongly favor the active conformation of Smo. In this model, the net signaling strength of Smo would be determined by the Smo fraction residing in the active conformation. Further studies will be needed to distinguish between the two models of Smo action.

1.2.3.2. Gprk2 and Ck2 have modest effects on Smo activation.

In addition to PKA and Ck1, two other kinases that phosphorylate Smo have been identified, Ck2 and Gprk2. Ck2 sites were identified in the Smo C-terminus downstream of the SAID and mutating these sites to Ala rendered Smo slightly less active and incapable of turning on the highest threshold target gene, A *en*. In terms of Smo regulation, Ck2 assumes only a minor role, but it might also be implicated in Ci phosphorylation and processing (Jia et al., 2010).

My PhD thesis focussed on Gprk2 and its role in Smo regulation. During my work, a competing group published a paper identifying four Gprk2 phosphorylation sites in Smo (Chen et al., 2010). The sites are grouped in two clusters, one within the SAID, the other one at the distal end of the Smo cytoplasmic tail. Only the first cluster seemed functionally relevant and phosphorylation at these sites facilitated Smo to adopt its most active conformation. Although mutating these putative Gprk2 sites resulted in a less active Smo variant, expression of this

construct *in vivo* failed to replicate all aspects of the *gprk2* mutant phenotype. The authors hypothesized that Gprk2 also stabilizes the active conformation of Smo and promotes dimerization of the Smo C-terminus in a kinase-independent fashion by directly binding to it (Chen et al., 2010). Although some experimental evidence was provided to support these claims, we had compelling preliminary data indicating that the mapping of Gprk2 sites was incomplete. We continued our studies focussing on a different set of Gprk2 phosphorylation sites and re-evaluated the importance of the published sites with our own tools.

1.2.4. The roles of the Hedgehog signaling complex in the pathway.

The HSC has two functional roles in the Hh pathway, one positive and one negative. First, in the presence of Hh, it bridges the signaling gap between membrane-integral Smo and the cytosolic/ nuclear transcription factor Ci (Figure 1.4B). Therefore, it acts downstream of Smo and converts Smo activity into transcriptional activity of full-length Ci^{155}. Second, the HSC plays a negative role in the pathway by promoting processing of Ci into Ci^{75} repressor in the absence of Hh (Figure 1.4A). As discussed above, the transcriptional outcome of the Hh pathway is determined by the balance of Ci^{75} and Ci^{155}. Due to its dual role in the Hh pathway, the HSC ultimately determines this balance.

In the absence of Hh, the HSC initiates processing of Ci into its transcriptional repressor form. Two proteins form the core of the cytosolic HSC: the kinesin-like Costal 2 (Cos2) and the Ser/Thr kinase Fused (Fu; Figure1.4). Cos2 acts mostly as a scaffold protein and engages with various pathway components in a Hh-dependent manner (Robbins et al., 1997). Whether it is a functional kinesin *in vivo* is unclear (Ho et al., 2005; Lum et al., 2003b); however Cos2 moves along microtubules in cultured cells (Farzan et al., 2008). In the absence of Hh, Cos2 sequesters full-length Ci and initiates Ci processing into Ci^{75} by recruiting the Ser/Thr kinases, PKA, Ck1 and glycogen synthase kinase 3 (Gsk3; Figure 1.4A) (Zhang et al., 2005). Phosphorylation triggers Ci ubiquitination followed by partial proteasomal degradation into Ci^{75} (Jia et al., 2005; Price and Kalderon, 2002). Interestingly, phosphorylation of Ci is strikingly similar to Smo phosphorylation. PKA phosphorylation primes further phosphorylation by the other two kinases making PKA the master kinase (Smelkinson et al., 2007). Therefore, like the HSC, PKA plays

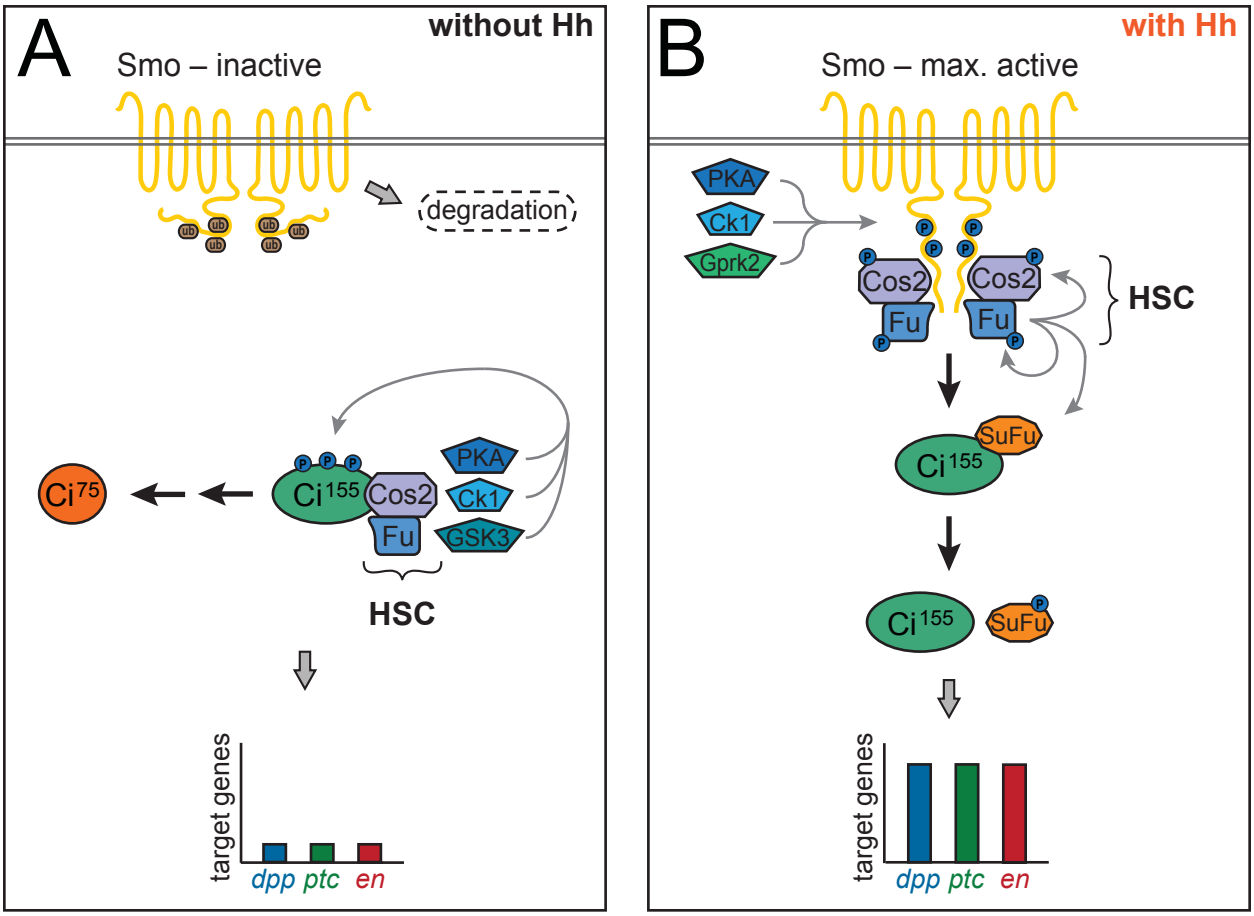

Figure 1.4. Regulation of Ci by the HSC.

(A) In the absence of Hh Smo is inactive and degraded. The scaffolding protein Cos2 of the HSC binds Ci^{155} and recruits the kinases PKA, Ck1 and GSK3 to Ci^{155}. Ci phosphorylation initiates proteasomal processing into the repressor form Ci^{75}. Consequently, the transcriptional response of the pathway is shut off. **(B)** Smo is phosphorylated by three kinases (PKA, Ck1 and Gprk2) in response to high doses of Hh. This shifts Smo in a maximally active state and allows dimerization of C-terminal domains. Smo recruits the HSC proteins Cos2 and the kinase Fu. Fu dimerizes and activates itself through trans-autophosphorylation. Fu also phosphorylates Cos2 triggering the release of Ci^{155} into the cytosol. SuFu antagonizes Ci by retaining it in the cytosol. Fu phosphorylates SuFu, disrupting the interaction between SuFu and Ci^{155}. Ci^{155} is now free to enter the nucleus where it drives expression of Hh responsive genes.

two opposing key roles in the Hh pathway. On one hand, it negatively regulates the pathway by promoting Ci processing (Chen et al., 1998). On the other hand, it promotes Hh signaling by activating Smo (Jia et al., 2004).

In the presence of Hh, the HSC engages Smo and releases full-length Ci^{155} into the cytosol. The opening and dimerization of Smo in response to Hh stimulation exposes Cos2 and Fu binding sites within the Smo C-terminal tail and leads to the recruitment of both proteins to

activated Smo (Jia et al., 2003). However, engagement of Fu is Cos2-dependent (Figure 1.4B). Through the dimerization of the cytoplasmic tails of Smo, Fu also dimerizes and this is sufficient to strongly activate Hh target gene expression. Mechanistically, Fu dimerization leads to Fu activation through trans-autophosphorylation (Figure 1.4B). This model explains how the various Smo activation states are converted into graded responses of downstream signaling. Only in the presence of high concentrations of Hh are the cytoplasmic tails of Smo fully dimerized, leading to maximal Fu activation. Modest Smo activity characterized by partial dimerization of the Smo C-terminus leads to modest Fu dimerization and a smaller increase in Fu activity (Shi et al., 2011; Zhang et al., 2011).

Fu acts as a kinase for two other pathway components, Cos2 and SuFu (Figure 1.4B). Fu phosphorylates Cos2 at at least two distinct sites, Ser^{572} and Ser^{931}. Interestingly, phosphorylation of Ser^{572} correlates with low level Hh signaling, whereas both serine residues are modified with a phosphate group at high levels of Hh signaling (Ranieri et al., 2012). Modification of Ser^{931} might require maximal Fu kinase activity only triggered by maximal dimerization of Fu and Smo C-terminal tails. Most likely as consequence of its phosphorylation, Cos2 releases full-length Ci^{155} into the cytosol in the presence of Hh (Ruel et al., 2003; Zhang et al., 2005). In this condition, Ci is no longer proteolytically processed and is, in principle, ready to enter the nucleus and promote Hh target gene expression. Ci^{155} gets further activated into a hyper-active but labile form required for the expression of the highest threshold Hh target genes (Ohlmeyer and Kalderon, 1998). The mechanism behind this further activation of Ci is not well understood, but most likely depends on other post-translational modifications of the protein.

Suppressor of Fused (SuFu) controls nuclear entry of Ci^{155}. Genetic analysis has identified SuFu as a negative pathway component acting downstream of Fu. Removal of Fu leads to a Hh loss-of-function phenotype, which is almost completely reverted by the additional loss of SuFu. This suggests that Fu counteracts the negative role of SuFu. However, the negative role of SuFu is minor, as the loss of SuFu alone has no effect on Hh signaling (Preat, 1992). Mechanistically, SuFu binds Ci and prevents its nuclear translocation by retaining it in the cytosol (Figure 1.4B) (Methot and Basler, 2000). Fu antagonizes SuFu most likely by phosphorylation (Figure 1.4B).

Fu phosphorylation sites in SuFu have been mapped but their functional relevance remains unclear (Zhou and Kalderon, 2011).

In summary, SuFu plays a minor role in antagonizing Ci. In flies, Ci activity is mostly counteracted by Cos2, which scaffolds Ci^{155} for phosphorylation leading to Ci^{75} processing (Smelkinson et al., 2007). Consequently, loss of Cos2 results in strong pathway activation (Grau and Simpson, 1987). This negative function of Cos2 is inhibited in the presence of Hh through Fu. Fu phosphorylates Cos2 and triggers the release of transcriptionally active Ci^{155}.

1.2.5. Dual role of PKA in *Drosophila* Hh signaling.

As detailed in the previous sections, PKA plays two opposing key roles in the Hh pathway. In the absence of Hh, it acts negatively on the pathway by restricting Ci activity. PKA is the master kinase for Ci phosphorylation which is the initial step leading to proteolytic Ci processing. In the presence of Hh, PKA becomes a positive regulator of Hh signaling, as it is also the key kinase for Smo activation. This complicated setup suggests that PKA activity must be tightly controlled for proper pathway function. However, whether kinase activity is controlled at all and how this would be achieved is still under investigation.

The biochemistry of PKA is well understood. In its inactive state, PKA exists as heterotetramer consisting of two catalytic and two regulatory subunits. The kinase function of the catalytic units is blocked by the regulatory subunits. The second messenger cAMP binds the regulatory subunits, resulting in the dissociation of the complex and release of free catalytic subunits. Due to this architecture, cellular cAMP levels correlate directly with PKA activity (Taylor et al., 1990). This led to the speculation that Hh signaling modulates cAMP levels and therefore controls PKA activity. The second messenger cAMP is often influenced by heterotrimeric G protein signaling, therefore, one would expect that G protein signaling might influence Hh signaling as well. This aspect of Hh signaling is discussed in more detail in section 1.4.3.

However, whether PKA activity is controlled at all by the Hh pathway is also under debate. An early study of Hh signaling in *Drosophila* embryos suggested cAMP-dependent regulation of PKA is not necessary for Hh signaling. *In vivo* expression of a cAMP insensitive

form of PKA did not alter Hh signaling in fly larvae (Ohlmeyer and Kalderon, 1997). A recent publication offered an alternative mechanism for controlling PKA activity based on spatial distribution. In the absence of Hh, the catalytic subunit of PKA (PKA-c) is in a cytosolic complex with Cos2 and Ci. In the presence of Hh, PKA-c dissociates from this complex and is recruited to Smo at the plasma-membrane. According to this model, the subcellular localization and PKA complex formation dictate whether PKA exerts a positive or negative role in Hh signaling (Li et al., 2014).

In conclusion, PKA plays both a positive and negative role in the Hh pathway. PKA activity is most likely regulated by Hh, possibly through modulating cAMP levels or controlling the spatial distribution and complex formation of active PKA subunits.

1.3. Conservation and divergence of Hh pathway components in mammals and *Drosophila*.

Most Hh pathway components were first discovered and cloned in *Drosophila* and vertebrate orthologs were identified based on sequence homology. In the following section, I will focus on mammalian Hh signaling and detail the similarities and differences compared to *Drosophila*.

1.3.1. The mammalian Hh signaling cascade is more complex than in *Drosophila* but follows the same principle arrangement.

Generally, Hh pathway genes are well conserved, but several gene duplications occurred in the vertebrate lineages. For instance, mammals have three paralogous Hh genes: Sonic (Shh), Indian (Ihh) and Desert (Dhh) (Echelard et al., 1993). All three isoforms are functionally relevant and characterized by spatially and temporally specific expression patterns. Nevertheless, Shh is the most widely expressed Hh variant in mammals (Ingham and McMahon, 2001). Of the two Ptc isoforms present in vertebrates (Ptc1 and Ptc2); Ptc1 assumes most functions whereas the loss of Ptc2 causes only a few abnormalities (Rahnama et al., 2004). The ortholog of *Drosophila* Ci, called Glioma associated oncogene (Gli), exists in three isoforms (Gli1, 2 and 3). Gli proteins are regulated in a similar fashion as Ci; phosphorylation by PKA, Ck1 and Gsk3 triggers partial

proteasomal degradation. However, the three isoforms assume more specialized functions. In mammals, Gli2 is the main transcriptional activator. Gli3 acts mainly as a repressor (Wang et al., 2000) but some examples of Gli3 as transcriptional activator have also been described (Bai et al., 2004). This suggests a certain degree of context dependency of Gli3 activator/repressor function. Gli1 plays a minor role as a transcriptional activator but it constitutes a positive feedback in the Hh pathway because it is also a transcriptional target of Hh (Hui and Angers, 2011).

Despite the fact that some components exist in several isoforms, the general architecture of the Hh pathway is the same in mammals and flies. Hh deactivates Ptc leading to Smo accumulation and activation. Active Smo ultimately controls the state of the bifunctional Gli transcription factors and shifts them to the active form. Nevertheless, important differences exist between the *Drosophila* and mammalian Hh pathway. I will focus on three major dissimilarities. The first one relates to the primary sequence of Smo. Mammalian species encode one Smo ortholog, showing a fair degree of conservation through large parts of the protein. However, the vertebrate Smo cytoplasmic tail differs greatly from its *Drosophila* counterpart. The second major difference lays in the downstream signaling between Smo and Gli. The signaling downstream of Smo is mediated in *Drosophila* by HSC proteins binding to its C-terminus. Not all HSC proteins are functionally relevant in mammals, consistent with the non-conservation of the Smo cytoplasmic tails and possibly explaining the dissimilarities in signaling. Mammalian Hh signaling differs in a third point from its *Drosophila* counterpart. It requires the presence of a primary cilium. The importance of this microtubule-based cellular compartment was only discovered over the last ten years and has added a whole new level of complexity.

1.3.2. The C-terminal tails of Smo orthologs differ throughout evolution but are regulated in an analogous fashion.

Smo proteins are well conserved throughout evolution and present in all three branches of the bilaterian lineage (Ingham et al., 2011). This is reflected in a high degree of sequence similarity throughout large parts of the protein including the N-terminal and transmembrane domains. However, of the cytoplasmic C-termini only about the 100 most membrane proximal amino-acids are broadly conserved (Maier et al., 2014). The rest of the tail diverges substantially. This

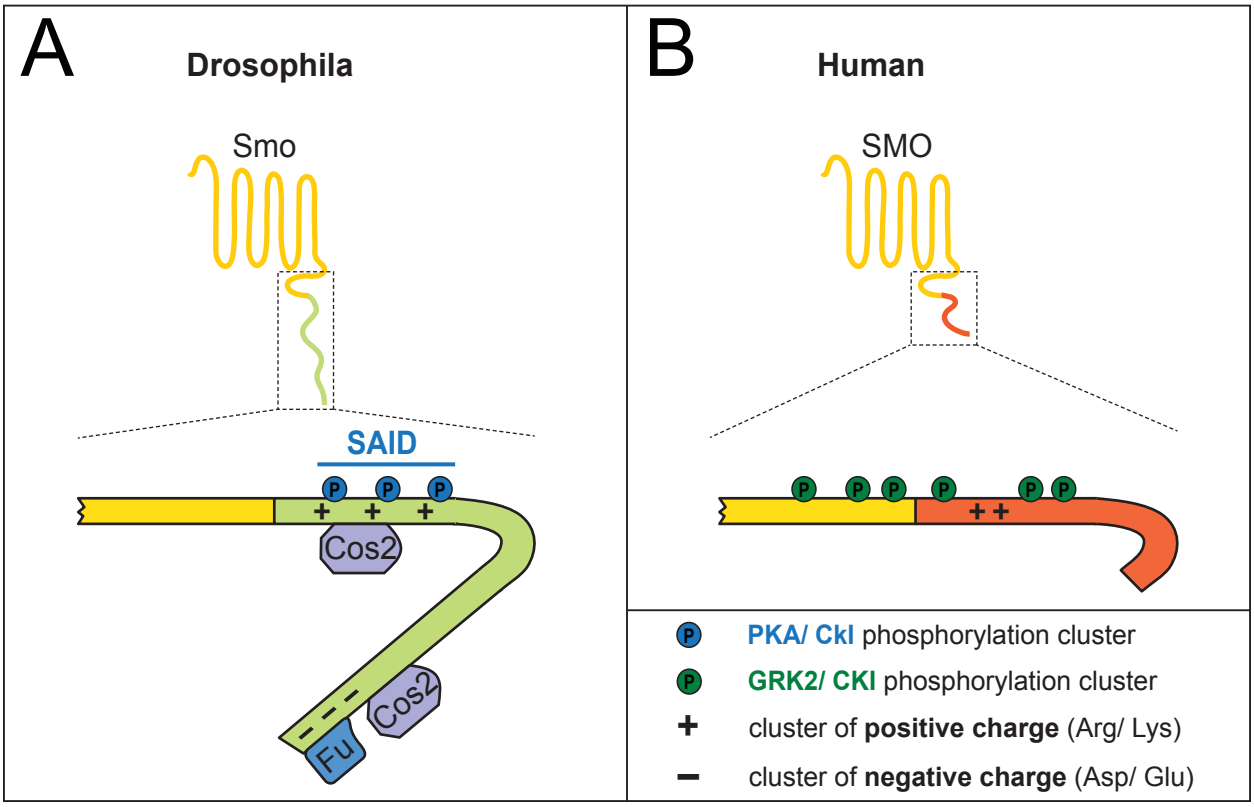

Figure 1.5. The cytoplasmic C-terminal tails of *Drosophila* and murine Smo proteins.

(A-B) Schematics of Smo C-terminal domains; shown for *D. melanogaster* **(A)** and *M. musculus* **(B)** Smo orthologues. Between the two species, only the membrane proximal part (~ 100 amino acids) is conserved (highlighted in yellow). **(A)** The non-conserved part in *Drosophila* (colored in green) harbors the SAID which is regulated by PKA and Ck1 phosphorylation. The open conformation exposes binding sites for Cos2 and Fu. **(B)** The non-conserved region in murine Smo (orange) is shorter than in *Drosophila*. Murine Smo proteins also undergo conformational changes triggered by GRK2 and Ck1α phosphorylation. Six regions of phosphorylation within the murine Smo C-terminal domain were mapped. The first two phosphorylation clusters, which are located in the conserved Smo sequence, are functionally most important for GRK2/Ck1α-driven Smo activation in mice.

distal, non-conserved part of the Smo terminus compromises roughly 100 residues in most Smo orthologs. However, arthropod Smo proteins encode a much longer tail of approximately 350 amino acids. Interestingly, all of the previously discussed regulatory elements of *Drosophila* Smo fall into this region including the SAID with the PKA/Ck1 phosphorylation sites and the Fu/Cos2 binding sites (Figure 1.5A) (Chen and Jiang, 2013). By controlling the conformational switch and signaling strength of Smo, PKA is the master regulator of *Drosophila* Smo (Zhao et al., 2007). However, mammalian Smo orthologs do not contain PKA phosphorylation sites and PKA is not thought to regulate them (Figure 1.5B). Nonetheless, a recent study confirmed that

mammalian Smo also undergoes a conformational switch in the presence of Hh and in response to phosphorylation (Chen et al., 2011). Chen and colleagues demonstrated that Ck1 and G protein-coupled receptor kinase 2 (GRK2) phosphorylate and activate Smo downstream of Shh stimulation (Figure 1.5B). Phosphorylation triggers a conformational switch by neutralizing positively charged residues in proximity to the phosphorylation sites and promotes dimerization of Smo C-terminal tails.

In summary, Ck1 and GRK2 assume the same function in vertebrate Smo as PKA/Ck1 do in *Drosophila*. Therefore, the mechanism of Smo activation in mammals is analogous but molecularly distinct from the one described for *Drosophila* Smo. The kinase-dependent regulation of the Smo C-terminal tails might represent an example of convergent evolution.

1.3.3. Signaling downstream of Smo to Ci is different in mammals compared to flies.

Orthologs of Cos2, Fu and SuFu are found in mammals but their functional relevance to Hh signaling has shifted (Ingham et al., 2011). The closest relative of Cos2 is Kinesin family member 7 (Kif7), which is capable of binding Gli proteins and promoting proteolytic processing of Gli (Cheung et al., 2009). As with Cos2, a positive role of Kif7 in Hh signaling has also been suggested (Cheung et al., 2009; Endoh-Yamagami et al., 2009; Liem et al., 2009). It is tempting to speculate that Kif7 also engages with Smo and that this interaction is crucial for its positive role in the pathway. Indeed, an interaction between Kif7 and the Smo C-terminal tail has been reported (Endoh-Yamagami et al., 2009). The details of this interaction remain unclear, however, a recent report suggested that it might be indirect as it required the presence of two cilia specific proteins (Yang et al., 2012) (see section 1.3.4.). Further studies are needed to clarify the interplay between Smo and Kif7 and functional consequence of their interaction.

A change in functional relevance between flies and mammals can also be observed for SuFu. SuFu exerts only a minor influence in the fly Hh pathway (Preat, 1992). However, in mice, loss of SuFu causes strong constitutive pathway activation indicating that SuFu is a major negative regulatory element of this system (Cooper et al., 2005; Svard et al., 2006). The presence of Shh antagonizes the negative role of SuFu, but how this is achieved at the molecular level remains unknown. In flies, Fu is thought to deactivate SuFu by phosphorylating it but the

ortholog of Fused, Serine/Threonine kinase 36 (STK36) is not required for mammalian Hh signaling and not considered a component of the pathway (Ingham et al., 2011). Another kinase might have replaced Fu in the vertebrate system.

To conclude, orthologs of Fu, Cos2 and SuFu are present in vertebrates. However, only Cos2 (Kif7) to some extent and SuFu are functionally conserved; the latter being a major inhibitor of pathway activity in mammals. However, the molecular mechanisms controlling these orthologs are not defined yet.

1.3.4. Vertebrate Hh signaling requires coordinated ciliary localization of the main pathway components.

The primary cilium is an evolutionarily ancient cellular organelle present in many different eukaryotes, from single celled organisms to humans. Anatomically, it can be described as a microtubule-based membrane protrusion. The maintenance of the cilium and its protein composition is controlled by intraflagellar transport (IFT) along microtubules. Motor proteins of the kinesin family mediate anterograde transport together with members of the IFTB protein complex. IFTB proteins cross-link the motor proteins with cilium-specific cargo. Similarly, retrograde transport is mediated by dynamin motors and IFTA proteins. As a result of the highly selective traffic, the cilium forms a distinct cellular compartment. A highly specialized example of a primary cilium is the other segment of rod photoreceptors; however, primary cilia are far more common and nearly every cell of the human body has at least one (Goetz and Anderson, 2010).

The link between the primary cilium and mammalian Hh signaling was established about ten years ago, when mutants lacking primary cilia were fund to display typical Hh loss-of-function phenotypes (Huangfu et al., 2003). The mutations disrupted two IFTB proteins, IFT172 and IFT88, and in the following years many more cilia-specific proteins were shown to influence Hh signaling. Collectively, these studies established the view that the cilium provides a compartment in which most of the vertebrate Hh signal transduction is taking place. This is achieved by highly selective transport of pathway components into the cilium in a Hh-dependent manner (Briscoe and Therond, 2013). For instance, in the absence of Hh, Ptc and other Hh co-

receptors localize to the cilium (Rohatgi et al., 2007), whereas Smo is absent (Humke et al., 2010; Kim et al., 2009). The Gli transcription factors traffic through the cilium and this process relies on Kif7 (Cheung et al., 2009; Endoh-Yamagami et al., 2009; Liem et al., 2009). Processing of Gli proteins into their transcriptional repressor forms is initiated at the ciliary base where the critical kinases (PKA, Ck1 and Gsk3) are located (Barzi et al., 2010; Fumoto et al., 2006; Sillibourne et al., 2002). Phosphorylation of Gli by these kinases triggers its ubiquitination and partial proteasomal degradation.

The composition of the cilium changes dramatically in the presence of Hh. Ptc exits and Smo enters the cilium. Smo enrichment is dependent on phosphorylation by GRK2 and Ck1α (Chen et al., 2011). Furthermore it requires the kinesin Kif3a and β-arrestins as scaffold proteins (Chen et al., 2004; Kovacs et al., 2008). The latter two proteins are implicated in vesicular trafficking, suggesting that Smo is delivered in vesicles to the cilium. Smo accumulates at the basolateral membrane of cilium through its interaction with two other proteins, Elis-van Creveld syndrome protein (ECV) and ECV2 (Dorn et al., 2012; Yang et al., 2012). The molecular details are still unknown, but ciliary accumulation and activation of Smo stops Gli processing and leads to the stabilization of full-length Gli proteins. Gli in complex with SuFu is trafficked into the cilium where both proteins accumulate. SuFu releases full-length Gli, which exits the cilium and drives target gene expression in the nucleus (Humke et al., 2010; Tukachinsky et al., 2010).

In summary, the cilium adds a new dimension to Hh pathway regulation in mammals. Proteins involved in growth and maintenance of the cilia as well as ciliary proteins specifically interacting with Hh pathway components are implicated in proper pathway function. Interestingly, the primary cilium is largely absent in most *Drosophila* cell types and only found in a few specialized cells such as photoreceptors or sperm cells. Consequently, Hh signaling does not require any ciliary structure in flies. However, some parallels can be drawn between accumulation of mammalian Ptc and Smo in cilium and their fly counterparts at the plasma membrane. In both systems, accumulation of either protein is antagonistic to the other one. Ptc is at the surface in the absence of Hh and Smo only in the presence of Hh. Furthermore, Smo accumulates only in its phosphorylated and active conformation. These parallels might suggest

that membrane accumulation of Ptc and Smo in flies is functionally analogous to their ciliary translocation in mammals.

1.4. Evaluation of Smo as a functional GPCR and the role of G protein signaling in the Hh pathway.

The cloning of *Drosophila* Smo in 1996 identified it as a putative GPCR (Alcedo et al., 1996; van den Heuvel and Ingham, 1996). Based on Smo loss-of-function mutants available at the time, a compelling model detailing the role of Smo G protein signaling in the Hh pathway was proposed (Alcedo et al., 1996). Now, almost 20 years later, the relationship between Smo, G protein signaling and the Hh pathway is still not well understood. There are at least two outstanding questions relating to the connection between G protein signaling and the Hh pathway. First, is Smo a functional GPCR capable of coupling to G proteins to initiate signaling? And second, if Smo activates G protein signaling, how does this affect the Hh pathway and what is the mechanism behind it? In the following section, I will introduce the GPCR family and heterotrimeric G protein signaling, and review their roles in Hh pathway.

1.4.1. Hallmarks of GPCR signaling and biology.

The GPCR family of seven transmembrane receptor consists of about 800 members in humans (Bjarnadottir et al., 2006) and about 100 in flies (Brody and Cravchik, 2000). Phylogenetic analyses led to the classification of GPCRs into five main groups based on the GRAFS (glutamate, rhodopsin, adhesion, frizzled/taste2, and secretin) system. According to this system Smo is part of group F, which also includes Frizzled proteins (Schioth and Fredriksson, 2005). Interestingly, similar to Smo, Frizzled proteins are also critically involved in embryonic development and tissue specification because their signaling is initiated by the Wnt morphogen (Logan and Nusse, 2004). Extensive sequence homology between GPCRs is usually only found among members of the same subgroup, but one structural feature is conserved among all family members. This defining feature is the heptahelical domain consisting of seven transmembrane alpha helices connected by intra- and extra-cellular loops. The heptahelical domain is critically involved in ligand binding, GPCR activation and downstream signaling. GPCRs are activated by

very diverse endogenous ligands covering single ions and volatile odorants as well as peptides and proteins. Due to the wide spectrum of physiological GPCR stimulants, GPCRs are involved in virtually every aspect of animal physiology and cell biology, ranging from sensing the cellular environment to cell motility and growth control. This profound impact of GPCRs in cell biology and physiology, together with their shared structural features, make GPCRs excellent targets for pharmaceutical research. Indeed, about 40% of medicinal drugs on the market affect GPCR signaling (Heng et al., 2013).

GPCRs are typically activated by ligand binding and then signal through heterotrimeric G proteins consisting of G_α, G_β and G_γ subunits. In their inactive state, these three proteins form a plasma membrane associated complex. GPCR activation results in the activation and dissociation of the G_α subunit from the remaining $G_{\beta\gamma}$ complex and initiates G protein signaling. Both moieties, the G_α protein and the $G_{\beta\gamma}$ complex, have signaling capabilities, although canonical G protein signaling is mediated through the G_α subunit. The G_α protein functions as a GTPase and hydrolyses GTP to GDP. However, the hydrolysis rate of the G_α is relatively slow, therefore, the G_α protein exists in two states, GTP- and GDP-bound. In the GTP-bound stage, the G_α protein engages in downstream signaling by regulating various effector proteins. In the GDP bound stage, the G_α is inactive and associates with the $G_{\beta\gamma}$ complex. GPCRs control G_α signaling by acting as Guanine nucleotide exchange factors (GEFs) facilitating the exchange of GDP for GTP within the G_α subunit. Therefore, GPCRs initiate heterotrimeric G protein signaling. However, GPCRs act as GEFs only in response to ligand binding and in their active conformation, assuring that signaling is only engaged after proper GPCR stimulation (Hamm, 1998).

The G_α proteins can be divided into four groups ($G_{\alpha s}$, $G_{\alpha i}$, $G_{\alpha q}$ and $G_{\alpha 12/13}$). Each groups affects a different set of molecular effectors, which are often metabolic enzymes for major second messengers in the cell. For instance, proteins of the $G_{\alpha s}$ group stimulate adenylyl cyclase (AC) and therefore increase cAMP levels. Some isoforms of the $G_{\alpha i}$ group decrease cAMP levels by inhibiting AC. Lipid-based second messengers and the release of Ca^{2+} are influenced by $G_{\alpha q}$ signaling, which regulates the activity of phospholipase C (Neves et al., 2002).

Termination of G protein signaling has multiple aspects. First, the activity of GPCRs needs to be inhibited to prevent further activation of G protein signaling. G protein-coupled

receptor kinases (GRKs) are capable of recognizing and phosphorylating active, ligand-occupied GPCRs. This is the first step in the process of homologous GPCR desensitization, which describes the termination and reconstitution of GPCR signaling (Claing et al., 2002). The mechanism of this process is discussed in more detail in section 1.5.2. Second, the activated GTP-bound Gα proteins need to switch to their inactive GDP-bound state. Gα proteins possess GTPase activity, converting GTP into GDP and therefore terminating their own activity automatically. However, their intrinsic hydrolysis rate is relatively slow and cannot account for the often abrupt reduction in G protein signaling. GTPase-activating proteins (GAPs) are a class of proteins which vastly accelerate GTP hydrolysis and are therefore negative regulators of G proteins. GAPs specific for Gα proteins are also known as Regulator of G protein Signaling (RGS) proteins and more than 30 RGS or RGS-like proteins exist in humans (Hollinger and Hepler, 2002). Once the Gα subunit is in its inactive state, it re-associates with the Gβγ complex, terminating Gβγ signaling at the same time.

In summary, GPCRs represent a large group of membrane receptor capable of recognizing vastly different ligands and regulating many aspects of cell biology. Prototypical GPCRs act as GEFs for the α subunit of heterotrimeric G proteins. Heterotrimeric G proteins can influence a large number of cellular signaling pathways, but signaling through the α-subunit often involves regulation of second messengers systems such as cAMP and lipid-derived messengers. G protein signaling is terminated by stopping GEF activity of active GPCRs and by catalyzing the transition of the Gα protein from the active into the inactive state.

1.4.2. Is Smo a functional GPCR and regulated like one?

The first question is whether Smo is a functional GPCR − i.e. does it couple to G proteins, initiate signaling and is it regulated like a typical GPCR? Several lines of evidence support all these aspects of Smo GPCR functionality. First, there are structural similarities. The heptahelical domain of GPCRs encodes the binding sites for receptor ligands. Ligand binding usually occurs at the extracellular site of plasma membrane and triggers conformational changes within the domain. These conformational changes affect the intracellular surface of the receptor and enable G protein coupling. It is therefore the conformation of the heptahelical domain which determines

whether the receptor resides in an active or inactive state (Rosenbaum et al., 2009). In Smo, the heptahelical domain is clearly defined and functionally relevant (Alcedo et al., 1996; van den Heuvel and Ingham, 1996). Although the natural ligand of Smo is still unknown, several chemicals acting as agonist and antagonists of vertebrate Smo were identified and shown to bind within this region (Mas and Ruiz i Altaba, 2010). In addition, several forms of constitutively active vertebrate Smo, isolated from basal cell carcinomas, show point mutations within the heptahelical domain (Lam et al., 1999; Reifenberger et al., 1998; Xie et al., 1998). Furthermore, point mutations of highly conserved residues in the third intracellular loop decreased the activity of *Drosophila* Smo (Nakano et al., 2004). Since the third loop is critically involved in G protein binding, this result might suggest that Smo directly engages with G proteins. Experimental evidence also supports one-to-one coupling of Smo to $G_{\alpha i}$. Transgenic expression of human Smo in *Xenopus* melanophores results in pigment aggregation, a process that can serve as bioassay for functional $G_{\alpha i}$ signaling in these cells (DeCamp et al., 2000). In *Drosophila* S2 cells, Hh stimulation lowered cAMP levels in a Smo- and $G_{\alpha i}$-dependent manner (Ogden et al., 2008). Direct coupling of mouse Smo exclusively to members of the $G_{\alpha i}$ family of G proteins was shown in several tissue culture systems, when both receptor and G protein were overexpressed (Riobo et al., 2006). A follow up study by the same group revealed that the efficacy of Smo towards $G_{\alpha i}$ is similar to that measured for 5-hydroxytryptamine1A (5-HT1A) receptor, a well defined $G_{\alpha i}$-coupled receptor. Stimulation of endogenously expressed Smo decreases cellular cAMP levels to about the same extent as stimulation of the 5-HT1A receptor does, suggesting that Smo-$G_{\alpha i}$ coupling is a physiologically relevant process (Shen et al., 2013).

Taken together, mounting evidence supports the notion that Smo is a functional GPCR that directly couples to and signals through $G_{\alpha i}$, resulting in a decrease of cellular cAMP levels. Furthermore, some other aspects of Smo behavior are also reminiscent of typical GPCRs. Like other GPCRs, Smo forms homodimers and dimerization of the cytoplasmic C-terminal domain of Smo is required for Smo signaling (Zhao et al., 2007). In addition, work by myself and others demonstrates that Smo is phosphorylated by GRKs and that Smo is regulated in part by homologous desensitization (Chen et al., 2010; Cheng et al., 2010). The biology of GRKs and of

homologous desensitization is introduced in section 1.5.2. and a common thread throughout my thesis.

1.4.3. The role of heterotrimeric G protein signaling in the Hh pathway.

If Smo is a functional GPCR, and possibly couples through $G_{\alpha i}$, what could be the role and mechanism of heterotrimeric G protein signaling in the Hh pathway? So far, this role is not well defined and highly controversial. I will summarize the current understanding and highlight some of the unresolved issues.

Smo-$G_{\alpha i}$ signaling plays a permissive role in the Hh pathway. Work in several systems supports the view that coupling of $G_{\alpha i}$ to Smo has a positive impact on Hh signaling. For instance, selective inhibition of $G_{\alpha i}$ signaling by overexpression of pertussis toxin (PTX) in zebrafish embryos causes mild Hh loss-of-function phenotypes (Hammerschmidt and McMahon, 1998). Similarly, $G_{\alpha i}$ is required for the the proliferation of cerebellar granular neural precursors (CGNPs), which is a Shh-dependent process in the mammalian cerebellum (Barzi et al., 2011). Furthermore, in *Drosophila*, $G_{\alpha i}$ is required for expression of low threshold Hh target genes such as *dpp* in the wing disc (Ogden et al., 2008). The proposed mechanism behind the positive role of $G_{\alpha i}$ in the Hh pathway states that Smo-$G_{\alpha i}$ signaling lowers cellular cAMP levels by decreasing PKA activity. PKA promotes proteasome-dependent Ci/Gli processing into a transcriptional repressor and therefore inhibits Hh target gene expression. Consequently, $G_{\alpha i}$ promotes Hh target gene expression by preventing PKA-dependent Ci/Gli processing. The already discussed Smo- and $G_{\alpha i}$-dependent drop in cellular cAMP concentrations fits nicely in this model (Ogden et al., 2008; Shen et al., 2013). Furthermore, in mouse embryonic fibroblasts, $G_{\alpha i}$ activity was essential for Gli activation (Riobo et al., 2006).

Although this model is consistent with the presented phenotypes, how $G_{\alpha i}$ signaling in flies selectively promotes Hh target gene expression via stabilization of full-length Ci without grossly affecting Smo needs to be further investigated. In vertebrates, the situation appears less complicated. PKA does not phosphorylate vertebrate Smo, therefore $G_{\alpha i}$ signaling should not affect Smo activity. Nevertheless, some studies have postulated a positive of role of PKA in

vertebrate Hh signaling (Milenkovic et al., 2009; Tiecke et al., 2007). The conundrum of how the dual roles of PKA are orchestrated might be present in the vertebrate system as well.

Smo-G protein signaling might affect some aspects of Hh signaling but it is not at the core of the Hh pathway. What is the relationship between Smo-G protein signaling and the canonical Hh machinery? First, Smo-G protein signaling might influence Hh signaling but it is most likely not part of the core Hh pathway. The fact that $G_{\alpha i}$ activation is not sufficient to overcome the requirement for Smo itself favors this view. Smo must have additional functions, required for propagation of the Hh signal. These functions depend on the Smo C-terminus, because its deletion abrogates Hh target gene expression but does not affect $G_{\alpha i}$ coupling. The fact that $G_{\alpha i}$ coupling and transcriptional pathway responses can be functionally uncoupled leads to the speculation that they represent two distinct Smo signaling modes (Riobo et al., 2006). On one hand, Smo-G protein signaling might control PKA-dependent Ci/Gli processing, but on the other hand, the Smo C-terminus undergoes conformational changes and affects Ci/Gli through the HSC. Further studies are needed to dissect the precise interplay of the two potential signaling modes.

Second, G protein signaling might only be required in some but not all tissues patterned by Hh. In addition, G protein signaling might affect only specific subsets of Hh target genes. These hypotheses might explain some of the contradictory results published in the literature. For instance, a large scale RNAi screen in a *Drosophila* cell culture model, aimed at discovering novel components of the Hh pathway, failed to identify any member of the heterotrimeric G protein family (Lum et al., 2003a). Furthermore, several studies reported that perturbations of G protein signaling *in vivo* have no effect on the Hh patterning. For instance, patterning of the chick neural tube, a well studied Hh-dependent process, was not affected by overexpression of $G_{\alpha i}$ (Low et al., 2008). Work in our lab demonstrated that overexpression of constitutive active forms of $G_{\alpha i}$ and $G_{\alpha s}$ did not grossly alter Hh target gene expression in the *Drosophila* wing disc (Cheng et al., 2012). This seems at odds with work by Ogden and colleagues, which demonstrated that $G_{\alpha i}$ is required for Hh target gene expression (Ogden et al., 2008). However, the authors focussed on *dpp* expression, a low threshold Hh target gene, whereas we examined exclusively medium to high threshold responses.

In summary, a positive role for Smo-dependent $G_{\alpha i}$ signaling has been described in several systems. However, in contrast to canonical pathway components, G protein signaling seems to modulate the Hh pathway rather than drive it. Furthermore, it might only be required in a tissue-specific manner and/or affect some specific Hh responses. Further experiments are needed to clarify these issues.

Global G protein signaling might influence the Hh pathway outcome as an example of signaling cross-talk. As established above, Smo-$G_{\alpha i}$ signaling modulates Hh pathway outcome most likely via changes in cellular cAMP concentrations, which affect PKA activity. This model implies that there could be signaling cross-talk, because the second messenger cAMP is regulated by a variety of signaling events. In particular, GPCRs coupling to either $G_{\alpha i}$ or $G_{\alpha s}$ can lead to substantial fluctuations of cAMP levels, possibly influencing Hh target gene expression (Neves et al., 2002). A recent publication which focussed on mammalian Hh signaling in the neural tube confirmed this model by identifying an active $G_{\alpha s}$-coupled GPCR, GRP161, in the cilium. GRP161 localizes to the cilium alongside Ptc in the absence of Hh. It restricts Hh signaling by locally increasing cAMP levels leading to PKA activation and Gli phosphorylation/ processing. In the presence of Hh, Ptc and GRP161 are cleared away from the cilium (Mukhopadhyay et al., 2013). The biology of GRP161 is far from understood and the mechanisms regarding its activation and localization are unknown. However, GRP161 illustrates that cAMP levels are regulated by proteins outside the core Hh pathway and that this profoundly impacts Hh signaling.

1.4.4. Non-canonical Smo and Hh signaling.

Most Hh studies focus on the patterning of model tissues such as the *Drosophila* wing disc or the mammalian neural tube. However, Hh and Smo signaling are implicated in many other processes and not all of these follow the paths outlined above. For instance, neurite outgrowth in mammalian tissue culture cells and patterning of the rat neural tube seems to depend on $G_{\alpha 12}$ signaling through RhoA, a small GTPase (Kasai et al., 2004). Furthermore, some responses triggered by Hh and Smo are independent of the Hh transcription factor. Shh-induced fibroblast migration is such an example. Here too, the small GTPases RhoA and Rac1 are implicated

(Polizio et al., 2011). Another example is the directed outgrowth of spinal commissural axons towards the ventral midline in the neural tube. Shh acts as a chemoattractant and the axon growth cones follow a Shh gradient. This process does not involve most of the canonical Hh pathway but leads to Smo-dependent activation of Src kinases (Yam et al., 2009).

In conclusion, Hh and Smo also use non-canonical routes to trigger additional signaling responses in various tissues and cell-types. Smo in particular might be a signaling molecule with many faces. These newly emerging Smo roles need further investigation and it should be noted that not every Smo response necessarily leads to changes in Hh target gene expression.

1.5. G protein-coupled receptor kinases.

GRKs are a subgroup of Ser/Thr kinases capable of phosphorylating GPCRs selectively in their active agonist-occupied state. This function was discovered even before the recognition of GPCRs as a family of signaling receptors and goes back to work on rhodopsin isolated from bovine retinas (Kuhn and Dreyer, 1972). Rhodopsin is the protein responsible for light detection in photoreceptor cells and later became a founding member of the GPCR superfamily (Dixon et al., 1986; Hargrave et al., 1983). Stimulation by light activates rhodopsin and triggers the phosphorylation of the receptor by opsin kinase (Weller et al., 1975). Opsin kinase was later renamed GRK1 and became the archetypical member of the GRK family (Lorenz et al., 1991).

1.5.1 GRK subgroups and structural organization.

In humans, there are seven GRKs encoded in the genome which can be subdivided into three groups based on sequence similarity. GRK1 and 7 are also known as visual GRKs because the expression of these kinases is, with few known exceptions, exclusively limited to photoreceptor cells. The GRK2 group consists of two members, GRK2 and 3, which are ubiquitously expressed throughout the body. GRK4, 5 and 6 constitute the GRK5 group. GRK4 is particularly highly expressed in the testis but was also found less abundantly in some other tissues such as the brain and kidney. Expression of GRK5 and 6 is ubiquitous and, like GRK2 and 3, starts as early as embryonic day 14 of development. Alternative splicing has only been described for GRK4 and 6, with four and three splice variants, respectively, adding up to a total count of 12 GRK variants in

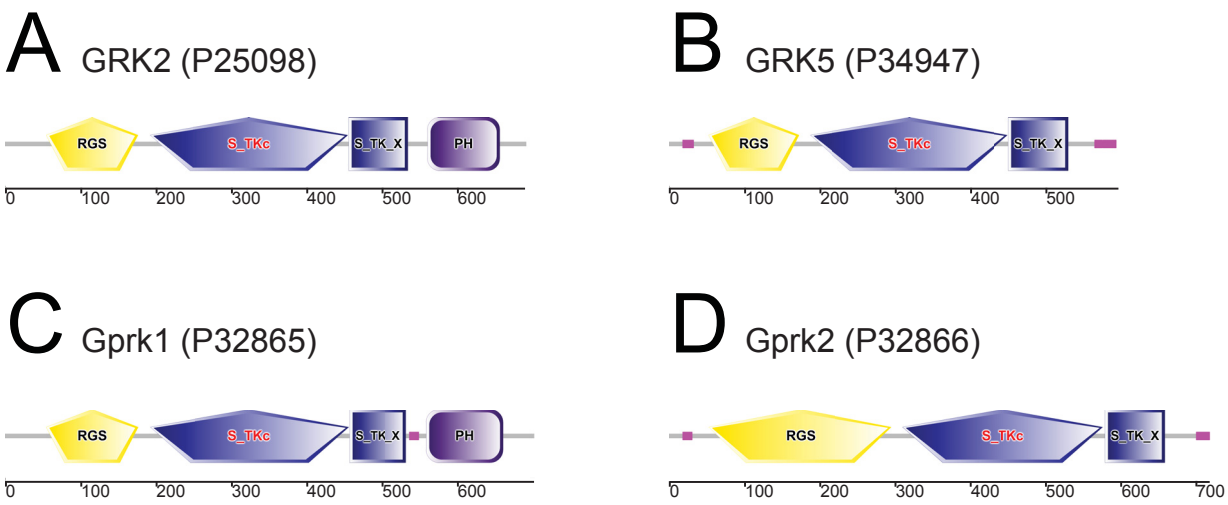

Figure 1.6. Domain organization of human and *Drosophila* GRKs

(A-D) Schematics of selected GRKs. Annotated are the RGS domain (yellow), the kinase domain (blue) and the PH domain (purple) if applicable. The domain arrangement of *Drosophila* Gprk1 **(C)** resembles that of human GRK2 **(A)**. Gprk2 found in *Drosophila* **(D)** shows homology to human GRK5 **(B)**. **Note:** Gprk2 encodes an unusually long RGS domain. Schematics were generated by a protein domain prediction software (http://smart.embl-heidelberg.de).

humans (Gurevich et al., 2012). This rather small number of GRKs stands in contrast to about 800 GPCRs present in the human genome (Bjarnadottir et al., 2006). The receptors outnumber the kinases by which they are regulated by about two orders of magnitude. This poses interesting questions when it comes to substrate specificity of GRKs.

All GRKs posess a highly conserved centrally located kinase domain which shows homology to those found in the AGC (protein kinase A, -G, -C) family of Ser/Thr kinases (Figure 1.6A, B) (Pearce et al., 2010). N-terminal to the kinase domaine is situated a regulator of G protein signaling (RGS) homology domain (RH; (Figure 1.6A, B). Differences between GRK isoforms are found at the N and C-termini. Roughly the first 25 amino acids at the N-terminus are specific to each GRK subgroup. The C-terminus varies largely between different GRK isoforms and mediates membrane targeting, which differs between GRK isoforms. For instance, GRK2 and 3 possess a Pleckstrin homology (PH) domain, which interacts with phospholipids and the β/γ subunits of heterotrimeric G proteins (Figure 1.6A). The G_{β} and G_{γ} proteins are only accessible as a result of active GPCR signaling, therefore, the membrane recruitment of GRK2/3 is coupled to GPCR signaling activity. Other GRKs are constitutively membrane associated due

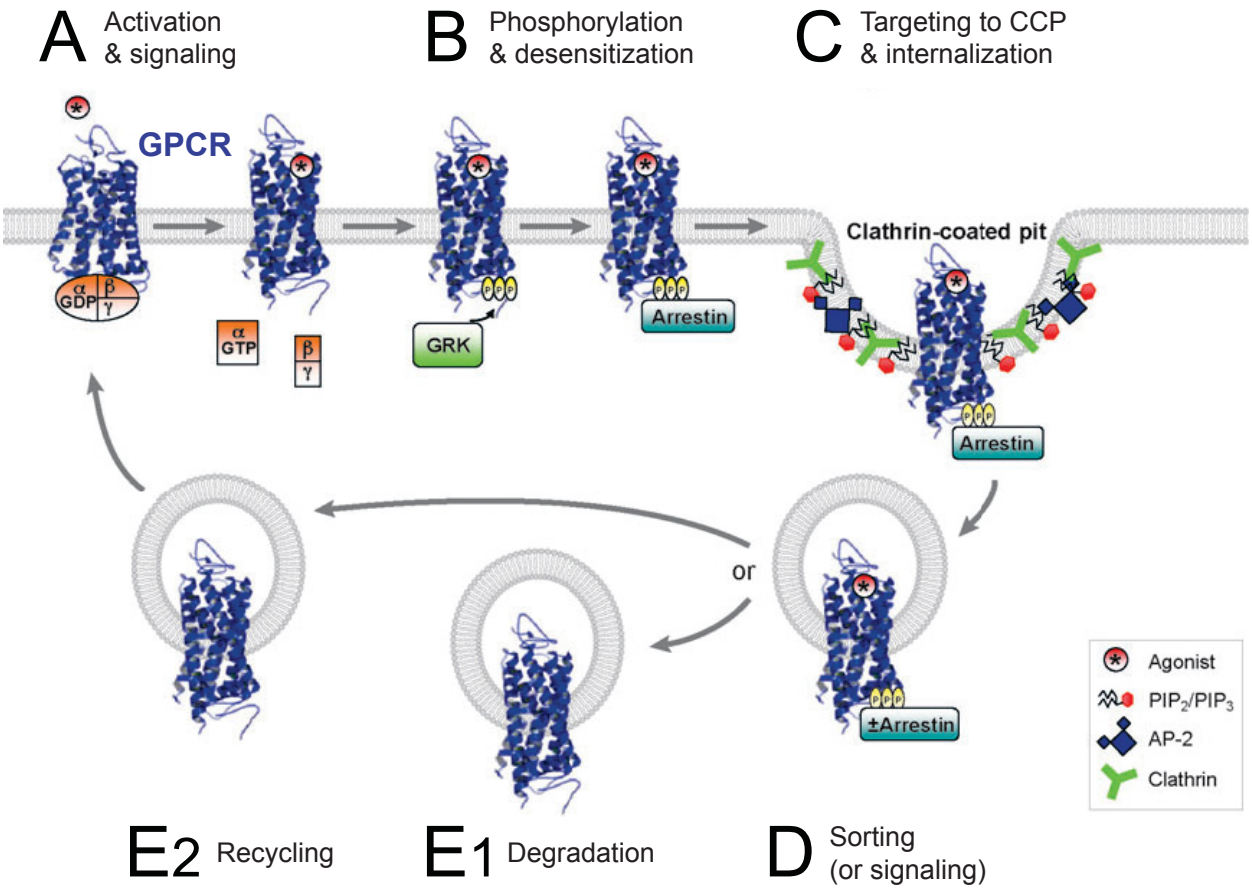

Figure 1.7. Homologous desensitization of GPCRs

(A) Agonist (*) binding to GPCRs leads to receptor activation, G protein coupling, and signal transduction. **(B)** GRKs phosphorylate the agonist-activated GPCR, initiating arrestin recruitment. Arrestin binding to the receptor inhibits G protein coupling and terminates signaling. **(C)** Receptor/arrestin complexes are then targeted to clathrin-coated pits (CCP), where arrestin forms a multicomponent complex with clathrin, adapter protein-2 (AP-2), and phosphoinositides, resulting in receptor internalization. Internalized GPCRs are sorted **(D)** to either degradation **(E1)** or recycling **(E2)** compartments. Figure copied with permission (Moore et al., 2007).

to post-translational modifications such as prenylation (GRK1/7) or palmitoylation (GRK4/6). In addition, GRK5 and 6 are capable of direct lipid binding through an amphipathic helix in their respective C-termini (Pitcher et al., 1998a).

1.5.2. Canonical function of GRKs: GPCR desensitization.

The canonical function of GRKs is the selective phosphorylation of prototypical GPCRs in their active, agonist-occupied state (Figure 1.7). GRK phosphorylation plays an integral part in the negative regulation of GPCR signaling and is therefore a relevant factor controlling the

appropriate strength and duration of GPCR signaling (Figure 1.7A). Phosphorylation of active GPCRs generates high affinity binding sites for β-arrestins, a family of scaffolding proteins. β-arrestin recruitment to the active receptors serves three purposes. First, it terminates G protein signaling by shielding the G protein binding site within the GPCR and preventing G_α activation (Figure 1.7B). Second, β-arrestins can act as scaffolds for signaling complexes and β-arrestin recruitment to active GPCRs can trigger G protein-independent signaling by these GPCRs. Third, β-arrestin binding initiates clathrin-dependent receptor endocytosis because β-arrestins recruit the adaptor protein 2 (AP2) complex to GPCRs (Figure 1.7C, D). Receptor endocytosis can lead to degradation via the lysosomal pathway (Figure 1.7E_1) or to recycling of the GPCR through the sorting endosome (Figure 1.7E_2) (Gurevich et al., 2012).

To summarize, GRK phosphorylate active GPCRs and terminate G protein signaling by initiating β-arrestin binding. β-arrestin enables the switch of some GPCRs to G protein-independent signaling and also triggers receptor turnover via endocytosis. Thus, together with β-arrestins, GRKs are key regulators of GPCR desensitization and profoundly impact GPCR signaling (discussed in section 1.4.1). Interestingly, similar to GRKs, there are only a very limited number of arrestin genes. Humans have only four arresins; expression of two is restricted to the visual system and the two others (β-arrestin1 and 2) are ubiquitously expressed (Premont and Gainetdinov, 2007).

1.5.3. Mechanisms of GRK function.

How can a group of just seven GRKs play such a central role in the regulation of about 800 potential GPCRs? Based on the numbers alone, each GRK must control multiple GPCRs. But what are the underlying mechanisms determining substrate specificity and kinase activity? This is a large field of extensive studies. In the following section, I will introduce the concepts explaining this conundrum and highlight a few examples of GPCR-GRK regulation.

GRKs interact with GPCRs via a conserved binding pocket. GRKs are capable of recognizing the active, ligand-occupied state of a GPCR. The precise details of the GPCR-GRK interaction have been mapped out by structural biologists. The number of GRK structures in complex with a GPCR is limited; nevertheless some characteristics of the interaction are defined.

It is thought that GPCRs share a common structural feature recognized by GRKs. Agonist binding leads to conformational changes within the GPCRs and exposes a GRK binding pocket with conserved physical properties. This explains why GRK phosphorylation does not seem to follow a consensus sequence. The size and surface charge of the binding pocket within the GPCR are conserved, not a specific motif in the primary sequence. Not surprisingly, the counterpart to the GPCR binding pocket in the GRK sequence falls into the highly conserved region of all seven GRKs, ensuring that all GRKs are capable of recognizing GPCR substrates. Furthermore, the interaction of GRKs with GPCRs via the binding pocket activates their catalytic activity by stabilizing the active conformation of the kinase domain. This ensures that GRKs are only activated in response to GPCR engagement (Gurevich et al., 2012).

One GRK regulates multiple GPCRs and conversely, a single GPCR can be phosphorylated by multiple GRKs. The model of the shared binding pocket present in GPCRs solves the problem of how a small number of GRK can regulate so many different GPCRs. However, this model implies that a single GPCR might be phosphorylated by several GRK isoforms (Gurevich et al., 2012). This has been known for a long time thanks to *in vitro* studies. For instance, Rhodopsin can be phosphorylated by all seven GRK isoforms (Benovic and Gomez, 1993; Benovic et al., 1986; Kunapuli et al., 1994). However, *in vitro* results are not necessarily matched *in vivo*, illustrated by the fact that Rhodopsin *in vivo* is solely controlled by GRK1 (Chen et al., 1999b). *In vitro* and *in vivo* data can even contradict each other. For example, in kinase assays, the muscarinic M3 receptor appears to be phosphorylated by GRK2 and 3 and not by GRK5 or 6 (Debburman et al., 1995). However, in tissue culture cells, GRK6 was demonstrated to regulate some aspects of muscarinic M3 receptor signaling (Luo et al., 2008). To further complicate the matter, multiple GRKs can phosphorylate the same GPCR at different sites, and this can bias the receptor into different signaling responses (Liggett, 2011). The phenomenon was dubbed GPCR phosphorylation barcoding and was described for the β_2-adrenergic receptor. This GPCR is phosphorylated at distinct set of Ser/Thr residues by GRK2 and GRK6 resulting in two different signaling outputs. Both kinases desensitize G_s-coupling but the β_2-adrenergic receptor also signals through the MAP kinase pathway via β-arrestin recruitment. For the latter signaling only GRK6 is required (Nobles et al., 2011).

In conclusion, the relationship between GPCRs and GRKs is complex *in vivo*. It is clear that each GRK isoform must be capable of phosphorylating multiple GPCR substrates. However, some GPCRs (e.g. Rhodopsin) are exclusively phosphorylated by a single GRK; others by several GRKs (e.g. muscarinic M3- and β_2-adrenergic receptors), indicating that GRKs are functionally redundant to a certain extent. The specific kinase-substrate relationship needs to be evaluated for each GPCR-GRK pair *in vivo*. It should also be pointed out that tissue-specific expression and spatial distribution of GRKs are also factors determining substrate specificity *in vivo*.

1.5.4. Non-canonical roles of GRKs.

In addition to the role of GRKs in GPCR signaling, a growing list of non-canonical GRK function has come into focus. There are several types of non-canonical signaling. Some rely on GRK phosphorylation of non-GPCR substrates, others are kinase-independent and are mediated by protein-protein interactions (Gurevich et al., 2012).

Non-GPCR substrates of GRKs include proteins located in various cellular compartments (Gurevich et al., 2012). For instance, GRK2 and 5 phosphorylate the receptor tyrosine kinase PDGFRβ located at the plasma membrane (Freedman et al., 2002). Membrane-receptor associated proteins are also known targets of GRK phosphorylation, for instance β-arrestin (Barthet et al., 2009). The fact that these types of proteins are non-GPCR substrates is not too surprising, because GRKs are typically active within this compartment of the cell. But GRK phosphorylation was also described for cytoskeletal proteins such as tubulin (Pitcher et al., 1998b) or members of the ERM family (Cant and Pitcher, 2005), which are cross-linkers between the cytoskeleton and the membrane. Even some nuclear proteins, such as transcription factors and histone deacetylases are GRK phosphorylated (Martini et al., 2008; Parameswaran et al., 2006). This highly diverse selection of non-GPCR substrates raises the question about the mechanism and specificity of these phosphorylation events. One possibility is so called high gain phosphorylation. Highly active GPCRs lead to strong activation of GRK kinases, which in turn phosphorylate not only GPCRs but also other substrates in close proximity. This type of GRK activity is less specific and probably a byproduct GRK activation through GPCRs. Another

possible explanation for non-GPCR substrate phosphorylation postulates that some of these substrates are activating the catalytic activity of GRK activity in a way similar to GPCR binding. This might be the more plausible model for substrates distant from the plasma membrane, such as nuclear proteins (Gurevich et al., 2012). Interestingly, GRK5 has a functional nuclear localization sequence (Johnson et al., 2004), suggesting that the functions of GRKs reach far beyond GPCR phosphorylation.

Catalytic activity-independent functions of GRKs are also well described. The RH domain present in each GRK mediates one such function. The RH domain is structurally similar to RGS proteins. RGS proteins are negative regulators of heterotrimeric G proteins, acting as GAPs for G_α-proteins to terminate G_α signaling (Hollinger and Hepler, 2002). However, the RH domains present in GRKs have little to no GAP activity. Nevertheless, the RH domains of GRK2 and 3 are functionally relevant, because they bind and sequester active $G_{\alpha q}$ subunits, specifically influencing signaling responses driven by that particular G protein isoform (Carman et al., 1999).

GRKs may potentially exert some of their functions solely through protein-protein interactions. GRK interacting proteins (GITs) were discovered as GRK binding partners but as not phosphorylation substrates (Premont et al., 1998). GITs are multi-domain scaffolding proteins and are involved in some aspects of cellular adhesion and cell migration. However, the connection between GRKs and GITs is not well understood.

Taken together, non canonical GRK functions have multiple facets. These include phosphorylation of non-GPCR substrates, kinase-independent functions, and recruitment of other proteins via protein-protein interactions.

1.5.5. Physiological roles of GRKs and loss-of-function phenotypes.

GRK knockout animals have been generated in order to study the physiological functions of GRKs. Although GRKs play such a crucial role in GPCR signaling, most of these mutants display surprisingly mild defects, possibly due to functional redundancies between GRKs. The only exception is the GRK2 knockout, which is embryonic lethal due to abnormal formation of the heart (Jaber et al., 1996). However, this malformation seems not to be the result of specific defects in the heart. GRK2 ablation in cardiac myocytes does not replicate the phenotype of the

whole animal knockout (Matkovich et al., 2006). The molecular mechanism of the GRK2 phenotype is not yet defined, but is currently attributed to a general role of GRK2 in development. GRK2 mutant embryos also displayed some Hh loss-of-function phenotypes (Chen et al., 2011; Philipp et al., 2008). This newly identified participation of GRKs in Hh signaling is discussed in further detail in section 1.5.6.

Further examination of GRK mutants revealed some distinctive phenotypes. For instance, GRK3 knockout mice lack any olfactory activity, possibly because GRK3 is the only GRK present at significant levels in the olfactory epithelium (Peppel et al., 1997). The situation is similar in rod photoreceptors, which express exclusively GRK1 (Weiss et al., 2001). In these cells, the rhodopsin response to light is terminated by GRK1 phosphorylation. Knockout of GRK1 or deletion of GRK1 phosphorylation sites in rhodopsin caused a prolonged signaling response (Chen et al., 1999b; Chen et al., 1995). Furthermore, extended exposure to dim light triggered rod photoreceptor degradation and apoptosis, suggesting that abnormal signaling is harmful to these cells (Chen et al., 1999b). Some phenotypes of germline knockouts present themselves only under specific circumstances. For instance, loss of GRK5 renders mice supersensitive to muscarinic, but not dopaminergic, stimulation (Gainetdinov et al., 1999).

Our understanding of how loss of GRK function affects GPCR signaling stems mostly from studies in human or murine tissue culture systems, which are more accessible for biochemical manipulations and assays. In these systems, loss of GRK function can lead to prolonged and exaggerated GPCR responses. For instance, loss of GRK2 results in elevated cAMP levels in response V2 Vasopression stimulation (Ren et al., 2005). Similarly, activation of the Angiotensin II Type1A receptor causes an inappropriate peak of the lipid derived second messenger DAG in GRK2 depleted cells (Violin et al., 2006). These dramatic signaling defects caused by depletion of a single GRK in cell culture systems are not necessarily reflected at the level of the whole animal. The discrepancies between tissue culture data and *in vivo* phenotypes observed in GRK knockout models suggest a high level of functional redundancy *in vivo*.

In summary, most GRK mutants display only minor phenotypic abnormalities, most likely due to functional redundancy of GRKs. Nevertheless, most GRK mutants are characterized by specific defects which present themselves in response to specific stimuli. Consistent with the

negative role of GRKs in GPCR-dependent heterotrimeric G protein signaling, depletion of GRKs in cell culture leads to excessive G protein responses.

1.5.6. GRKs participate in vertebrate Hh signaling.

A connection between Hh signaling and GRKs was initially established in vertebrates. Depletion of zGRK2/3 in zebrafish causes several defects associated with mild Hh loss-of-function defects (Philipp et al., 2008). The same is true for GRK2 knockout mouse embryos, which display defects in limb development and neural tube patterning (Chen et al., 2011; Philipp et al., 2008). The phenotypes in both model organisms suggest that GRK2 is required for Hh signaling.

Smo belongs to the GPCR family and therefore, the most straight forward model postulates that GRK2 influences the Hh pathway by regulating Smo. If GRK2 treats Smo in an analogous fashion to any other GPCR, one would expect that GRK2 phosphorylates Smo and triggers β-arrestin-dependent Smo internalization. This has been confirmed in mammalian tissue culture systems. GRK2 phosphorylates Smo which leads to β-arrestin recruitment (Chen et al., 2004), and these two events are required for the expression of Hh-responsive reporter genes (Meloni et al., 2006). The positive role of β-arrestin in the Hh pathway was confirmed *in vivo*. Zebrafish morphants depleted for β-arrestin2 show similar Hh defects as zGRK2/3 morphants (Wilbanks et al., 2004).

The mechanism behind the positive role of GRK2 and β-arrestins in vertebrate Hh signaling has been uncovered in recent years and has two aspects. First, Smo phosphorylation by GRK2 and Ck1α is required for Smo activation (Chen et al., 2011). Second, GRK2 phosphorylation leads to β-arrestin binding (Chen et al., 2004; Meloni et al., 2006), internalization and trafficking of Smo into the cilium (Chen et al., 2011) via the kinesin motor protein Kif3a (Kovacs et al., 2008). These two aspects also highlight important differences between the Hh pathways in mammals and in *Drosophila*. Fly cells lack the cilium and the key kinases responsible for Smo activation are PKA and Ck1. This suggests that if a fly GRK participates in the Hh pathway, the mechanism behind it is most likely not conserved.

1.5.7. GRKs in *Drosophila* and their role in Hh signaling.

The *Drosophila* genome encodes two GRKs, Gprk1 and Gprk2 (Figure 1.6C, D). Gprk1 is structurally related to the vertebrate GRK2 subgroup, evident by the presence of a PH domain (Figure 1.6A, C). Gprk2 shares homology with the kinases of the mammalian GRK5 group (Figure 1.6B, D) (Cassill et al., 1991). Similar to the situation in vertebrates, the approximately 100 fly GPCRs (Brody and Cravchik, 2000) far outnumber the two GRKs. However, GRK function is not extensively studied in *Drosophila*. Gprk1 was identified as a visual GRK promoting rhodopsin phosphorylation (Lee et al., 2004) but not much is known otherwise. Gprk2 is slightly better represented in the literature; it has been mainly analyzed in the context of circadian rhythm (Chatterjee et al., 2010; Tanoue et al., 2008), egg development (Lannutti and Schneider, 2001; Schneider and Spradling, 1997) and synuclein phosphorylation (Chen and Feany, 2005). Synuclein is a non-GPCR substrate of GRKs, linked to Parkinson's disease in humans. Analogous to vertebrates, one of the two GRKs in flies − Gprk2 − participates in the Hh pathway (Chen et al., 2010; Cheng et al., 2012; Cheng et al., 2010; Maier et al., 2014; Molnar et al., 2007) and this has attracted some intense research by our lab and other research teams around the globe. I will introduce some results of these studies in the following sections as background information to my work. My contribution to the current understanding of the multiple roles Gprk2 plays in the *Drosophila* Hh pathway are presented in the result section of this thesis.

1.5.7.1. *gprk2* mutants display a Hh loss-of-function defect.

To study the physiological function of Gprk2 several tools have been used: knockdown via RNA interference (RNAi) (Molnar et al., 2007), mutant alleles (Chen et al., 2010; Schneider and Spradling, 1997), and defined chromosomal deletions and transgenic knockouts (Cheng et al., 2010). *gprk2* knockdown animals or mutants develop normally and show no obvious phenotypes when cultured at the usual temperature of 25^{o}C (Cheng et al., 2010). However, some defects occur during egg morphogenesis and mutant females are sterile due to a role of Gprk2 in ovaries (Schneider and Spradling, 1997). The most striking *gprk2* loss-of-function phenotype presents itself when knockdown or mutant animals are raised at elevated temperatures such as 29^{o}C (Cheng et al., 2010; Molnar et al., 2007). In these conditions the adult wings show a reduction of

the L3-L4 area, reminiscent of a mild Hh defect (see Figure 1.1C). This was confirmed in developing wing discs, which display either loss or strong reduction of high threshold Hh target genes expression (Chen et al., 2010; Cheng et al., 2010; Molnar et al., 2007).

1.5.7.2. Role of Gprk2 in the Hh pathway.

The mutant phenotypes suggest that *gprk2* is required for Hh target gene expression. This seems reminiscent of the situation in vertebrates. In that system, GRK2 affects Smo in two ways. First, phosphorylation of Smo by GRK2 and Ck1α activates Smo and promotes dimerization of Smo C-terminal tails. Second, GRK2 phosphorylation is required for arrestin-dependent Smo internalization and translocation of Smo into the cilium.

Role of Gprk2 and β-arrestin in Smo trafficking. Loss of Gprk2 causes Smo accumulation at the plasma membrane in a hypo-phosphorylated state, whereas overexpression of Gprk2 causes downregulation of Smo proteins levels in wing discs (Cheng et al., 2010). This implies that Gprk2 phosphorylates active Smo, leading to Smo internalization and degradation. This model is consistent with the prototypical GPCR-GRK relationship and implies the involvement of arrestins in this process. However, the data on arrestins only partially fits with this hypothesis. Overexpression of the only typical β-arrestin in flies (Kurtz, Krz) leads to downregulation of Smo and also causes a loss-of-function Hh phenotype. The Smo-Krz-interaction can be visualized in tissue culture cells. Although the overexpression studies indicate a negative role of Krz in Smo regulation, Krz loss-of-function experiments fail to produce any Smo or Hh phenotype (Molnar et al., 2011). This could suggest that under physiological conditions Krz plays only a minor role in Smo regulation. Alternatively, other fly arrestins could functionally compensate for the loss of Krz. The *Drosophila* genome encodes two visual arrestins (Arr1 and Arr2) as well as one non-typical arrestin (CG32683) (Molnar et al., 2011) and further studies are needed to rule out functional redundancy. In addition, as discussed in section 1.2.3.1, Smo turnover is also regulated by ubiquitination and proteasome-dependent degradation. It has been proposed that the arrestin and ubiquitination pathway act in parallel and with overlapping functions (Li et al., 2012). In conclusion, arrestin-dependent internalization might play a role in *Drosophila* Smo degradation. However, this role is minor; most likely because turnover of Smo

is also controlled by ubiquitantion and the proteasome. Therefore, the role of arrestins in flies differs compared to the vertebrate system.

Role of Gprk2-dependent Smo phosphorylation and summary of my results. As described earlier, Smo activation in flies is thought to be mediated by PKA and Ck1 phosphorylation within the SAID. Gprk2 could have an auxiliary function in this process that is required for maximal Smo activation. This would explain why loss of Gprk2 only affects high threshold Hh target genes. To test this model, the phosphorylation sites need to be mapped and functionally characterized. This is the core of my PhD thesis. However, during my PhD studies, a competing group published Gprk2 phosphorylation sites (GPS) within Smo (Chen et al., 2010). They concluded that Gprk2 indeed stabilizes the active conformation of Smo by phosphorylating Ser/Thr residues in the SAID. In addition, the authors claimed that Gprk2 has a kinase-independent function by scaffolding and stabilizing dimers or oligomers of Smo C-termini (Chen et al., 2010). At the time of this publication, our preliminary results indicated that the group might have missed some Gprk2 phosphorylation sites. I continued my mapping studies and also re-evaluated the published sites.

In the first chapter of my results (Chapter 3), I locate Gprk2-dependent Smo phosphorylation to four Ser/Thr clusters in the membrane-proximal Smo C-terminus. These sites do not overlap with the the published GPS sites and in fact, our analysis suggest that the GPS sites are not primarily regulated by Gprk2. Phosphorylation within the four clusters enhances Smo activity and increases dimerization of the C-terminal tails. However, blocking Gprk2 phosphorylation by mutating the Ser/Thr residues to Ala resulted in a modest decrease of Smo activity *in vivo* and failed to replicate the full spectrum of the *gprk2* mutant phenotype.

The fourth chapter of my thesis establishes that Gprk2 influences the Hh pathway in an additional and indirect way by controlling cellular cAMP levels and PKA-dependent Smo activation. We demonstrate that loss of Gprk2 decreases cellular cAMP concentrations and that the *gprk2* mutant phenotype can be rescued by genetically increasing cAMP levels or mimicking full PKA phosphorylation of Smo. We conclude that Gprk2 is not an essential component of the *Drosophila* Hh pathway. However, Gprk2 influences Smo activity in two ways: by direct phosphorylation and indirectly by keeping PKA activity at a permissive level for Hh signaling.

In the last chapter of my results (Chapter 5), we hypothesize that regulation of Smo by GRKs represents an evolutionarily ancient mechanism of controlling Smo activity. Three of the four Gprk2 phosphorylation clusters in fly Smo overlap with regulatory sites in the mouse protein and are highly conserved among the bilaterian linages. GRKs seem to serve a common function in Smo regulation, because most GRK phosphorylation sites fall into the conserved core of Smo. We find that a C-terminally truncated *Drosophila* Smo mutant (Smo^{core}) consisting of the highly conserved core including most GRK phosphorylation sites, signals in a strictly Gprk2-dependent manner *in vivo*. Smo^{core} lacks all previously known regulatory elements of fly Smo but we identify a novel Gprk2-dependent binding site for Cos2. Through the identification and characterization of Smo^{core}, we speculate that the mechanisms behind Smo regulation throughout the bilaterian species are more similar then previously recognized.

1.6. Starting point of my PhD project.

I started my PhD in January 2009. At that time, the link between GRKs and Hh signaling was just emerging in the literature. The Hh related *gprk2* loss-of-function phenotype was already published but the study was based on RNAi-mediated *gprk2* knockdown (Molnar et al., 2007). Our lab had generated several *gprk2* null alleles and another PhD student, Shuofei Cheng, had already begun phenotypic analyses. I will introduce our *gprk2* mutant alleles and show the essential *gprk2* mutant phenotype at the beginning of the Results section (Chapter 3). Later, I will focus on my main research object, the phosphorylation of Smo by Gprk2.

Chapter 2: Material & Methods.

2.1. Fly strains.

Transgenic flies generated for the context of this thesis.

***gprk2^{del1}* and *gprk2^{del2}*.** These two deletions were generated using FRT-site-bearing transposable elements as described (Parks et al., 2004). These deletions remove sequences located between *pBac{RB}e01955* and *pBAC{WH}f06602* (*gprk2^{del1}*) or *pBac{WH}f00526* and *p{XP}d09952* (*gprk2^{del2}*). The presence of the deletions was verified by genomic PCR and Southern blotting (not shown). The *gprk2^{del1}* deletion removes four genes (*lox*, *CG11333*, *CG11334*, and *CG12063)* in addition to *gprk2*, and is homozygous viable at 25°C and semi-lethal at 29°C. The *gprk2^{del2}* allele is identical to *Df(3R)gprk2* (Molnar et al., 2007). This deletion likely disrupts the promoter of the neighboring *CG11337* gene, as it is homozygous lethal at 25°C, but viable in trans to other *gprk2* null alleles.

***gprk2^{KO}*.** The *gprk2^{KO}* allele were generated by "ends-out" homologous recombination (Gong and Golic, 2003). To generate targeting constructs, upstream and downstream homology arm fragments (3.4 and 4.0 kb, respectively) were PCR amplified and cloned into the pW25 vector. The resulting targeting constructs were transformed into flies. After the crosses to generate potential recombinants with the targeting constructs mapping to the correct chromosome, homologous recombination events were identified by genomic PCR across each arm of homology. Multiple independent targeting events were identified for each gene. The *gprk2^{KO}* allele is homozygous viable at 25°C and semi-lethal at 29°C.

UAS-Gprk2. The expression plasmid was constructed by cloning the 3058 nucleotide *Eco*RI/*Xho*I insert fragment from EST LD21923 into pUAST. This fragment contains the full-length *gprk2* coding sequence, plus 602 and 328 nucleotides of 5′ and 3′ untranslated sequences, respectively. Transgenic flies were generated by standard P-element-mediated transgenesis.

UAS-Smo transgenics. All *UAS-Smo* variant transgenic fly strains were generated by recombining the appropriate p*UAST-attB* transgenes into the 65B2 *attP* locus using the *PhiC31* system (Bischof et al., 2007).

UAS-smo$^{3'UTR}$-dsRNA. Flies carrying a chromosome 2 insertion of the *UAS-smo$^{3'UTR}$-dsRNA* transgene were generated by standard P-element-mediated transgenesis.

Other fly strains and their sources.

p{XP}d09952, *pBac{WH}f00526*, *pBac{RB}e01955*, and *pBAC{WH}f06602* were from the Exelixis Collection at Harvard Medical School (Thibault et al., 2004). *UAS-G$_{\alpha i}^{Q205L}$* transgenic animals were provided by J. Knoblich IMBA, Austria. The following stocks were obtained from the Bloomington *Drosophila* Stock Center: *ap-GAL4*, *nub-GAL4*, *dpp^{10638}* (*dpp-LacZ*), *UAS-Dicer*, *UAS-G$_{\alpha s}^{Q215L}$, tubP::GAL80^{ts}*, *w;hs-I-SceI,hs-FLP*.

2.2. DNA constructs.

Plasmids cloned during my PhD project.

The integrity of all newly generated constructs was verfied by diagnostic restriction digest, and sequencing.

Smo constructs. For expression of Smo mutants, we first flanked wt and Smo^{SD} (Jia et al., 2004) coding sequence with an *Eco*RI and a *Not*I site at the 5' and 3' end, respectively. Next, we silently mutated codons 458 and 459 of these coding sequences to introduce an *Eco*RV site. Restriction digest of wt or Smo^{SD} coding sequence released a

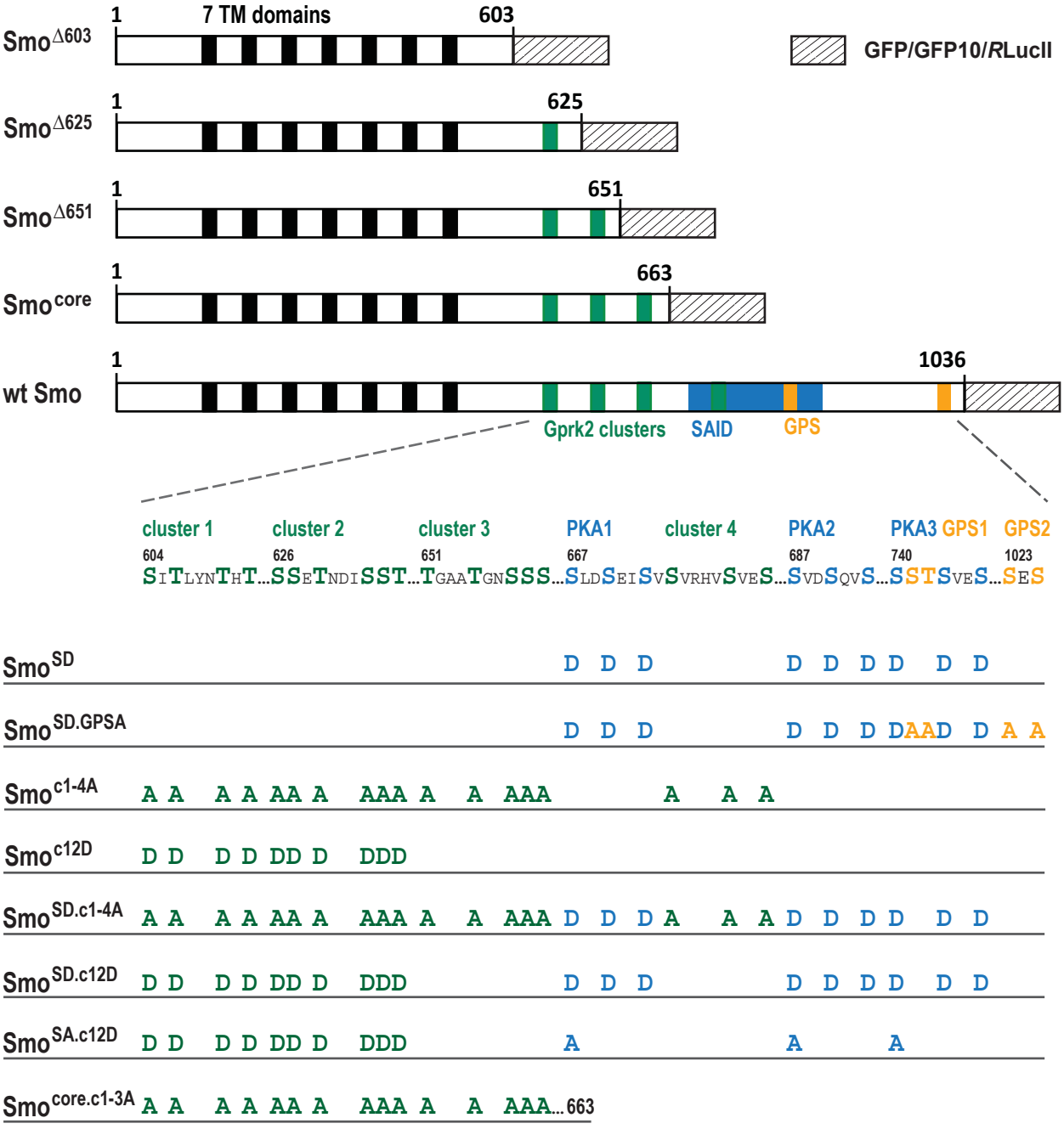

Figure 2.1. Overview of Smo constructs.

The seven transmembrane domains are indicated as black boxes. The four clusters of Ser/Thr residues phosphorylated by Gprk2 (three juxtamembrane, one in the SAID) are highlighted in green. The PKA/CkI phosphorylation sites in the SAID are highlighted blue and the two GPS clusters (Chen et al., 2010) are yellow. The shown Ser/Thr→Asp or Ser/Thr→Ala substitutions match in color and position to the mentioned phosphorylation sites. All constructs carry either a GFP, GFP10 or *R*LucII tag (hatched boxes).

1023 nt fragment between the new *Eco*RV and an internal *Eco*RI site. This stretch of DNA contains codons 458-798 and harbors all our Gprk2 and PKA phosphorylation sites was then subcloned into *pBluescript* (*pBS*). In addition, the C-terminal portion of Smo (728 nt DNA fragment corresponding to codons 797-1036) was cut out by digesting wt Smo with *Eco*RI and *Not*I and also subcloned in (*pBS*). The resulting constructs were used as templates for multiple rounds of PCR-based site-directed mutagenesis in order to mutate the four GPS sites (Chen et al., 2010) or our Gprk2 sites (Figure 2.1). The modified *Eco*RV-*Eco*RI or *Eco*RI-*Not*I fragments were then cloned back into full-length Smo expression plasmids.

To generate Smo truncations (Smo^{core} - amino acids 1-663, $Smo^{\Delta 651}$ - amino acids 1-651, $Smo^{\Delta 625}$ - amino acids 1-625 and $Smo^{\Delta 603}$ - amino acids 1-603; Figure 2.1) Smo sequences between the *Eco*RV site at codon 458-459 and the indicated 3′ codon were PCR amplified, introducing a 3′ *Not*I site. The resulting *Eco*RV-*Not*I fragments were cloned into Smo expression vectors.

All Smo constructs were C-terminally tagged with either GFP, GFP10 or *R*LucII (Figure 2.1). The tags were engineered as a cassette flanked by *Not*I and *Kpn*I restriction sites. Coding fragments were cloned into expression constructs for use in cell culture [*pRmHa3.puro* (Denef et al., 2000) containing the *metallothionein* promoter] and flies [*pUAST-AttB* (Bischof et al., 2007)].

UAS-smo-3′UTR-dsRNA was generated by cloning a genomic PCR-generated fragment containing nucleotides 2L:281756..281981 of the *smo* 3′-UTR. The 226 nt long fragment was cloned between the EcoRI-AvrII sites and in the opposite orientation between the NheI-XbaI sites of *pWIZ* (*Drosophila* Genomics Resource Centre).

Gprk2 constructs. wt Gprk2 coding sequence was cloned downstream of a Myc-epitope tag in *pRmHa3.puro*. To generate catalytically inactive forms of Gprk2, point mutations changing $Lys^{338/339}$→Met [$Gprk2^{kd1}$ (Chen et al., 2010)] or Asp^{453}→Asn [$Gprk2^{kd2}$] were generated by PCR mutagenesis.

Cos2 plasmid. A C-terminal luciferase-tagged Cos2 expression construct used in BRET assays was engineered by flanking the Cos2 coding sequence at the 5′ and 3′ end with an *Eco*RI and a *Not*I site, respectively. The resulting *Eco*RI-*Not*I fragment was cloned into *pRmHa3.puro.* The *R*LucII cassette described above was cloned downstream of the Cos2 sequence at the *Not*I site.

Fu construct. Fu coding sequence was cloned downstream of a Myc-epitope tag in *pRmHa3.puro*.

EPAC constructs. To prepare the EPAC-BRET plasmid, a fragment encoding the cAMP binding portion of human Epac1 (amino acids 148-881) fused to GFP10 and *R*LucII at the amino- and carboxy-termini, respectively (provided by Michel Bouvier, UdM, Canada), was subcloned into *pMT.puro* to generate *pMT.puro/GFP10-EPAC-RLucII_T781A,F782A*. As a control for background emission, we prepared a construct encoding the same protein lacking the GFP10 moiety.

$G\alpha_s^{Q215L}$ and $G\alpha_i^{Q205L}$ expression vectors. Coding sequences of $G\alpha_s^{Q215L}$ and $G\alpha_i^{Q205L}$ were PCR amplified from genomic DNA from flies bearing appropriate UAS-transgenes (Connolly et al., 1996; Schaefer et al., 2001) and subcloned downstream of a Myc-epitope tag in *pRmHa3.puro*.

Other plasmids and their sources.

pRmHa3.puro/Hh^N encodes an active N-terminal fragment of *Drosophila* Hh (Denef et al., 2000). For *ptc-luc* reporter assays a mixture of the following constructs was used: *pRmHa3/Ci* (a gift from S. Cohen, Denmark), *pGL.basic/ptcΔ136-luc*(Chen et al., 1999a), and *pRL/CMV* (Promega).

2.3. Generation of dsRNA.

DNA templates for *in vitro* transcription of dsRNA were generated by PCR. Forward and reverse primers included T7 (5′-TAATACGACTCACTATAGGGAGA-3′) and T3 (5′-AATTAACCCTCACTAAAGGGAGA-3′) promoter sequences, respectively. Top and bottom strand RNAs were generated using MEGAscript T7 and T3 *in vitro* transcription kits (Ambion, Life Technologies). The resulting single-stranded RNAs were mixed in equal amounts, and heated to 95 °C followed by slow cooling to room temperature to anneal.

Table 1. List of dsRNA fragments used in this study.

dsRNA	target sequence
gprk2 CDS	nt 372..870 of Gprk2 cDNA
gprk2 5‘UTR	nt 27259182..27259345 of genomic scaffold 3R
gprk2 3‘URT	nt 27282732..27283011 of genomic scaffold 3R
smo CDS	nt 1024..1529 of Smo cDNA
smo 3‘UTR	nt 281756..281981 of genomic scaffold 2L
β-*galactosidase* (β -*gal*)	nt 2226..2736 of *E. coli lacZ* gene (NCBI-Accession: V00296)
GFP	nt 64..559 of EGFP coding sequence

2.4. Antibodies.

Smo antibodies. Mouse α-Smo (20C6, developed by P.A. Beachy) was used for immuno-stainings and immuno-precipitation (Developmental Studies Hybridoma Bank, created by the NICHD of the NIH and maintained at the Department of Biology, University of Iowa). For western blot applications we first used a rat α-Smo (Denef et al., 2000) raised against amino acids 560-1036 of the Smo C-terminus (a gift from S. Cohen, Denmark). We later re-made this antibody by immunizing guinea pigs against the same His-tagged fragment of the Smo C-terminus as previously described (Denef et al., 2000). α-pSer^{604} and α-pThr^{610}/pThr^{612} phosphospecific antisera were generated by GenScript. Rabbits were immunized with phosphorylated peptides (KGRL{pS}ITLYNTHC or CSITLYN{pT}H{pT}DPVGL), and antibody was isolated from serum by modified peptide affinity column purification and unmodified peptide cross-adsorption.

Preparation of α-Gprk2 antibody. A portion of the sequence encoding the C-terminus of Gprk2 (amino acids 560-714) was PCR amplified (5′ primer: AATAAGGATCCAACGGTCGCATGGGCGGG; 3′ primer: TATATGAATTCTCAGCTTTCGACCGTCGTG). The product was digested with *Bam*HI and *Eco*RI and cloned into *Bam*HI/*Eco*RI-digested pGEX4T-1 (Invitrogen). Bacterially expressed GST-fusion protein was purified with glutathione

agarose (Pierce) under native conditions according to the manufacturer's instructions. Guinea pigs were injected with 50-100 µg of purified fusion protein mixed with Sigma Adjuvant (Sigma), at 3-week intervals. For immunostainings, serum was affinity purified using the AminoLink® Plus Immobilization Kit as per manufacturer's instructions (Pierce).

List of other antibodies.

mouse: α-Col (M. Crozatier, Université Paul Sabatier Toulouse, France); α-myc (Santa Cruz Biotechnology). α-En (4D9; developed by C. Goodman), α-Ptc (ApaI; developed by I. Guerrero) and α-alpha-Tubulin (12G10) were obtained from the Developmental Studies Hybridoma Bank.

rat: α-Ci^{155} (T. Kornberg, University of California, United States)

rabbit: α-β-galactosidase (Santa Cruz Biotechnology or Molecular Probes), α-GFP (Torrey Pines Scientific); α-Moesin (a gift from D. Kiehart, Duke University, United States).

2.5. Fly crosses, immunostainings, mounting and measurements of adult wings.

Unless otherwise indicated flies were cultured and crossed at 25 °C. For expression of Smo^{SD} variants, flies were mated at 25 °C and 0-48 h old offspring transferred to 29 °C to inhibit $GAL80^{ts}$ and activate *apGAL4*-dependent transgene expression. For experiments involving rescue of dsRNA-mediated Smo depletion, crosses included a *UAS-Dcr* transgene and were carried out at 27 °C to maximize the *smo* dsRNA phenotype while minimizing the ectopic effects of transgenic Smo overexpression. For experiments in a $gprk2^{KO}/gprk2^{del1}$ mutant background, flies were mated at 25 °C and 0-48 h old offspring transferred to the restrictive temperature of 29 °C (Cheng et al., 2010).

For processing of adult wings, flies were collected in 50% ethanol/50% glycerol. After rinsing with water, wings were transferred into a drop of Faure's solution on glass slides and cover-slipped. Wing images were analyzed using the polygon selection tool in ImageJ 1.42q to outline and measure the areas bounded by L3 and L4 veins and total wing areas for at least five wings of each genotype. Statistical significance was tested using the Student's *t*-Test.

For imaginal disc analyses, wandering third instar larval wing discs were dissected in phosphate-buffered saline (PBS) and kept on ice for a maximum of 20 min before fixation in PBS/0.2% Tween (PBT) containing 4% parafomaldehyde for 20 min. Discs were washed three times in PBT, followed by incubation for 30 min in PBT with 0.1% BSA (BBT). Primary antibodies were diluted in BBT, added to the discs and incubated over night at 4 °C. After four washes with PBT, the discs were incubated with fluorescently-labeled secondary antibodies (Invitrogen and Jackson ImmunoResearch Laboratories) diluted in BBT, for 2 hours at room temperature. After four to five more washes with PBT, discs were mounted on slides in mounting medium (10% PBS, 90% glycerol, 0.2% n-propyl gallate), cover-slipped, and imaged using a Zeiss LSM700 confocal microscope.

2.6. Imaginal disc lysates and λ–phosphatase treatment.

Wing/haltere/leg imaginal disc complexes were dissected in PBS as described above. After collection od an appripate number of discs, the PBS buffer was removed and the tissue was lysed in lysis buffer [50mM Tris pH 7.5, 150 mM NaCl, 1% NP and containing 120 µg/ml AEBSF (Sigma), 1x protease inhibitors (Roche) and 1x phosphatase inhibitors (Roche)] for 15 min on ice. Insoluble material was removed by microcentrifugation for 15 min at 12,000 x *g* and 4 °C and the sample was fractionated by SDS-PAGE (see section 2.10). For some

experiments, a portion of the lysate was first incubated with 400U λ–phosphatase (New England Biolabs) in a 30 µl reaction volume containing 1X reaction buffer and 2 mM $MnCl_2$.

2.7. cAMP measurements of whole larvae extracts.

Freshly-hatched larvae from 4 h embryo collections were transferred to food vials (40 per vial). Larvae were cultured at 29˚C for 4 days. cAMP concentrations for 6 independent groups of 8 wandering third-instar larvae of each genotype were measured using the CatchPoint cAMP 384-well Bulk Fluorescent Assay Kit (Molecular Devices). Briefly, 8 larvae were homogenized in 300 µl of CatchPoint lysis buffer, and lysates were snap-frozen. After thawing, lysates were spun twice at 18,000 x *g* and 4˚C in a microcentrifuge and insoluble material and fat were removed. Measurements of cAMP in the soluble lysates were made according to manufacturer's instructions. cAMP measurements were normalized to protein concentrations in the lysates as determined by DC Protein Assay (BioRad). Protein concentrations varied by less than 11% between genotypes.

2.8. Cell culture, dsRNA treatment, transfections and *ptc-luciferase* reporter assays.

Drosophila S2 cells were cultured at 25 °C unless otherwise indicated. Most experiments were performed using S2-R+ cells grown in *Drosophila* Schneider's medium (Lonza) supplemented with 10% fetal bovine serum (Gibco) and 50 U/ml penicillin and streptomycin (Gibco). Exceptionally, experiments for Figures 3.1K, L; 3.2C, E; 3.3 and 4.1D, E were performed using *Drosophila* S2 cells adapted to growth in serum-free medium (EX-CELL 420, Sigma), which show more pronounced Smo phosphoshifts due to a higher basal level of phosphorylation (Cheng et al., 2012). In two of these experiments cells were treated for 2 h with Hh-conditioned or S2-conditioned medium prior to lysis. (Figure 3.1K; 3.2C). For Hh treatments, S2 cells stably transfected with a puromycin-selectable pMT vector containing sequences encoding an active N-terminal fragment of Drosophila Hh (Hh^N) were selected in 10 µg/ml puromycin. Hh-conditioned medium was prepared by culturing these cells in the absence of puromycin and inducing Hh^N expression with 0.5 mM $CuSO_4$. After the cells reached confluence, the medium was harvested, clarified by centrifugation for 5 min at 1000 x g, and sterile filtered. Control conditioned medium was obtained by treating wild-type S2 cells the same way.

dsRNA treatments. Depletion of endogenously expressed *mRNAs* was achieved by dsRNA treatments typically over five days. The amounts of dsRNA administered to the growth medium of S2 cell are specified in the following sections. For experiments involving treatment with more than one dsRNA, the total amount of RNA added to cells was equalized with the use of β-*gal* dsRNA.

Biochemical analysis. ~$1x10^6$ cells were typically plated on day 1 in 24 well plates in 0.5 ml of complete Schneider's medium and each well was transfected with 100-250 ng of the indicated *pRmHa.puro* expression constructs using X-tremeGENE HP transfection reagent (Roche) according to manufacturer's instructions. On day 2, the cells of each well were split into 2 new wells of a 24 well plate and treated with 5 µg of the indicated dsRNA. On day 3 to 4, a second dose of dsRNA was applied and transgene expression was induced by addition of $CuSO_4$ to a final concentration of 0.5 mM. Cells were harvested and processed on day 7.

***ptc-luc* reporter assays.** S2-R+ cells were transfected in 24 well plates on day 1 of the experiment as described above. 100 ng *pRmHa/Ci*, 75 ng *pGL.basic/ptcΔ136-luc,* 75 ng *pRL/CMV* and 100 ng of each additional expression

plasmid (Smo/Gprk2 variant; Hh^N, as indicated) were typically used. Total DNA amounts in the transfection mix were normalized using empty *pRmHa.puro* vector. On day 2 the cells were split into 4 wells of a 96 well plate and each well was treated with 0.5-1 µg dsRNA. On day 3 or 4 transgene expression was induced by addition of $CuSO_4$ and a second dose of dsRNA was administered. Cells were processed on day 7 and luciferase activity measured using the Dual Luciferase Reporter system (Promega) according to manufacturer's instructions. Assays were performed at least two times in quadruplicate, and the data was pooled. Statistical significance was assessed using two-tailed Student's *t*-tests.

2.9. Bioluminescence resonance energy transfer (BRET) experiments.

cAMP measurements using the EPAC-BRET biosensor. dsRNA-treated S2 cells were transiently transfected with *pMT.puro/GFP10-EPAC-RLucII_T781A,F782A*, encoding the EPAC-BRET cAMP sensor protein. In the unbound state, the GFP10 and *R*LucII moieties of this protein are in proximity such that the energy generated by *R*LucII after oxidizing its substrate coelenterazine (DeepBlueC) is transferred to GFP10, causing it to fluoresce. cAMP binding to the EPAC1 domain induces a conformational shift that decreases this intramolecular BRET (Jiang et al., 2007). 48 hours after induction of sensor expression, cells were harvested, washed once with PBS, and transferred in PBS to white-walled, clear-bottomed 96 well plates. DeepBlueC (Biotium) was added at a final concentration of 5 µM and one to four minutes later emissions at 400 nm (*R*LucII, donor) and 515 nm (GFP10, acceptor) were measured using a PHERAstar microplate reader (BMG Labtech). The BRET signal was calculated as the ratio of GFP10 : *R*LucII emission. The values were corrected for background emission by subtracting the BRET signal obtained using S2 cells transfected in parallel with a biosensor protein that lacks the GFP10 moiety, to yield the net BRET signal. Graphs represent the composite results from two independent experiments, each with triplicate or quadruplicate measurements.

Smo dimerization. S2-R+ cells were transfected with 100 ng of the Smo^{SD}-RLucII variant, 300 ng of the Smo-GFP10 variant and 100 ng of ^{myc}Gprk2 (if applicable) per well of a 24-well plate. Background emission was determined by transfecting S2 cells only with the Smo^{SD}-RLucII construct along with the appropriate amount of Mock-DNA. BRET measurements were performed on day 7 as described above. Assays were performed at least two times in quadruplicate, and the data was pooled.

Recruitment of Cos2 to Smo truncations. 75 ng of Cos2-RLucII, 300 ng of the indicated Smo-GFP10 variant, and 75 ng ^{myc}Fu plasmids were transfected. Cells were re-plated in 4 wells of a white-walled 96-well plate and subjected to dsRNA treatments and transgene induction as described above. BRET measurements were performed on day 7 as described above. Assays were performed at least two times in quadruplicate, and the data was pooled.

2.10. Immunoprecipitations, cell surface biotinylation, SDS-PAGE, and immunoblotting.

S2 cells expressing Smo-GFP variants were lysed in lysis buffer [50mM Tris pH 7.5, 150 mM NaCl, 1% NP and containing 120 µg/ml AEBSF (Sigma), 1x protease inhibitors (Roche) and 1x phosphatase inhibitors (Roche)] for 15 min on ice. Insoluble material was removed by microcentrifugation for 15 min at 12,000 x *g* and 4 °C. The sample was kept on ice and endogenous Smo was precipitated by adding α-Smo (20C6) for 2 h followed by adding protein A/G beads (Pierce) for 1 h protein. Transgenically-expressed Smo variants were enriched by adding α-GFP mAb

agarose (MBL International) to soluble extracts and samples incubated on ice for 2h. Beads were washed 2-3 times in 1 volume of lysis buffer and precipitated proteins extracted by addition of 1x SDS-PAGE sample buffer and heating at 75 °C for 6 min. For most experiments, proteins were fractionated by SDS-PAGE on standard polyacrylamide gels. For Figure 3.3B, Phos-tag acrylamide (Wako Pure Chemicals Industries, Ltd.) was added to a final concentration of 7.5 mM to improve resolution of phosphoproteins (Kinoshita et al., 2006). Fractionated proteins were transferred to nitrocellulose membranes using a wet transfer apparatus and immunoblotted according to standard methods. Quantitation of signal intensity was performed using the Gels>Plot Lanes function of ImageJ 1.42q. Plots were normalized to equal total signal intensity (area under the curve), to correct for differences in loading.

Cell surface biotinylation. Cells were washed, and cell surface proteins labelled with 1 mg/ml Sulfo-NHS-SS-Biotin (Pierce) as described (Denef et al., 2000). After purification, strepatavidin-agarose-bound proteins were recovered by suspension in 1x SDS–PAGE sample buffer and incubation at 50°C for 10 min to cleave the disulfide bond, followed by denaturation for 5 min at 75°C prior to SDS-PAGE.

2.11. Preparation and analysis of LC-MS/MS samples.

Immunoaffinity purification of Smo. S2-R+ cells were plated in 1 to 3 wells per condition of a 6-well plate and transfected with 2.5 µg/well of *pRmHa3.puro/Smo^{SD}-GFP* as above. A day later, medium was replaced and 20 µg/well control (*β-gal*) or *gprk2* dsRNA was added to the cells. After three days of growth, the cells were harvested and replated in a 10-cm plate, along with 100 µg/plate of the appropriate dsRNA. Smo^{SD} expression was induced by addition of 0.5 mM $CuSO_4$. 2-3 d later, cells were washed with ice-cold PBS and lysed in 3 ml RIPA buffer for 15 min on ice. Lysates were cleared by microcentrifugation for 15 min at 12,000 x *g* and 4 °C. Smo^{SD}-GFP was immunoprecipitated using α-GFP mAb agarose for 2 h at 4 °C with rotation. Beads were washed 4 times with ice-cold RIPA buffer before addition of 1x SDS-PAGE sample buffer and heating at 75°C for 6 min. Samples were frozen at -80°C and typically 2 to 3 such preps were pooled for subsequent analysis. Pooled samples were fractionated by SDS-PAGE on 4-15% polyacrylamide gradient gels (BioRad), stained using Colloidal Blue (Life Technologies) according to manufacturer's protocol, and the band corresponding to Smo was excised from the gel.

Protein digestion. Gel pieces were washed with water for 5 min and destained twice with the destaining buffer (50 mM ammonium bicarbonate, acetonitrile) for 15 min. An extra wash of 5 min was performed after destaining with a buffer of ammonium bicarbonate (50 mM). Gel pieces were then dehydrated with acetonitrile. Proteins were reduced by adding the reduction buffer (10 mM DTT, 100 mM ammonium bicarbonate) for 30 min at 40 °C, and then alkylated by adding the alkylation buffer (55 mM iodoacetamide, 100 mM ammonium bicarbonate) for 20 min at 40 °C. Gel pieces were dehydrated and washed at 40 °C by adding ACN for 5 min before discarding all the reagents. Gel pieces were dried for 5 min at 40 °C and then re-hydrated at 4 °C for 40 min with enzyme solution. Tryptic digestion was performed with a 6 ng/µl solution of sequencing grade trypsin from Promega in 25 mM ammonium bicarbonate buffer, incubated at 58 °C for 1 h and stopped with 15 µl of 1% formic acid/2% acetonitrile. Chymotryptic digestion was performed with a 40 ng/µl solution (Roche) in 100 mM Tris HCl- 25, mM CaCl2, pH 8 buffer, incubated at 25 °C for 4 h and stopped with 15 µl of 1% formic acid/2% acetonitrile. Supernatant was transferred into a 96-well plate and peptide extraction was performed with two 30-min extraction steps at room

temperature using the extraction buffer (1% formic acid/50% ACN). All peptide extracts were pooled into the 96-well plate and then completely dried in vacuum centrifuge. The plate was sealed and stored at −20 °C until LC-MS/MS analysis. Protein digestion with Asp-N was performed in solution on tryptic digests. Samples were re-solubilized in a 50 mM ammonium bicarbonate buffer and 1 ng of Asp-N was added to each sample. Samples were incubated at 37 °C for 3h.

Liquid chromatography/tandem mass spectrometry (LC-MS/MS) analysis. Prior to LC-MS/MS, peptide extracts were re-solubilized under agitation for 15 min in 11 µl of 0.2% formic acid and then centrifuged at 2000 rpm for 1 min. The LC column was a C18 reversed-phase column packed with a high-pressure packing cell. A 75 µm i.d. Self-Pack PicoFrit fused silica capillary (New Objective, Woburn, MA) of 15 cm length was packed with the C18 Jupiter 5 µm 300 Å reverse-phase material (Phenomenex, Torrence, CA). This column was installed on the Easy-nLC II system (Proxeon Biosystems, Odense, Denmark) and coupled to the LTQ Orbitrap Velos (ThermoFisher Scientific, Bremen, Germany) equipped with a Proxeon nanoelectrospray ion source. The buffers used for chromatography were 0.2% formic acid (buffer A) and 100% acetonitrile/0.2% formic acid (buffer B). During the first 12 min, 5 µl of sample were loaded on column with a flow of 600 nl/min and, subsequently, the gradient went from 2-80% buffer B in 60 min at a flow rate of 250 nL/min and then came back at 600 nL/min to 2% buffer B for 10 min. LC-MS/MS data acquisition was accomplished using an eleven scan event cycle comprised of a full scan MS for scan event 1 acquired in the Orbitrap which enables high resolution/high mass accuracy analysis. The mass resolution for MS was set to 60,000 (at m/z 400) and used to trigger the ten additional MS/MS events acquired in parallel in the linear ion trap for the ten most intense ions. Mass over charge ratio range was from 360 to 2000 for MS scanning with a target value of 1,000,000 charges and from ~1/3 of parent m/z ratio to 2000 for MS/MS scanning with a target value of 10,000 charges. The data-dependent scan events used a maximum ion fill time of 100ms and 1 microscan. Target ions already selected for MS/MS were dynamically excluded for 25s. Nanospray and S-lens voltages were set to 0.9-1.8 kV and 50 V, respectively. Capillary temperature was set to 225°C. MS/MS conditions were: normalized collision energy, 35 V; activation q, 0.25; activation time, 10 ms.

Peptide identification and quantification. The peak list files were generated with extract_msn.exe (version January 10, 2011) using the following parameters: minimum mass set to 600 Da, maximum mass set to 6000 Da, no grouping of MS/MS spectra, precursor charge set to auto, and minimum number of fragment ions set to 10. MS/MS spectra were queried against the Smo^{SD} sequence using Mascot 2.3 (Matrix Science). The mass tolerances for precursor and fragment ions were set to 10 ppm and 0.6 Da, respectively. Search parameters allowed for up to two missed enzyme cleavages. Oxidation of methionine and phosphorylation of serine, threonine and tyrosine were allowed as variable modifications while carbamidomethyl was set as a fixed modification. Matches for phosphopeptides were validated manually. In a few cases (twice phosphorylated species of cluster 1 peptide W.AKRKDFEDKGRLSITLY.N in Chymotrypisin digest, once and twice phosphorylated species of the cluster 3 peptide R.MALTGAATGNSSSHGPR.K in trypsin + AspN digests), the phosphopeptides were not confirmed by MS2, but were detected in full scan with mass accuracies of less than 2 ppm, and eluted with very similar retention times to other phosphospecies of the same peptide. Peptides were quantitated by manual integration of precursor ion LC spectra using Qual Browser (Xcalibur from Thermo Scientific) (Chelius and Bondarenko, 2002; Neilson et al.,

2011). For each phosphopeptide identified, the relative level of phosphorylation in each sample was calculated as the ratio of the amount of phosphorylated : non-phosphorylated forms of the peptide.

2.12. Smo sequence analysis.

Multiple sequence alignment of full-length Smo proteins from nine bilaterian animal species was generated with Clustal-Omega. The species and accession numbers corresponding to the sequences used were: *Homo sapiens* (NP_005622.1), *Mus musculus* (NP_795970.3), *Danio rerio* (NP_571102.1), *Paracentrotus lividus* (AEX61000.1), *Platynereis dumerilii* (ADK38671.1), *Drosophila melanogaster* (NP_523443.1), *Apis mellifera* (XP_395373.3), *Tribolium castaneum* (NP_001127850.1), *Daphnia pulex* (EFX80809.1).

Chapter 3: Results – part I

Mapping and functional characterization of Gprk2 phosphorylation sites in Smo.

3.1. Characterization of *gprk2* mutant alleles and loss-of-function phenotypes.

GRKs are implicated in Hh signaling and Smo regulation in several systems including flies, zebrafish, and mouse (Chen et al., 2004; Meloni et al., 2006; Molnar et al., 2007; Philipp et al., 2008). In *Drosophila*, *gprk2* has been studied in the patterning of the wing imaginal disc, an embryonic tissue that develops into the adult wing and part of the fly body wall. Depletion of *gprk2* via RNAi caused a reduction in Hh target gene expression in this tissue, reminiscent of the phenotypes obtained by Smo impairment. *gprk2* mRNA was expressed throughout the wing disc, but was upregulated in a narrow stripe of A cells close to the A/P compartment border in a Hh-dependent manner. The study concluded that *gprk2* is required for Hh target gene expression. Furthermore, because it also seemed to be a Hh target gene, *gprk2* forms a positive feedback loop in the Hh pathway. The authors proposed that *gprk2* most likely acts on Smo, but mechanistic insight into the nature of this regulation was lacking (Molnar et al., 2007).

Our work aimed to provide a detailed mechanistic explanation behind the role of Gprk2 in *Drosophila* Hh signaling. To our advantage, we had already generated transgenic *gprk2* mutant fly lines in our lab. This allowed us to study the function of *gprk2* in the Hh pathway without possible complications arising from RNAi-dependent gene knockdown. I will preface my results section with the confirmation that our *gprk2* mutant alleles behave as clean protein null mutations.

3.1.1. Our *gprk2* null alleles abrogate Gprk2 protein levels below detection limits.

We generated three *gprk2* mutant alleles either by defined chromosomal deletions or by homologous recombination (Figure S1A). Engineered piggyBAC transposable elements flanking the whole ($gprk2^{del2}$) or part of the *gprk2* locus ($gprk2^{del1}$) were used to excise genomic DNA. The $gprk2^{KO}$ allele, created by homologous recombination, replaced most of the exons encoding the Gprk2 kinase domain with a marker transgene. Both deletion alleles, $gprk2^{del1}$ and $gprk2^{del2}$, affect neighboring genes, hence, trans-heterozygous combinations of the three *gprk2* alleles were used to obtain clean *gprk2* null phenotypes (Figure S1A). We first validated that the Gprk2 protein was eliminated in animals carrying any trans-heterozygous combination of the three *gprk2* alleles. To visualize Gprk2, we raised an antiserum targeting the C-terminus of the protein.

The antibody works well on western blots and revealed a robust Gprk2 signal in lysates derived from wt third instar wing discs. Gprk2 protein was not detectable in wing disc lysates isolated from *gprk2* mutant animals possessing any combination of *gprk2* alleles (Figure S1B). We conclude that all three trans-heterozygous genotypes eliminate Gprk2 expression and behave as clean *gprk2* nulls. We observed no phenotypic difference between the three combinations and we used them interchangeably in all our studies. Unless otherwise indicated, any of these three combinations is further refereed as *gprk2* mutant ($gprk2^{-/-}$).

We next assessed the pattern of *gprk2* expression in the wing disc by using a *gprk2-LacZ* enhancer trap and immunofluorescence staining of the LacZ protein. *gprk2* transcription was upregulated in A compartment cells (identified by expression of Ci), close to the A/P compartment boundary (Figure S1C). Immunofluorescence staining of Gprk2 protein showed a uniform expression pattern throughout the disc. Gprk2 protein levels were slightly elevated in the form of a stripe running along the A/P axis in the center of the disc, which is in line with the increase in *gprk2* transcription revealed by the enhancer trap (Figure S1C). The lack of Gprk2 staining in $gprk2^{KO}$ mutant clones within an otherwise wt wing disc confirmed the specificity of the antibody signal (Figure S1D). In all, our expression profile of *gprk2* in wing discs confirms the observations made by Molnar and colleagues. The up-regulation of *gprk2* transcription and protein levels in a narrow stripe of A compartment cells is consistent with the identification of *gprk2* as a Hh target gene (Molnar et al., 2007).

3.1.2. *gprk2* mutants display a Hh loss-of-function phenotype.

To test whether our *gprk2* mutant alleles could replicate the published Hh loss-of-function phenotype observed in *gprk2* knockdown animals, we first analyzed adult fly wings (Molnar et al., 2007). *gprk2* mutants had smaller wings compared to wt animals (Figure 3.1A-C). In particular the area between longitudinal veins 3 and 4 (L3 and L4) of the adult fly wing was strongly reduced in *gprk2* mutants, reminiscent of a typical Hh loss-of-function phenotype (Figure 1.1C). We quantified this reduction by measuring and calculating the ratio of the L3-L4 wing region over the total wing size. *gprk2* mutants were characterized by a significant 19% to 30% reduction compared to the wt ratio set to a 100% (Figure 3.1D). Patterning of the adult fly

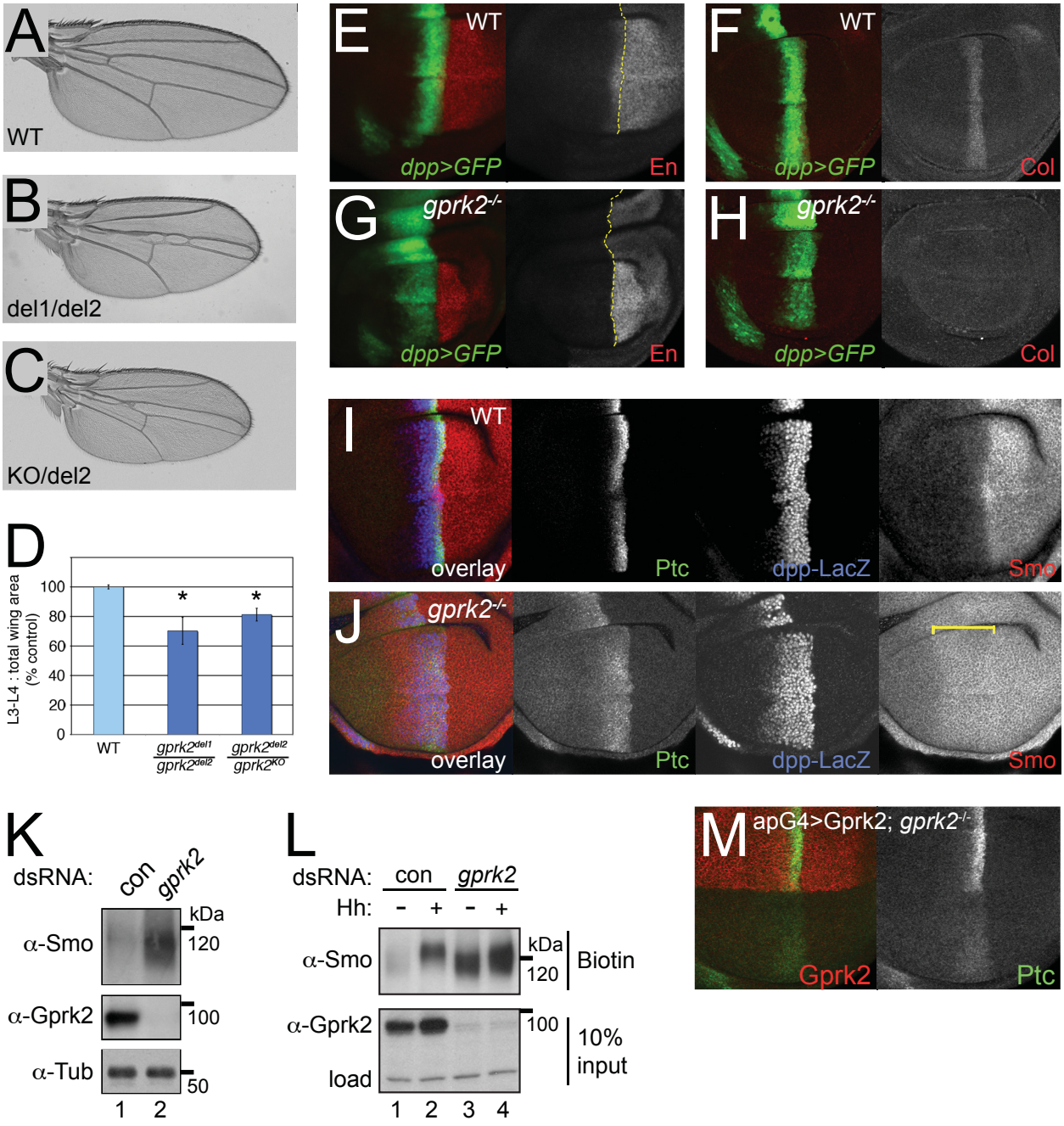

Figure 3.1. Impaired Hh signaling and ectopic accumulation of Smo in *gprk2* mutant Hh-responding cells.

(A-D) The L3-L4 area of adult fly wings is reduced in *gprk2* mutants. Wings of flies raised at 29°C. Genotypes are: **(A)** wild-type (w^{1118}); **(B)** $gprk2^{del1}/gprk2^{del2}$; **(C)** $gprk2^{KO}/gprk2^{del2}$. **(D)** Measurements of wings as presented above: wild-type (w^{1118}; n=7), $gprk2^{del1}/gprk2^{del2}$ (n=6), and $gprk2^{del2}/gprk2^{KO}$ (n=11). *, significantly smaller than wild-type (p<.001; *T*-test).

[*continued on next page*]

Figure 3.1. Impaired Hh signaling and ectopic accumulation of Smo in *gprk2* mutant Hh-responding cells. [*continued*]

(E-J) High threshold Hh target genes are lost or reduced in *gprk2* mutants and Smo accumulates in *gprk2* mutant Hh-responding cells. Confocal micrographs of wing discs, oriented with A compartment to left, D compartment up. Wing disc from wild-type **(E, F, I)** or *gprk2* mutant animals **(G, H, J)** raised at 29°C. **(E-H)** GFP expressed under the control of *dpp*-GAL4 (green channel) was used to mark the A/P boundary (yellow dotted lines in **E** and **G**). Disc were immunostained for En (**E**, **G**, red channel) or Collier (**F**, **H**, red channel). Expression of A En and Col, which are both high-threshold Hh targets is absent in *gprk2* mutants at 29°C. **(I, J)** Immunofluorescence staining of a wild-type **(I)** or *gprk2* mutant **(J)** wing disc with antibodies recognizing Ptc (green), Smo (red) and nuclear β-galactosidase expressed from a *dpp-LacZ* enhancer trap (blue). Hh-dependent Ptc expression is strongly reduced. Ectopic Smo is indicated by a yellow bracket. **(K)** Smo accumulates in Gprk2 depleted S2 cells. S2 cells were treated with dsRNAs targeting *gfp* (Control) or *gprk2*. Lysates were separated by SDS-PAGE and immunoblotted with antibodies against Smo (*top*) and Gprk2 (*middle*). Samples were run in parallel on a higher percentage gel and re-probed with antibody against α-Tubulin to ensure equal loading (*bottom*). **(L)** Gprk2 promotes Smo turnover from the plasma membrane. S2 cells were pretreated with dsRNA targeting *gfp* (Control) or *gprk2*, and then incubated for 2 h with control (-) or HhN (+) conditioned medium. Cell surface proteins were then labeled by surface biotinylation. After lysis, biotinylated proteins were recovered by avidin-mediated affinity purification, and separated by SDS-PAGE. Smo was detected in the biotin-labeled surface protein fraction by immunoblotting (*top*). 1/10 of the input was run separately and probed with an antibody against Gprk2 (*middle*). A background band served as a loading control (load) to ensure that the starting samples had equivalent amounts of protein (*bottom*). **(M)** Immunofluorescence staining of a wing disc from a *gprk2* mutant animal raised at 29°C, in which transgenic expression of Gprk2 (red) in the D compartment was driven with *ap*-GAL4. Re-expression of Gprk2 specifically rescued Ptc expression (green).

wing is determined at embryonic and larval stages through expression of Hh-responsive genes in the wing imaginal disc (see section 1.1.2.1.). We examined Hh target gene expression in third instar wing discs by immunostaining. In a wt wing disc, Hh target genes were expressed in the A compartment but expression was limited to a few cell rows proximal to the A/P boundary, generating a stripe in the middle of the disc. Low threshold target genes such as *decapentaplegic* (*dpp*) were turned on in a broad stripe (Figure 3.1I). In contrast, medium to high threshold targets such as *patched* (*ptc*), *collier* (*col*) and A *engrailed* (*en*) were detectable as gradually more narrow stripes closer to the A/P border (Figure 3.1E, F, I). *en* was also expressed in the P-compartment independently of Hh (Figure 3.1E). In *gprk2* mutants, the expression of *dpp*, visualized with the use of an *dpp-LacZ* enhancer trap, seemed unaffected (Figure 3.1J). However, transcription of medium to high threshold Hh-responsive genes was substantially affected by the removal of Gprk2. The high Hh threshold target genes *col* and A *en* were completely lost in *gprk2* mutants (Figure 3.1G, H). P *en* was not impaired by removal of Gprk2 (Figure 3.1G).

Protein levels of Ptc, a medium threshold Hh target gene, were strongly reduced in *gprk2* mutants (Figure 3.1J). To validate that the reduction of Hh target gene expression is specific to the loss of *gprk2*, a genetic rescue experiment was performed. Transgenic Gprk2 was expressed in *gprk2* mutant animals in the D compartment of the disc using the *apterous*-Gal4 (*ap*-Gal4) driver. As shown in Figure 3.1M, Ptc expression was restored dorsally where transgenic Gprk2 was expressed but remained low in the V compartment of the disc.

We conclude that Gprk2 is exclusively required for expression of medium to high threshold Hh target genes. This differs to a certain extent from the published *gprk2* RNAi phenotypes, which seemingly affected all Hh target genes (Molnar et al., 2007). In addition, it is worth noting that the presented phenotypes were only obtained by culturing the flies at 29°C. *gprk2* mutants kept at the usual temperature of 25°C showed no signs of Hh defects. Genetic experiments in our lab suggested that the temperature-dependent nature of the phenotype is caused by partial functional redundancy. The *Drosophila* genome encodes two GRK orthologues, Gprk1 and Gprk2 (Cassill et al., 1991). Work from our group has demonstrated that *gprk1* mRNA is expressed in wing disc (Cheng et al., 2010). Furthermore, we generated and analyzed *gprk1* knock-out animals. Loss of *gprk1* alone was not sufficient to impair Hh signaling even at 29°C. We could not analyze *gprk1*/*gprk2* double mutants due to embryonic lethality. However, flies carrying only one functional *gprk1* allele in a homozygous *gprk2* mutant background showed Hh signaling defects at 25°C. Collectively, these data suggests that, compared to *gprk2, gprk1* exerts only a minor role in Hh signaling (Cheng et al., 2010).

3.1.3. Gprk2 promotes downregulation of Smo protein.

A connection between Gprk2 and Smo protein levels was already established in the *gprk2* knockdown study (Molnar et al., 2007). *smo* mRNA is uniformly expressed throughout the wing disc. However, the stability of Smo proteins is post-translationally regulated (Denef et al., 2000). In wt wing discs, Smo proteins accumulate in the P compartment. Smo protein levels further increase in the very first rows of A cells close to the A/P boundary and then gradually decrease to low levels in the far A part of the disc (Figure 3.1I). Similar to the observation by Molnar and colleagues, we noticed ectopic accumulation of Smo in the A compartment in *gprk2* mutants

(Figure 3.1J; yellow bracket). Ectopic Smo levels were similar to those in the P compartment and the accumulation seemed to extended throughout the Hh-responsive zone of the wing disc. The fact that the expression of the *dpp-LacZ* enhancer trap matched the ectopic Smo domain supports this notion (Figure 3.1J). Based on this observation, we propose that Gprk2 downregulates Smo in Hh-stimulated cells. This hypothesis is appealing because GRKs are known to drive the internalization of active GPCRs from the plasma membrane into the endocytic pathway (see section 1.5.2.). Smo is a member of the GPCR superfamily and internalization and degradation of active Smo could therefore be Gprk2-dependent. To test this hypothesis more directly, we used *Drosophila* S2 cells, a cell culture line. Gprk2 was expressed in these cells and treatment with a *gprk2*-specific dsRNA depleted the endogenous protein below detection limits (Figure 3.1K). Analogous to the *in vivo* observations, we noticed an increase in total Smo levels (~ 3-fold compared to knockdown control; Figure 3.1K). To test whether Smo accumulates at the plasma membrane, I performed a cell surface biotinylation assay. In brief, S2 cells were incubated with either *gprk2* or control dsRNA, and in the presence or absence of Hh stimulation. Plasma membrane proteins were then covalently labelled with a biotin tag, precipitated by streptavidin agarose and analyzed by western blot. Hh treatment activated Smo and triggered its accumulation at the plasma membrane (Denef et al., 2000). Consistent with this notion, we noticed a 3-fold increase of Smo levels compared to unstimulated cells (Figure 3.1L; lane 1 vs 3). It should be pointed out that, even without Hh, a small fraction of Smo localized at the membrane (Figure 3.1L; lane 1), most likely because a small fraction of Smo resided in an active state. Interestingly, depletion of Gprk2 under this condition resulted in 3.6-fold increase in surface Smo levels (Figure 3.1L; lane 1 vs 2). This increase matched the elevation of total Smo protein shown in Figure 3.1K and suggestes that Smo mostly accumulates at the plasma membrane. We propose that Gprk2 promotes the turnover of active Smo from the plasma membrane. Depletion of Gprk2 causes enrichment of basally active Smo at the membrane even in the absence of Hh. Knocking-down *gprk2* also increased the membrane pool of Smo in the presence of Hh (1.6-fold; Figure 3.1L; lane 3 vs 4), again suggesting that Gprk2 is required for the downregulation of active Smo. However, Hh stimulation might have saturated membrane Smo levels, resulting a less pronounced Smo accumulation in response to Gprk2 depletion. In

conclusion, our data supports the hypothesis that Gprk2 promotes Smo turnover from the plasma-membrane, consistent with the canonical role of GRKs in GPCR regulation.

3.2. Gprk2 is a Smo kinase.

The canonical function of GRKs acts to phosphorylate active GPCRs at the plasma membrane. Phosphorylation triggers the recruitment of arrestins, terminates GPCR signaling and leads to clathrin-dependent receptor internalization. Based on the fact that Smo is a member of the GPCR superfamily and that Gprk2 promotes Smo internalization, we speculated that Gprk2 regulates Smo in the same way that it regulates any GPCR. If this model is true, Gprk2 should directly phosphorylate Smo.

3.2.1. Loss of Gprk2 renders Smo hypo-phosphorylated.

The first evidence in support of this hypothesis came from immunoblot analysis of Smo proteins expressed in wing discs. Lysates of wing disc from wt or *gprk2* mutant animals cultured at 29°C were fractioned. Compared to wt lysates, Smo bands migrated faster on the blot and appeared shifted downwards in *gprk2* mutants (Figure 3.2A). Removal of all post-translationally added phosphate groups by λ-phosphatase treatment eliminated the electro-mobility (EM) shift between wt and *gprk2* mutant Smo proteins, confirming that the initial difference reflects a reduction in phosphorylation in the mutants (Figure 3.2B). It is worth noting that Smo isolated from *gprk2* mutants still strongly responded to the λ-phosphatase treatment in the form of a large downwards shift (Figure 3.2B). This suggests that Gprk2 affects only a distinct subset of all Smo phosphorylation sites. This is not too surprising because Smo is a hyper-phosphorylated protein in wing disc (Denef et al., 2000) and other kinases such as PKA and Ck1 are known to phosphorylate it. We next tested whether Smo responds in a similar way in S2 cells depleted of endogenously expressed Gprk2 by RNAi treatment. In control cells, we detected two Smo bands; a faint signal at the bottom most likely representing un-phosphorylated Smo, whereas the bulk of the signal appeared as a diffuse band above, corresponding to phosphorylated Smo protein (Figure 3.2C, lane 1). As expected, Hh treatment promoted Smo stabilization and phosphorylation, as evident by a 1.9-fold increase in Smo signal and intensification of the upper

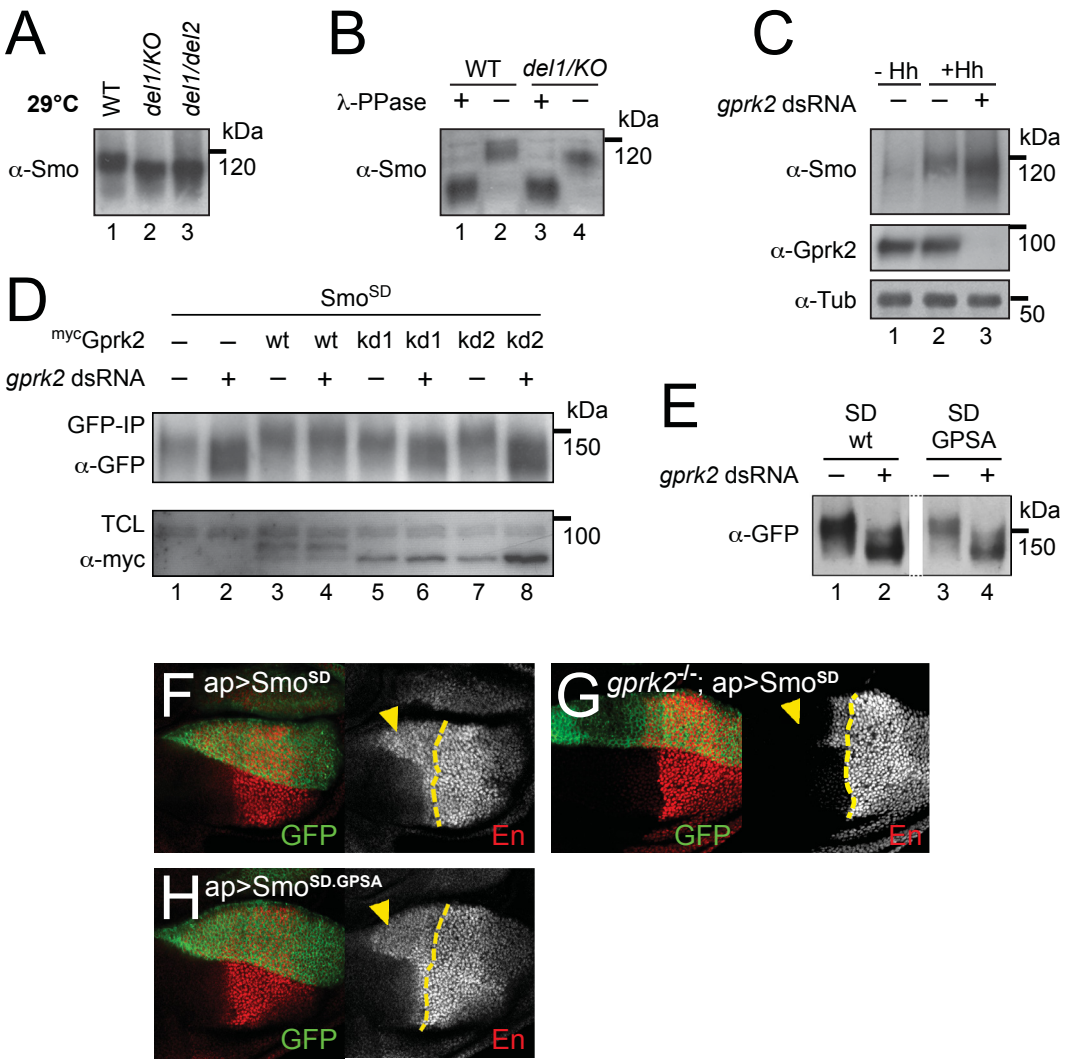

Figure 3.2. Gprk2 promotes Smo phosphorylation but not exclusively at the published GPS sites.

(A-D) Gprk2 promotes Smo phosphorylation in a catalytic activity-dependent manner. **(A)** Immunoblot analysis of wing disc lysates probed with antibody against Smo. Lysates were prepared from wild-type (w^{1118}), $gprk2^{del1}/gprk2^{KO}$, and $gprk2^{del1}/gprk2^{del2}$ larvae cultured at 29°C **(B)** Wing disc lysates prepared from wild-type or $gprk2^{del1}/gprk2^{KO}$ larvae were treated with (+) or without (-) λ-phosphatase and immunoblotted with antibody against Smo. **(C)** S2 cells were pretreated with dsRNA targeting *gfp* (-) or *gprk2*(+), and then incubated for 2 h with control (- Hh) or Hh^N (+ Hh) conditioned medium. Lysates were separated by SDS-PAGE and immunoblotted with antibodies against Smo (*top*) and Gprk2 (*middle*). Samples were run in parallel on a higher percentage gel and re-probed with antibody against α-Tubulin to ensure equal loading (*bottom*). **(D)** Western blot analysis of GFP immunoprecipitates (*top*) or total-cell lysates (*bottom*) of S2 cells with or without Gprk2 depletion, transfected with Smo^{SD}-GFP along with empty vector (-) or various forms of Myc-tagged Gprk2. The blots were probed with anti-GFP (*top*) or anti-Myc (*bottom*) antibodies. Re-expression of wild-type (lane 4) but not kd1 (lane 6) or kd2 (lane 8) Gprk2 mutants rescued the Smo phosphoshift in Gprk2-depleted cells, confirming that the Gprk2 mutants are catalytically inactive.

[*continued on next page*]

Figure 3.2. Gprk2 promotes Smo phosphorylation but not exclusively at the published GPS sites. [*continued*]

(E-H) GPS1 and GPS2 are not the principal Gprk2 phosphorylation sites in Smo. **(E)** Western blot analysis of GFP immunoprecipitates from S2 cells expressing Smo^{SD}-GFP or $Smo^{SD.GPSA12}$-GFP, with or without Gprk2 depletion. The blot was probed with anti-GFP antibody to visualize tagged Smo protein. All bands are from the same exposure of a single blot with intervening lanes removed. Although $Smo^{SD.GPSA12}$-GFP has putative Gprk2 phosphorylation sites mutated to nonphosphorylatable Ala, it still undergoes a similar phosphoshift as Smo^{SD}-GFP in response to depletion of the kinase. **(F-H)** Confocal micrographs of wing discs, oriented with A compartment to left, D compartment up. Smo variants - Smo^{SD}-GFP (F, G) or $Smo^{SD.GPSA12}$-GFP (H) - were expressed in the D compartment using *ap-GAL4*. Discs are wild-type (F, H) or *gprk2* mutant (*G*) background. Discs were immunostained to reveal En expression. Yellow dotted lines: A/P compartment boundaries based on domains of Ci expression (not shown). Both Smo^{SD}-GFP and $Smo^{SD.GPSA12}$-GFP drive comparable ectopic expression of En in dorsal A cells (arrowheads) - compare to wild-type ventral A cells. $Smo^{SD.GPSA12}$-GFP fails to reproduce the *gprk2* mutant phenotype characterized by the loss of ectopic A En expression. Genotypes in F-H: *ap-GAL4/+;UAS-*Smo^{SD}*-GFP/tubP::GAL80*^{ts} (F); *ap-GAL4/+;UAS-*Smo^{SD}*-GFP,gprk2*^{del1}*/gprk2*^{KO} (G); *ap-GAL4/+;UAS-*$Smo^{SD.GPSA}$*-GFP/tubP::GAL80*^{ts} (H).

Smo band (Figure 3.2C, lane 2). Gprk2 depletion prior to Hh stimulation caused the upper band to migrate faster, giving it a compressed appearance (Figure 3.2C). In addition, it further elevated Smo levels (2.6-fold higher than Hh treated cells), as already demonstrated (Figures 3.1K; 3.2C). In conclusion, both *in vivo* and in tissue culture cells, loss of Gprk2 causes Smo to accumulate in a hypo-phosphorylated state.

3.2.2. Gprk2-dependent Smo phosphorylation requires Gprk2 kinase activity.

We next attempted to determine whether the impairment of Smo phosphorylation is specific to the loss of Gprk2 via a rescue experiment. For this experiment, we decided to use the Smo^{SD} protein with the three PKA/Ck1 phosphorylation clusters mutated to Asp, mimicking phosphorylation and activation of Smo by these two kinases (Jia et al., 2004). Smo^{SD} is easier to express in S2 cells and does not require Hh stimulation for activation, therefore, it offered some practical advantages over wt Smo. Importantly, in response to Gprk2 depletion, Smo^{SD} also accumulated and underwent a similar EM shift compared to wt Smo (compare Figures 3.2D, lane 1, 2 with 3.2C). This suggests that Gprk2 regulates sites in Smo other than the PKA/Ck1 phosphorylation sites and established Smo^{SD} as a valid tool for monitoring Gprk2-dependent Smo phosphorylation.

For the rescue experiment, we depleted endogenously expressed Gprk2 via treatment with dsRNAs targeting the 5′ and 3′UTR of the *gprk2* transcript. Our *gprk2* overexpression constructs lack the UTRs and are therefore insensitive to the *gprk2* knockdown procedure. Re-expression of a wt *gprk2* construct rescued Smo^{SD} phosphorylation in the absence of the endogenous protein, confirming that the Smo^{SD} EM shift is Gprk2-specific (Figure 3.2D, lane 4 vs 2). The rescue depends on catalytic activity of Gprk2 as two kinase-dead mutant forms (kd1: $Lys^{338,339}$→Met and kd2: Asp^{453}→Asn) failed to rescue Smo phosphorylation (Figure 3.2D; lane 6, 8). In conclusion, we can use the described mobility shift assays of Smo^{SD} as a read-out for Gprk2-mediated Smo phosphorylation. We expect Gprk2 to directly phosphorylate Smo, although we did not formally rule out the possibility of an indirect mechanism involving other kinases.

3.2.3. Published Gprk2 phosphorylation sites can not fully account for Gprk2-dependent Smo phosphorylation and regulation.

Gprk2 phosphorylation sites in Smo have been mapped in a recent publication by the Jiang group. The authors proposed four Ser/Thr residues located at two different clusters (GPS1 and GPS2) within the Smo C-terminus as Gprk2 substrates (Chen et al., 2010). We mutated both clusters or all four Ser/Thr residues to non-phosphorylatable Ala residues in the SD backbone ($Smo^{SD.GPSA12}$; Figure 2.1) and tested the behavior of this mutant in our mobility shift assay. To our surprise, the response of $Smo^{SD.GPSA12}$ to Gprk2 depletion was indistinguishable to that of Smo^{SD}, suggesting that mutating the GPS clusters has not grossly changed Gprk2-dependent phosphorylation of Smo^{SD} (Figure 3.2E). This implies that other Gprk2 phosphorylation sites must exist within Smo.

In their study, the authors noted only a minor signaling impairment with the $Smo^{SD.GPSA12}$ mutation *in vivo* and they therefore proposed an additional kinase-independent function of Gprk2 in Smo regulation (Chen et al., 2010). To validate their findings, we made our own Smo^{SD} and $Smo^{SD.GPSA12}$ transgenic flies. By using the *Φ*C31-based integration system, all Smo expression constructs were incorporated into the same genomic locus to ensure equal transcription of the transgenes. Expression of Smo^{SD} in the D compartment of the wing disc using the *ap*-Gal4 driver

led to Hh-independent ectopic A *en* expression throughout the A compartment (Figure 3.2F), consistent with the constitutive activity of Smo^{SD} (Jia et al., 2004). In a *gprk2* mutant background Smo^{SD} failed to turn on ectopic *en* consistent with the requirement of Gprk2 for Hh target gene expression (Figure 3.2G; arrowhead). However, En was still expressed in the Hh-responsive zone of the A compartment (Figure 3.2G). This surprising finding suggests that Gprk2 is not absolutely required for Hh signal transduction. This is likely because mimicking full PKA/ Ck1 phosphorylation of Smo and the presence of Hh are sufficient to turn the highest known Hh target gene, *en*, on. On the other hand, Smo^{SD} requires Gprk2 for promoting Hh signaling in the far A region of the disc. Some aspects of this conundrum will be discussed in the the second result chapter of this thesis (Chapter 4).

We next examined the Hh signaling output driven by $Smo^{SD.GPSA12}$ expressed in the wing disc. Interestingly, in our hands, $Smo^{SD.GPSA12}$ promoted far A *en* expression to the same extent as Smo^{SD} (Figure 3.2H). Our observations differ from the data presented by Chen and colleagues. We have no explanation for this discrepancy. However, technical differences such as different gene expression drivers, staining and imagining techniques used could be contributing factors. In conclusion, we find that $Smo^{SD.GPSA12}$ fails to replicate the phenotype caused by loss of Gprk2 and has only a minor, if any, effect on Hh target gene expression. Together, with the observation that $Smo^{SD.GPSA12}$ is still phosphorylated by Gprk2, we propose that other Gprk2 sites must exist in Smo. We anticipate that these additional phosphorylation sites are of functional importance for Hh signaling.

3.3. Mapping of Gprk2 phosphorylation sites.

Since the beginning of my PhD studies, I worked towards the identification of Gprk2 phosphorylation sites within Smo. We decided to use two approaches. The first was based on cloning Smo variants and testing these mutants in our EM shift assay. For the second approach, we used a highly sensitive label-free quantitative liquid chromatography/tandem mass spectrometry (LC-MS/MS) method to directly monitor Gprk2-dependent Smo phosphate modifications.

3.3.1. Discovery of three Gprk2 phosphorylation clusters in Smo truncations.

To identify functionally important Gprk2 phosphorylation sites, we expressed a series of GFP-tagged C-terminally truncated Smo mutants in S2 cells and tested their response to Gprk2 depletion in our EM shift assay. We noted that the $Smo^{\Delta 663}$ construct (Figure 2.1), which is truncated at amino acid 663 and lacking ~75% of the Smo C-terminus, is phosphorylated by Gprk2 as is evident by a mobility shift in response to Gprk2 depletion (Figure 3.3A). The migration of the $Smo^{\Delta 603}$ band, a Smo mutant truncated at amino acid 603 (Figure 2.1), was not affected by loss of Gprk2 (Figure 3.3 A). This suggests that the intervening 60 amino acids harbor potential Gprk2 phosphorylation sites. This stretch encodes a total of 15 Ser/Thr residues, grouped into three clusters (c1 to c3; Figure 3.4A). Mutating all 15 Ser/Thr residues to non-phosphorylatable Ala ($Smo^{\Delta 663.c1\text{-}3A}$) rendered the protein insensitive to Gprk2 phosphorylation (Figure 3.3A). Interestingly, 9 of the 15 sites are known in the literature to be phosphorylated in response to Hh stimulation (Figure 3.4A), but the responsible kinase remains unknown (Zhang et al., 2004). These nine residues are located throughout all three Gprk2 phosphorylation clusters and our work suggests that Gprk2 is the kinase responsible for the phosphorylation at these and potentially all 15 Ser/Thr residues in the Smo C-terminus between amino acid 603 and 663.

To further validate whether Gprk2 phosphorylates sites within all three clusters, we analyzed single cluster mutations. We modified our mobility shift assay by separating protein samples on PhosTag-containing SDS-PAGE gels. PhosTag specifically retards phosphorylated proteins and increases the resolution of the EM shifts. Under these conditions, the $Smo^{\Delta 603}$ signal appeared as a high molecular weight smear, extending from about 100kDa to the top of the gel (Figure 3.3B, C). Gprk2 depletion or mutation of all three Gprk2 clusters had the same effect on the appearance of $Smo^{\Delta 603}$. In both cases, the smearing was strongly reduced and the signal of the 100 KDa band was increased, indicating that most, if not all, phosphate modifications were removed under these conditions (Figure 3.3B, C). Each single cluster mutation in the presence of endogenously expressed Gprk2 caused a modest decrease of the smearing but the faster migrating bands were more prominent (Figure 3.3B, C). Therefore, each of the single cluster mutations seemed to give a partial mobility shift compared to the full shift observed when all

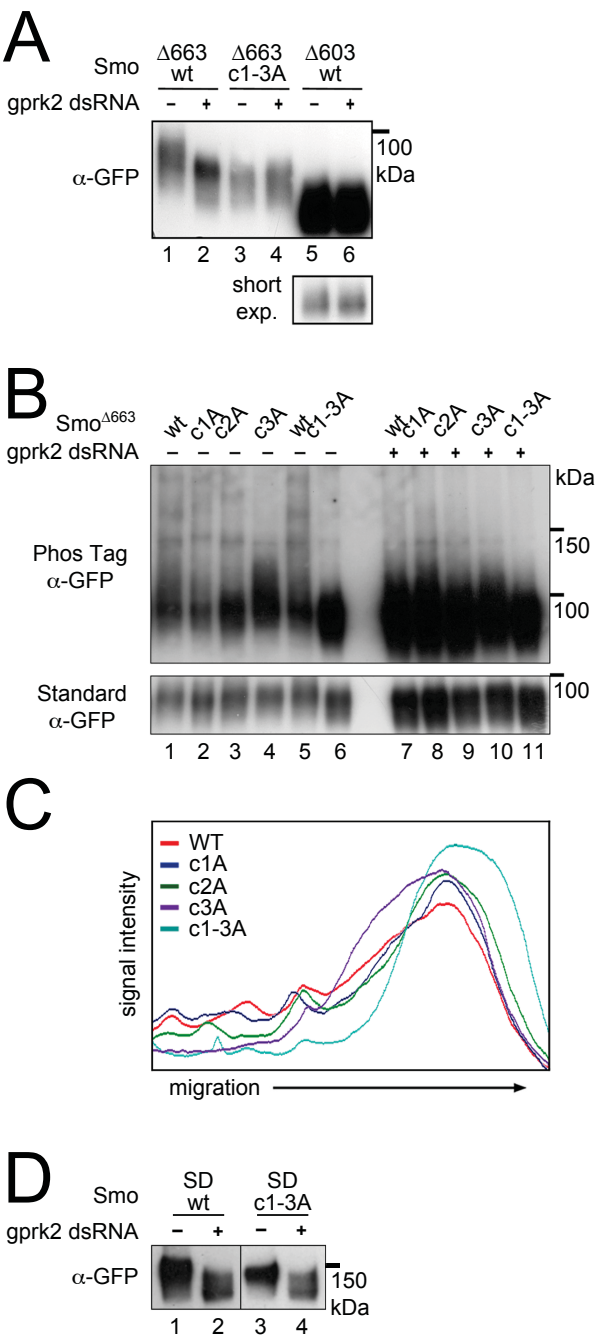

Figure 3.3. Gprk2 phosphorylates Smo within several clusters located in the cytoplasmic tail.

(A) Immunoblot analysis of truncated GFP-tagged Smo molecules, expressed in cells treated +/- *gprk2* dsRNA. Ala substitution of all three Ser/Thr clusters eliminates Gprk2-dependent phosphorylation of Smo. **(B)** Immunoblot analysis of Smo^{core}-GFP or mutants with one or all three Gprk2 phosphorylation clusters mutated to Ala, expressed in cells +/- *gprk2* dsRNA. Samples were separated on Phos-Tag-conjugated (*top panel*) or standard (*bottom panel*) SDS-PAGE gels. **(C)** Plot of signal intensity versus migration distance for the immunoblot of Smo^{core}-GFP mutants (-*gprk2* dsRNA conditions, left side of panel **(B)**. Ala substitutions within each Ser/Thr cluster increased Smo mobility, suggesting sites in all three clusters are phosphorylated. **(D)** Additional Gprk2 phosphorylation sites outside of clusters 1, 2, and 3 exist in Smo. Western blot analysis of GFP immunoprecipitates from S2 cells expressing Smo^{SD}-GFP or $Smo^{SD.c1-3A}$-GFP, with or without *gprk2* depletion. The blot was probed with anti-GFP antibody to visualize tagged Smo protein. All bands are from the same exposure of a single blot with intervening lanes removed. $Smo^{SD.c1-3A}$-GFP migrates as a tighter band than Smo^{SD}-GFP in control cells, suggesting that it is less phosphorylated. However, it still undergoes a phosphoshift in response to depletion of the kinase, indicating that additional Gprk2 phosphorylation sites exist.

three clusters are non-phosphorylatable. This suggests that Gprk2 uses sites located within all three identified Gprk2 clusters.

We next engineered the Ala substitutions of all three Gprk2 clusters in the full-length Smo^{SD} backbone. The resulting Smo variant, $Smo^{SD.c1-3A}$, migrated faster compared to Smo^{SD}, confirming that we have reduced Gprk2 phosphorylation (Figure 3.3D). However, $Smo^{SD.c1-3A}$

still responded to Gprk2 depletion by substantially shifting down (Figure 3.3D). Overall, this suggests that additional Gprk2 sites must exist in full-length Smo.

3.3.2. Mass-spec analysis reveals a fourth cluster of Gprk2 phosphorylation in Smo.

To specifically identify Gprk2 phosphorylation sites, we used a label-free semi-quantitative liquid chromatography/tandem mass spectrometry (LC-MS/MS) method as a second and complimentary approach. In brief, large quantities of Smo^{SD} were purified from S2-R+ cells treated with *gprk2* or control dsRNA. After digesting with the appropriate proteases, both samples were subjected to LC-MS/MS analysis and the abundance of individual Smo phosphopeptides was quantified. We normalized phosphorylated peptides to their non-phosphorylated form and compared the obtained ratios between the two conditions. This allowed us to express changes in phosphopeptide abundance in response to Gprk2 depletion as differential ratio relative to the control knockdown. The results are summarized in Table 2 and Gprk2-dependent Smo phosphorylation sites are presented schematically (Figure 3.4A). A more detailed analysis of the MS data is shown in the supplementary material (Table S1). We confirmed that Gprk2 phosphorylates all four sites in cluster 1 (Ser^{604}, Thr^{606}, Thr^{610}, Thr^{612}) and three out of five sites in cluster 3 (Ser^{658}, Ser^{659}, Ser^{660}). Phosphopeptides corresponding to these sites were strongly downregulated (generally 9-fold or higher) in response to Gprk2 depletion, which is in agreement with the robust effect we observed in our mobility shift assays. We were unable to obtain any peptide covering Gprk2 cluster 2, most likely due to technical limitations of the LC-MS/MS technique. However, four of the six sites (Ser^{626}, Ser^{627}, Thr^{629}, Ser^{633}; Figure 3.4A) are known to be phosphorylated after Hh treatment (Zhang et al., 2004). We speculate that at least some of these sites are used by Gprk2, because GRKs often phosphorylate multiple Ser/ Thr residues located within a larger stretch of their GPCR substrates. The fact that Gprk2 phosphorylates the neighboring Ser/Thr cluster (c1 and c3) supports this idea. The mass spectrometry experiments led us also to the identification of an additional fourth Gprk2 phosphorylation cluster consisting of three Ser residues (Ser^{674}, Ser^{679}, Ser^{682}). These sites are located between the first and second PKA/Ck1 phosphorylation clusters within the Smo autoinhibitory domain (SAID; Figure 3.4A) The drop in phospho-peptide abundance following

Table 2. Fold downregulation of Smo^{SD} peptide phosphorylation in Gprk2-depleted cells

Region (amino acids)	Phosphosite	T+AN1	T+AN2	T	C
cluster 1 (604-612)	**S**ITLY/NTHT	*nd*	*nd*	*nd*	10.0
	SI**T**LY/NTHT	*nd*	*nd*	*nd*	*nd*
	SI**T**LY/NTHT	*nd*	*nd*	*nd*	6.0
	SITLY/N**T**HT	*nd*	*nd*	*nd*	88.2
	SITLY/NTH**T**	*nd*	*nd*	*nd*	23.9
	SITLY/N**T**H**T**	*nd*	*nd*	*nd*	51.9
cluster 2 (626-635)	SSETNDISST	*nd*	*nd*	*nd*	*nd*
cluster 3 (651-660)	TGAATGN**S**SS TGAATGNS**S**S TGAATGNSS**S**	6.8	8.9	11.7	*nd*
	TGAATGN**SS**S TGAATGN**S**S**S** TGAATGNS**SS**	11	16.4	13.0	*nd*
	TGAATGN**SSS**	12.2	8.8	*nd*	*nd*
cluster 4 (675-683)	**S**VRHVSVES	*nd*	*nd*	4.7	*nd*
	SVRHV**S**VES	7.4	3.2	11.7	*nd*
	SVRHV**S**VES	**	**	26.9	*nd*
	SVRHV**S**VE**S**	34.2	7.1	12.2	*nd*
	SVRHV**S**VE**S**	*nd*	*nd*	28.0	*nd*
GPS1 (738-745)	RED**S**TDVE	0.9	1.2	1.9	2.0
	REDS**T**DVE	2.4	1.6	1.3	2.0
	RED**ST**DVE	5	2.4	3.2	4.7

**, signal in Gprk2-depleted cells too low to measure. T, trypsin; AN, AspN; C, chymotrypsin

gprk2 depletion was in the same range as observed for cluster 1 and cluster 3 sites, arguing that these sites are *bona fide* Gprk2 sites. This is in contrast to relatively minor change in the phosphorylation of GPS1 (Ser^{741}, Thr^{742}). Here, loss of Gprk2 resulted only in a 2-4-fold phosphorylation decrease, raising the possibility that another kinase might also phosphorylate these residues (Table 2).

In conclusion, our results from Smo mobility shift experiments and phospho-proteomic analysis suggest that Gprk2 phosphorylates Smo within four clusters located in its C-terminus.

3.3.3. Mobility shift assays and phospho-specific antisera validate our mapping results.

To test whether we have identified all Gprk2 phosphorylation sites, we mutated all Ser/Thr sites located within the four Gprk2 clusters to Ala in the Smo^{SD} backbone. The resulting mutant ($Smo^{SD.c1\text{-}4A}$; Figure 2.1) seemed insensitive to Gprk2 depletion. $Smo^{SD.c1\text{-}4A}$ did not display any EM shift on an immunoblot and migrated at the same height as Smo^{SD} in response to *gprk2* knockdown. (Figure 3.4B). Therefore, we conclude that our four Gprk2 phosphorylation clusters most likely cover all Gprk2 phosphorylation sites present in Smo.

To further validate our mapping results, we generated two phospho-specific antisera against cluster 1 sites (anti-Smo-pS^{604} and anti-Smo-pT^{610}/pT^{612}). Both antibodies detected Smo^{SD} or Hh-stimulated wt Smo proteins on a western blot (Figure 3.4C, D). As expected, Ala mutants of cluster 1 sites in either wt or Smo^{SD} background were not recognized by either antibody, suggesting that they both reliably detect their corresponding phospho-epitopes (Figure 3.4C, D). More importantly, Gprk2 deletion strongly reduced reactivity of both antibodies in the two tested conditions (Figure 3.4C, D). This confirms that the three sites probed with the phospho-specific antibodies are *bona fide* Gprk2 sites and validates the results obtained by mutagenesis and LC-MS/MS analysis.

3.4. Functional characterization of Gprk2-dependent Smo regulation in S2 cells.

To test the functional consequences of Smo phosphorylation throughout Gprk2, we took advantage of the *ptc-luciferase* (*ptc-luc*) transcriptional reporter assay. This method allows the quantitative evaluation of Hh pathway activity in our tissue culture system, S2-R+ cells. The assay is based on the promoter of the Hh target gene *ptc*, which drives expression of a firefly Luciferase transgene. The firefly Luciferase signal is normalized to the emission of *Renilla* Luciferase, which is expressed under the control of a constitutive promoter and therefore correlates to the number of cells transfected.

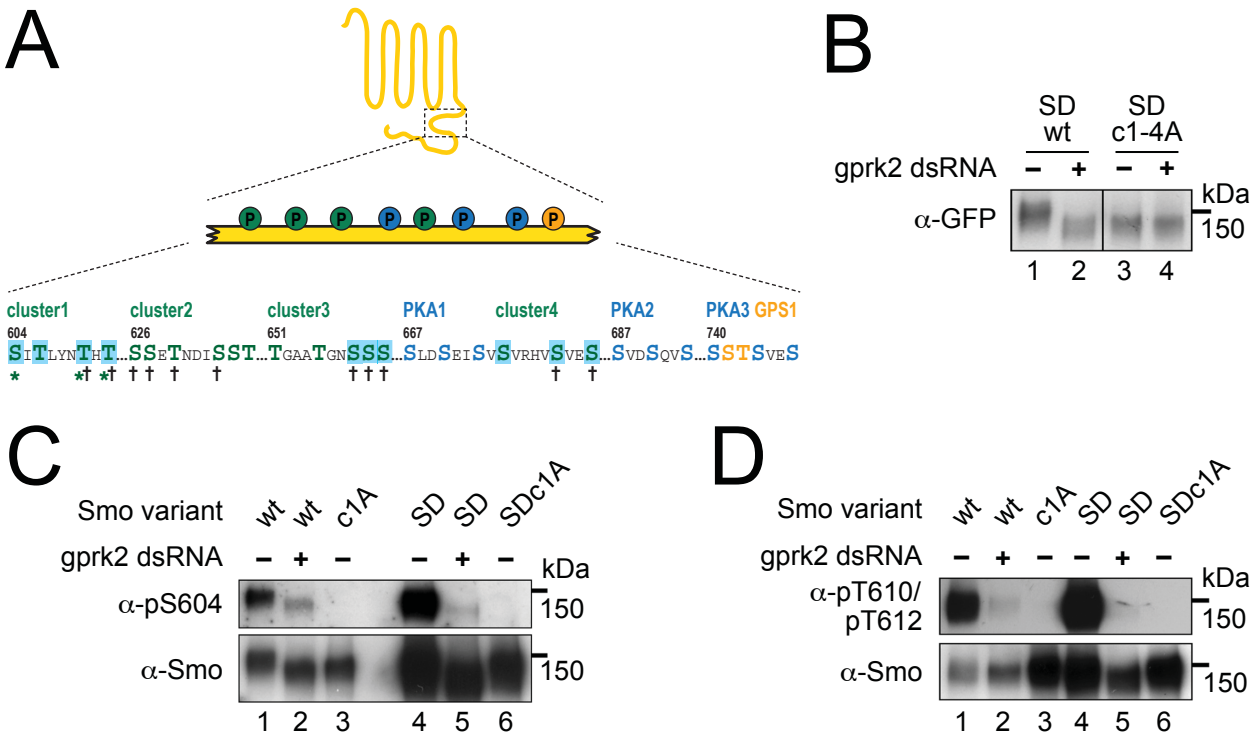

Figure 3.4. Identification of four Gprk2 phosphorylation in Smo.

(A) Schematic of relevant phosphorylation site within the Smo C-terminus. Shown are the four Gprk2 clusters verified by mutagenesis and electro-mobility shift assay. Highlighted in turquoise are sites confirmed by LC-MS/MS analysis. *, sites validated by phospho-specific antisera. †, known phosphorylation sites in Smo in response to Hh stimulation (Zhang et al., 2004). PKA sites - blue - and GPS sites - yellow - (Chen et al., 2010) for reference. **(B)** Immunoblot analysis of Smo^{SD} or $Smo^{SD.c1-4A}$ expressed in cells treated +/- *gprk2* dsRNA. Ala substitution of all four Ser/Thr clusters eliminates Gprk2-dependent phosphorylation of full-length Smo. **(C, D)** Immunoblot of Smo^{WT}, Smo^{c1A}, Smo^{SD}, or $Smo^{SD.c1a}$, expressed in cells +/- *gprk2* dsRNA. Blots were probed with Smo antisera: anti-pS^{604} **(C)** or anti-pT^{610}/pT^{612} **(D)**. Phosphorylation at both sites was strongly decreased by *gprk2* depletion.

3.4.1. Target gene expression downstream of Smo^{SD} requires phosphorylation of Gprk2 sites.

Smo^{SD} was constitutively active and promoted ectopic Hh target gene expression in the *Drosophila* wing disc in a Gprk2-dependent manner (Figure 3.2F, G). We first tested whether Gprk2 is also required for Smo^{SD}-driven *ptc-luc* reporter activity in S2 cells. As expected, the expression of Smo^{SD} led to a robust induction of the reporter gene (Figure 3.5A; second bar, set to a 100%), about 10-fold over basal levels (Figure 3.5A; first bar, 9.2%). Knockdown of *gprk2* by treating the cells with a mixture of dsRNA targeting the UTRs of endogenous *gprk2* mRNA notably reduced signaling activity of Smo^{SD}. In this condition, reporter activity was about 5-fold

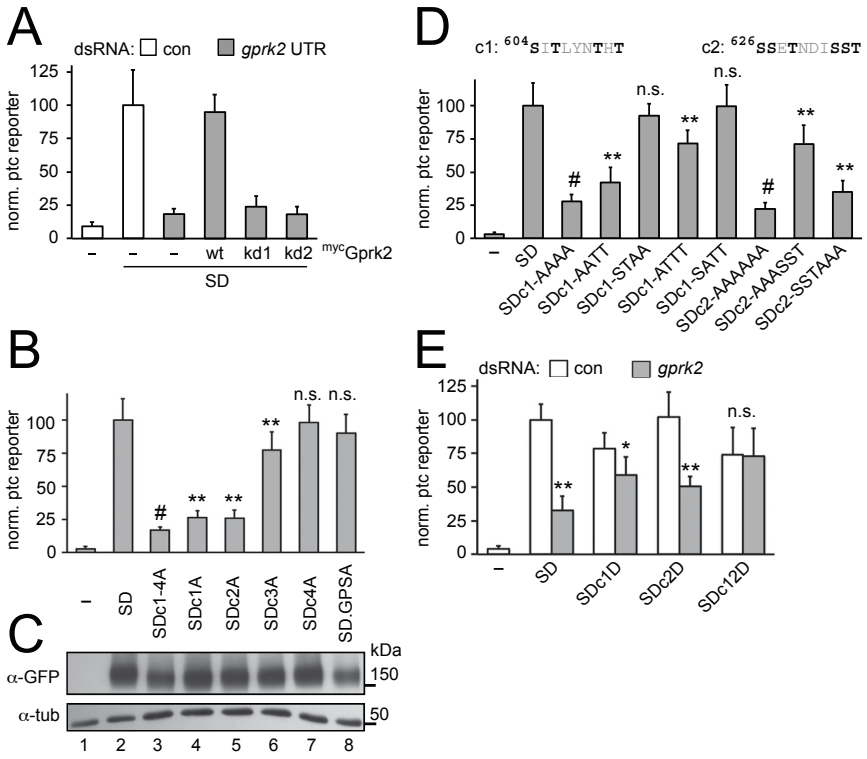

Figure 3.5. Gprk2 promotes target gene expression downstream of Smo^{SD} in S2 cells in a catalytic activity-dependent manner.

(A) Rescue of Smo^{SD}-GFP-driven *ptc-luc* reporter activity in *gprk2*-depleted S2-R+ cells. Smo^{SD}-GFP was transfected in S2 cells along with the indicated Gprk2 variants and *ptc-luc* activity (normalized to *pCMV-renilla*) was measured. Treatment of cells with *gprk2 5'-* and *3'-UTR* dsRNAs reduced *ptc-luc* reporter activity, and this was fully rescued by re-expressing wild-type Gprk2 but not kinase-dead Lys$^{338/339}$→Met (kd1) or Asp^{453}→Asn (kd2) mutants of Gprk2. Data represent mean ± standard deviation. **(B)** *ptc-luc r*eporter assay of Gprk2 phosphosite Ala mutants. Ala substitutions at phosphorylation cluster 1 and 2 most strongly impair Smo activity. **, significantly lower than Smo^{SD}, p<.001, *T*-test. #, significantly lower than Smo^{SDc1A} and Smo^{SDc2A}, p<.01. n.s., not significantly different from Smo^{SD}. **(C)** Immunoblot analysis of Gprk2 phosphorylation cluster Ala mutant Smo^{SD}-GFP variants. Proteins were expressed at similar levels. **(D)** Multisite phosphorylation within Gprk2 phosphorylation cluster 1 and 2 is important for Smo^{SD} activation. *ptc-luc* reporter activity driven by Smo^{SD} variants with a subset of sites within cluster 1 or 2 mutated to Ala. Mutation of Ser^{604} and Thr^{606} (Smo$^{SD.c1AATT}$) significantly reduced activity (**, p<0.001 vs Smo^{SD}), but not as much as mutation of all four residues (#, p<0.001 vs Smo$^{SD.c1AATT}$). Mutation of Ser^{604} and Thr^{606} individually (Smo$^{SD.c1ATTT}$ and Smo$^{SD.c1SATT}$) had much less effect than mutating both. Mutation of both Thr^{610} and Thr^{612} in cluster 1 (Smo$^{SD.c1STAA}$) had no significant effect on Smo activity. The situation was similar for cluster 2, where mutating just three residues in either half of the cluster (Smo$^{SD.c2AAASST}$ and Smo$^{SD.c1SSTAAA}$) reduced activity (**, p<0.001 vs Smo^{SD}), but both had less effect than mutating all six (#, p<0.001 vs Smo$^{SD.c2AAASST}$ or Smo$^{SD.c2SSTAAA}$). **(E)** *ptc-luc* reporter assay of cells treated with dsRNA targeting *β-gal* (control) or *gprk2* and expressing the indicated Smo^{SD}-GFP phosphosite Asp variants. The Gprk2 cluster 1 and 2 phosphomimetic form of Smo^{SD} no longer responds to depletion of the kinase. * and **, significantly lower than the respective *β-gal* dsRNA control, p<.01 and .001, respectively. n.s., not significantly different from control.

downregulated (Figure 3.5A; third bar, 18.4%), but still significantly elevated over basal levels. This is consistent with our *in vivo* observations, where loss of Gprk2 greatly impaired but did not completely block Smo^{SD} signaling in the A part of the wing disc (Figure 3.2G and data not shown). To test whether the reduction in Smo^{SD}-driven reporter activity is specific to the loss of Gprk2, a rescue experiment was performed. As shown in Figure 3.5A, Smo^{SD}-dependent *ptc-luc* reporter activity could be restored by expressing the wt Gprk2 protein. The rescue required catalytic activity of Gprk2 because kinase-dead mutants of Gprk2 (Figure 3.5A, bar 5, 6) failed to reinstate Smo^{SD} signaling. Western blot analysis of cell extracts complementing this experiment demonstrated that Gprk2 has no effect on Smo^{SD} protein levels or stability, ruling this out as a possible explanation for the observed changes in reporter activity (Figure 3.2D). In addition, the blot demonstrated that phosphorylation of Smo^{SD} also requires catalytically active Gprk2. Therefore, phosphorylation and signaling activity of Smo^{SD} correlate with each other. Taken together, we propose, that direct phosphorylation of Smo^{SD} by Gprk2 is necessary and sufficient for inducing its maximal signaling activity.

If the proposed model is accurate, mutation of all Gprk2 phosphorylation sites to non-phosphorylatable Ala residues should replicate the reduction of Smo^{SD} signaling seen in the absence of Gprk2. Indeed, in a *ptc-luc* reporter assay, $Smo^{SD.c1\text{-}4A}$ yielded roughly 20% of the Smo^{SD}-driven reporter activity (Figure 3.5B), which is nearly identical to the observed drop in Smo^{SD} signaling following *gprk2* knock down. It is worth pointing out, however, that $Smo^{SDc1\text{-}4A}$ still increased reporter transcription significantly over basal levels. Phosphorylation within cluster 1 and 2 seems to be mainly responsible for Smo^{SD} activation, as mutating the corresponding sites within each cluster alone ($Smo^{SD.c1}$ and $Smo^{SD.c2}$) strongly impaired reporter activity. However, both mutants were significantly more active than $Smo^{SD.c1\text{-}4A}$, suggesting that phosphorylation within both clusters is required. Mutation of the third Gprk2 cluster had a weak effect on *ptc-luc* reporter activity, whereas blocking phosphorylation at the fourth cluster or at the published GPS sites had no significant effect on *ptc-luc* reporter activity (Figure 3.5B). All Smo^{SD} variants were expressed at similar levels (Figure 3.5C), therefore, we conclude that Gprk2 phosphorylation within cluster 1, 2 and to a lesser extent within cluster 3 is necessary for full activation of Smo^{SD} signaling.

3.4.2. Smo^{SD} gets activated through multisite phosphorylation within clusters 1 and 2.

In an attempt to single out critical Ser/Thr residues for Smo^{SD} activation, we mutated various subsets of Gprk2 cluster 1 and cluster 2 sites. None of the tested single or double Ser/Thr to Ala substitutions in cluster 1 was sufficient to replicate the full effect of mutating all four sites, but some variants significantly decreased reporter activity (Figure 3.5D). Similar results were obtained for cluster 2 sites as well, where we tested two subsets, each exchanging three out of the six cluster 2 sites (Figure 3.5D). These results suggest that multisite phosphorylation of cluster 1 and 2 sites is required for Smo^{SD} activation rather than the phosphorylation of distinct and critical residues. The fact that some mutations displayed partial responses in the reporter assay could indicate a graded activation of Smo^{SD}, depending on the phosphorylation extent.

We have shown that multisite phosphorylation of cluster 1 and 2 sites is required for Smo^{SD} activation, and we next wondered whether it is also sufficient. We mimicked the negative charges of the phosphate groups by mutating the Ser/Thr residues within cluster 1 and 2 to Asp (Asp). The resulting Smo^{SD} variant, $Smo^{SD.c12D}$ (Figure 2.1), should activate *ptc-luc* reporter expression to a comparable extent as Smo^{SD} and independently of the absence or presence of Gprk2. This seems to be true as $Smo^{SD.c12D}$ did not respond to Gprk2 depletion and induced strong reporter gene activity. However, $Smo^{SD.c12D}$ yielded only about 75% of the Smo^{SD} signal (Figure 3.5E). This might be due to the fact that Asp substitutions are not perfectly mimicking the full charge of the phosphate modification. Under physiological conditions, the negative charge of phosphorylated Ser/Thr residues is higher than the one produced by an Asp residue (Pearlman et al., 2011). Consistent with our previous results from the Ala substitutions, we observed that both single cluster mutants ($Smo^{SD.c1D}$ and $Smo^{SD.c2D}$) were only partially resistant to *gprk2* knockdown (Figure 3.5E). Taken together, this implies that phosphorylation at both clusters is required and sufficient to promote full Smo^{SD} signaling.

3.4.3. Gprk2 regulates the signaling output of Hh-activated wt Smo.

So far we focussed on the effect Gprk2 has on the signaling response of constitutively active Smo^{SD}. We next addressed whether Gprk2 also affects normal, Hh-dependent Smo signaling using *ptc-luc* reporter assays. As shown in Figure 3.6A, Gprk2 depletion in S2 cells reduced Hh-

induced endogenous Smo signaling by about 70%. As expected, re-expression of a wt *gprk2* transgene almost completely restored reporter activity, implying that Gprk2 is required for Hh signaling in the same way as it is for Smo^{SD} (Figure 3.6A). If this notion is correct, one would expect that mutating all Gprk2 phosphorylation sites to Ala in a wt Smo backbone should also decrease the Hh response independently of Gprk2. To visualize the effect of the resulting Smo variant ($Smo^{c1\text{-}4A}$; Figure 2.1) in a *ptc-luc* reporter experiment, expression of endogenous Smo needs to be eliminated. We depleted endogenous Smo by targeting the 3′UTR of the *smo* transcript with dsRNA. The knockdown was efficient, as it reduced Hh-induced endogenous Smo signaling by 86% (Figure 3.6B). Our *smo* transgenes are insensitive to the knockdown procedure, because they lack the 3′UTR sequence. As expected, expression of wt Smo in this setup rescued *ptc-luc* reporter activity and exceeded endogenous Smo signaling (Figure 3.6B). In contrast, $Smo^{c1\text{-}4A}$ had only very limited signaling capabilities. It yielded a reporter signal of 24% of the endogenous Hh response, which was roughly 2-fold higher than residual endogenous Smo signaling activity (Figure 3.6B). The strong signaling impairment of Hh-induced $Smo^{c1\text{-}4A}$ is in agreement with the weaker *ptc-luc* reporter output driven by the $Smo^{SDc1\text{-}4A}$ mutant. Mutating the Gprk2 clusters individually in the wt Smo background also recapitulated the results from the Smo^{SD} *ptc-luc* reporter experiments. Ala substitution of the four cluster 1 sites (Smo^{c1A}) or six cluster 2 sites (Smo^{c2A}) caused a significant reduction of *ptc-luc* reporter activity but both mutants retained substantially higher signaling competence than $Smo^{c1\text{-}4A}$ (Figure 3.6B). Blocking of the phosphorylation at cluster 3 (Smo^{c3A}) or cluster 4 (Smo^{c4A}) caused only a minor, non-significant reduction of the reporter response (Figure 3.6B). Therefore, as already described for Smo^{SD}, phosphorylation within cluster 1 and 2 is crucial for proper signaling of wt Smo.

To validate that mutating the Gprk2 clusters did not affect Smo expression and subcellular localization, we determined cell surface expression of $Smo^{c1\text{-}4A}$. Following Hh stimulation and cell surface biotinylation we detected more $Smo^{c1\text{-}4A}$ protein at the membrane relative to wt Smo (Figure 3.6C). This result is consistent with the membrane accumulation of wt Smo in Gprk2-depleted cells (Figure 3.1L) and $Smo^{c1\text{-}4A}$ replicates this phenotype independently of Gprk2 itself. These results strongly limit the possibility that the lack of $Smo^{c1\text{-}4A}$ activity is due to improper protein expression or localization.

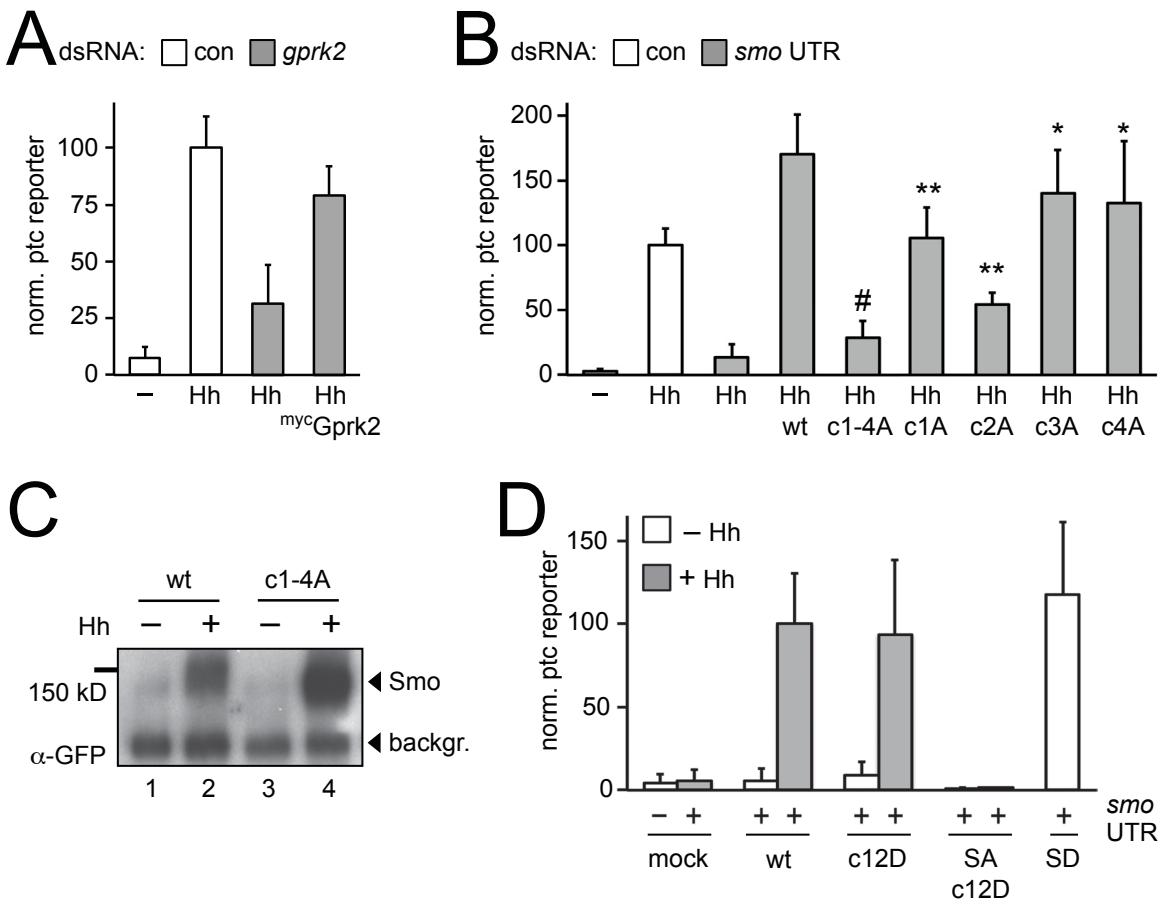

Figure 3.6. Gprk2 regulates the signaling activity of wt Smo in S2 cells.

(A) Rescue of *ptc-luc* reporter activity in *gprk2*-depleted S2-R+ cells. Treatment of cells with *gprk2 5'-* and *3'-UTR* dsRNAs reduced Hh-dependent *ptc-luc* reporter activity, and this was rescued by re-expressing wild-type Gprk2. For this experiment, cells were cultured at the restrictive temperature for Gprk2 of 29°C. **(B)** *ptc-luc* reporter assay of control or *smo 3'UTR* dsRNA-treated cells, transfected without (-) or with a Hh^N expression vector along with the indicated Smo-GFP variants. Ala substitution of all four cluster 1 or all six cluster 2 phosphorylation sites impairs Smo activity but not as strongly as mutation of all four Gprk2 clusters (18 sites). **, $p<.00001$ vs Smo^{WT}. #, $p<.0001$ vs Smo^{c1A} and Smo^{c2A}. $p<.01$. n.s., not significantly different from Smo^{SD}.(**, $p<0.001$ vs Smo^{WT}). Cluster 3 or 4 mutations have modest effects on signaling activity. *, $p<.05$ vs Smo^{WT}. **(C)** Immunoblot analysis of cell-surface wild-type Smo-GFP and Smo^{c1-4A}-GFP in cells treated with or without Hh. Cell surface proteins were labeled by surface biotinylation. After lysis, biotinylated proteins were recovered by avidin-mediated affinity purification, and separated by SDS-PAGE. Smo was detected in the biotin-labeled surface protein fraction by immunoblotting with anti-GFP antibody. A background band served as a loading control to ensure that the starting samples had equivalent amounts of protein. Mutation of the Gprk2 phosphorylation sites did not impair the ability of Smo to reach the cell surface in response to Hh. **(D)** *ptc-luc* reporter assay of cells treated with *smo 3'UTR* dsRNA and transfected with or without a Hh^N expression vector, along with empty vector (mock) or the indicated Smo-GFP, Smo^{SA}-GFP, or Smo^{SD}-GFP variants. The Gprk2 phosphomimetic form of Smo does not show constitutive activity.

Analogous to the Smo^{SD} *ptc-luc* reporter experiment series, we tested the effect of mimicking Gprk2 phosphorylation within the first two clusters. We substituted the corresponding ten Ser/Thr sites to Asp in a wt Smo backbone (Smo^{c12D}; Figure 2.1). In a *ptc-luc* reporter assay, signaling of Smo^{c12D} was Hh-dependent and the behavior of this mutant was practically identical to wt Smo (Figure 3.6D). We conclude that mimicking Gprk2 phosphorylation is not sufficient to activate Smo independently of Hh. This stands in contrast to the role PKA and Ck1 have in Smo activation. Mutating the three PKA/Ck1 cluster to Asp (Smo^{SD}) resulted in constitutive, Hh-independent activity (Figure 3.6D). Our result suggest that Gprk2 targets Smo molecules already phosphorylated by PKA/Ck1. In support of this idea, we found that simulating Gprk2 phosphorylation in a Smo variant, which could not be phosphorylated by PKA/Ck1 ($Smo^{SA.c12D}$; Figure 2.1), was constitutively inactive, even in the presence of Hh (Figure 3.6D). Taken together, we conclude that Gprk2 acts downstream of PKA/Ck1, consistent with typical GRK biology, which postulates that GRKs preferentially target active GPCRs.

3.5. Gprk2 phosphorylation promotes Smo dimerization.

Hh-dependent Smo activation by PKA/Ck1 phosphorylation triggers a conformational change of Smo, which results in the dimerization of Smo C-terminal tails. In a study by the Jiang group, the authors measured engagement of Smo C-termini and found a direct correlation to Smo signaling activity (Zhao et al., 2007). The quantification of the dimerization was based on fluorescence resonance energy transfer (FRET) efficiency between Smo molecules tagged at the C-terminus with CFP or YFP, respectively. FRET between the two tags was low in the absence of Hh or when PKA/Ck1 phosphorylation was prevented, implying that the Smo tails are not interacting with each other. FRET efficiency increased in the presence of Hh and was constitutively high when Smo^{SD} was expressed. FRET requires close proximity of the fluorophores, suggesting that the cytoplasmic tails of Smo are dimerized under these conditions.

We speculated that Gprk2 phosphorylation could contribute to the dimerization of Smo C-terminus downstream of PKA/Ck1. In other words, in order to achieve complete dimerization and therefore its most active state, Smo requires direct phosphorylation of Gprk2. To test this hypothesis, we modified the published FRET-based assay into a bioluminescence resonance

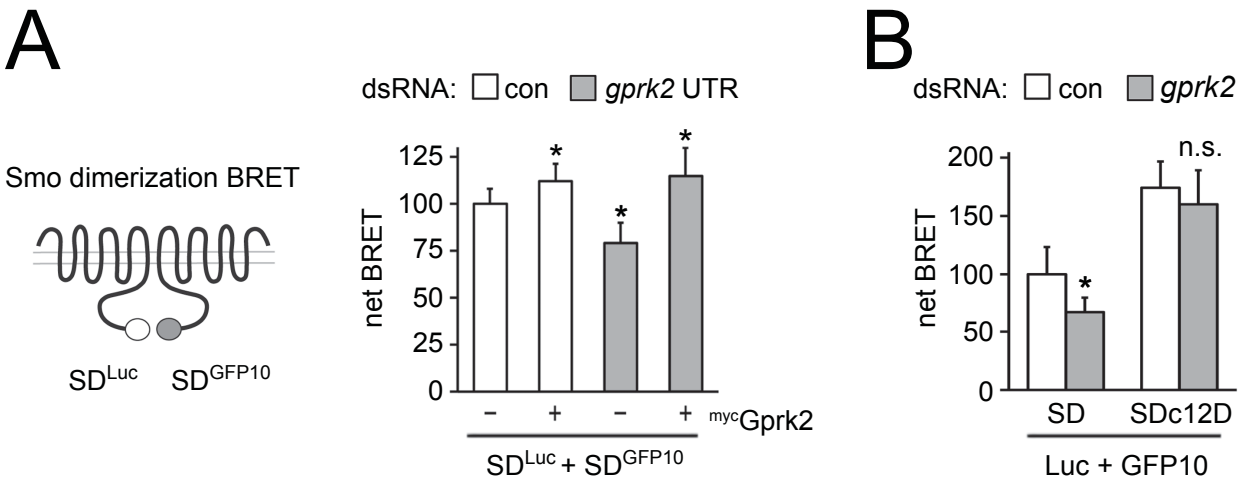

Figure 3.7. Gprk2 promotes Smo dimerization.

(A) BRET efficiency between C-terminally GFP10- and RLucII-tagged Smo^{SD} variants in S2-R+ cells. Cells were treated with control or *gprk2* dsRNA and transfected without (-) or with (+) myc-tagged Gprk2 in addition to the Smo variants. Data are expressed as mean net BRET ± standard deviation. Gprk2 promotes Smo dimerization. *, significantly different from control condition, $p<.001$. **(B)** BRET efficiency between C-terminally GFP10- and RLucII-tagged Smo^{SD} or $Smo^{SD.c12D}$ in S2 cells. Cells were treated with dsRNA targeting *β-gal* (control) or *gprk2* prior to transfection of the indicated Smo variants. The Gprk2 phosphomimetic form of Smo does not respond to *gprk2* depletion. *, significantly lower than control, $p<.01$. n.s., not significantly different from control.

energy transfer (BRET) application allowing us to measure Smo dimerization in intact cells. We tagged Smo^{SD} at the C-terminus either with *Renilla* Luciferase II or GFP10, and co-expressed the two Smo^{SD} variant in S2 cells. Following addition of the Luciferase substrate, GFP10 and Luciferase signals were measured and BRET ratios were calculated. Non-specific background BRET was subtracted from all datasets to yield net BRET. Expression of the two Smo^{SD} constructs in S2 cells under control conditions resulted in a robust net BRET (Figure 3.7A , set to 100%). Gprk2 depletion significantly reduced net BRET, whereas overexpression of the kinase increased BRET. The observed changes are specific because re-expression of Gprk2 in cells depleted of the endogenous protein restored net BRET to control levels (Figure 3.7A). These results suggest, that Gprk2 regulates dimerization of Smo^{SD} and imply that the loss of Smo^{SD} signaling following *gprk2* knockdown is caused by incomplete engagement of Smo^{SD} C-terminal tails.

This notion was further validated by the fact that mimicking phosphorylation of Gprk2 clusters 1 and 2 in the Smo^{SD} backbone ($Smo^{SD.c12D}$) increased net BRET between Smo C-

termini compared to net BRET levels observed for Smo^{SD} molecules (Figure 3.7B). Moreover, it rendered this mutant insensitive to the loss of Gprk2, consistent with the behavior of $Smo^{SD.c12D}$ in *ptc-luc* reporter assays (Figure 3.7B). Taken together, our studies in S2 cells indicate that Gprk2 directly enhances dimerization of active Smo. In particular, phosphorylation within the first two Gprk2 cluster is a prerequisite for Smo to shift into its most active state, which is required for efficient Hh target gene expression.

3.6. Analysis of Smo mutants *in vivo.*

So far we have characterized the effect of Gprk2-dependent Smo phosphorylation in tissue culture cells. In this system, *gprk2* knockdown or mutation of Gprk2 phosphorylation sites in Smo gave the same results: accumulation of Smo at the cell membrane and reduced signaling activity. To validate whether the same is true *in vivo*, we made transgenic flies expressing either wt Smo or the $Smo^{c1\text{-}4A}$ mutation. The transgenes were incorporated at the same genomic site using the *Φ*C31 recombination system as mentioned. This procedure ensures comparable expression of each construct.

3.6.1. Mutation of Gprk2 phosphorylation sites in Smo causes a modest Hh signaling defects and fails to replicate the *gprk2* mutant Hh phenotype.

To evaluate the consequences of eliminating Gprk2 phosphorylation sites in Smo, we first analyzed the adult wing phenotypes of our Smo transgenic flies. To circumvent any complications arising from the presence of endogenous Smo, an RNAi transgene was co-expressed that targeted the 3′UTR of the *smo* transcript. Smo mutant and RNAi transgenes were driven by *nubbin*-Gal4 (*nub*-Gal4), inducing expression throughout the wing pouch region of the developing wing disc. Analysis of wing patterning confirmed that endogenous Smo was efficiently depleted. As a control, the *smo* RNAi was co-expressed with GFP and the resulting wing was drastically smaller than a wt wing (Figure 3.8A, B). Hh signaling is responsible for patterning the central region of the wing which was essentially absent in the *smo* knockdown control (Figure 3.8B). Re-expression of wt Smo restored normal development of the wing and even gave signs of a slight gain-of-function, as evident by the perturbations in the A part of the

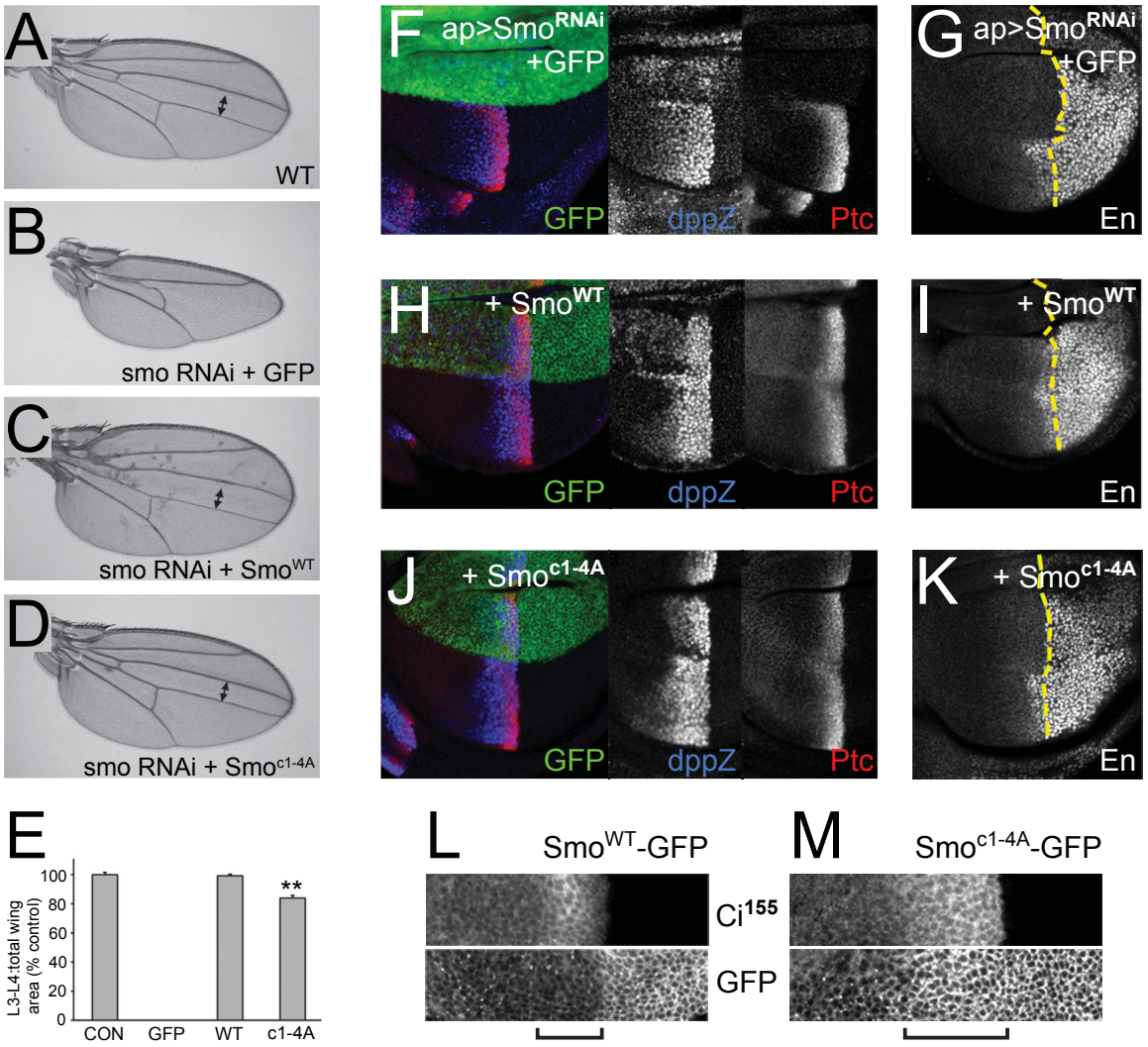

Figure 3.8. Loss of direct Gprk2 phosphorylation causes modest signaling defects *in vivo*.

(A-E) Smo$^{c1\text{-}4A}$ substantially but not fully rescues development of wings depleted of endogenous Smo. **(A)** Wild-type wing. **(B)** Depletion of endogenous Smo from the entire wing by *nub-GAL4* driven expression of a *smo 3'-UTR* dsRNA transgene (along with GFP as a negative control) led to loss of the central region of the wing patterned by Hh. **(C)** Reintroduction of wild-type Smo^{WT}-GFP expression rescued the central region of the wing and gave a slight Hh gain-of-function phenotype (A compartment overgrowth, ectopic vein defects). **(D)** Reintroduction of Smo$^{c1\text{-}4A}$-GFP expression largely rescued the central region of the wing. However, the space between veins 3 and 4 (indicated by two-headed arrow) remained narrower than in controls, indicating that signaling was lower than normal. **(E)** Measurements of the area bounded by veins 3 and 4 as a proportion of total wing area for the indicated genotypes. Data represent mean ± standard deviation for 5 wings of each genotype. **, significantly lower than Smo^{WT}-rescued wings, $p<.001$. Genotypes in A-D: *UAS-Dcr/+;nub-GAL4/+* (A); *UAS-Dcr/UAS-GFP;nub-GAL4/UAS-smo$^{3'UTR}$-dsRNA* (B); *UAS-Dcr/+;nub-GAL4/UAS-smo$^{3'UTR}$-dsRNA;UAS-Smo^{WT}/+* (C); *UAS-Dcr/+;nub-GAL4/UAS-smo$^{3'UTR}$-dsRNA;UAS-Smo$^{c1\text{-}4A}$/+* (D).

[*continued on next page*]

Figure 3.8. Loss of direct Gprk2 phosphorylation causes modest signaling defects *in vivo.* [*continued*]

(F-K) Gprk2 phosphorylation is required for maximal Smo activity *in vivo*. Confocal micrographs of wing discs, oriented with A compartment to left, D compartment up. Endogenous Smo was depleted from the D compartment by *ap-GAL4*-driven expression of *smo 3'UTR* dsRNA and replaced with GFP **(F, G)**, Smo^{WT}-GFP **(H, I)**, or $Smo^{c1\text{-}4A}$-GFP **(J, K)**. Immunostaining: Ptc and *dpp-LacZ* **(F, H, J)**; En **(G, I, K)**. *Dotted lines*: A/P compartment boundary (based on Ci immunostaining, not shown). $Smo^{c1\text{-}4A}$ rescued Dpp and Ptc but not En expression. **(L, M)** Gprk2 phosphorylation promotes Smo turnover. GFP fluorescence in D compartment of wing discs with endogenous Smo depleted and replaced with Smo^{WT}-GFP **(L)** or $Smo^{c1\text{-}4A}$-GFP **(M)**. *Brackets*: Hh-responding cells (identified by increased Ci^{155} immunostaining). The Gprk2 non-phosphorylatable form of Smo accumulates ectopically in Hh-responding cells. Genotypes in F-M: *UAS-Dcr/UAS-GFP;ap-GAL4,dpp^{10638}/UAS-smo$^{3'UTR}$-dsRNA* (F, G); *UAS-Dcr/+;ap-GAL4,dpp^{10638}/UAS-smo$^{3'UTR}$-dsRNA;UAS-Smo^{WT}-GFP/+* (H, I, L); *UAS-Dcr/+;ap-GAL4,dpp^{10638}/UAS-smo$^{3'UTR}$-dsRNA;UAS-Smo$^{c1\text{-}4A}$-GFP/+* (J, K, M).

wing (Figure 3.8C). Surprisingly, the $Smo^{c1\text{-}4A}$ mutation also almost completely rescued the loss of endogenous Smo. However, at a closer look, the mutation did not show any gain-of-function phenotypes and the L3:L4 inter-vein area was slightly reduced (Figure 3.8D, two headed arrow). The ratio of L3:L4 over total wing size was 16% lower compared to wt, consistent with a mild suppression of Hh signaling (Figure 3.8E). However, $Smo^{c1\text{-}4A}$ failed to replicate the full severity of the *gprk2* mutant phenotype. Loss of Gprk2 resulted in a more pronounced wing phenotype (19-30% reduction of the ratio between the L3:L4 area over the total wing size; Figure 3.1D). Therefore, we conclude that, *in vivo*, Gprk2 phosphorylation of Smo plays only a minor role in Smo activation and Hh signaling. $Smo^{c1\text{-}4A}$ does not completely mimic the *gprk2* mutant phenotype, hence, an additional role of Gprk2 in the Hh pathway likely exists.

Further immunohistochemical analysis of Hh target gene expression in the wing disc support this notion. To this end, we used a similar setup as above, but the two transgenes, *smo* 3′UTR RNAi and Smo expression constructs, were now under the control of *ap*-Gal4. This driver induces expression only in the dorsal half of the wing disc. Depletion of endogenous Smo eliminated *ptc* and *en* expression, intermediate and high threshold Hh target genes, respectively. Protein levels for *dpp*, a low threshold Hh target gene, were strongly reduced (Figure 3.8F, G). In agreement with the results seen in adult wings, re-expression of wt Smo rescued the expression of all the analyzed Hh target genes in the Hh-responsive zone. Staining for *dpp* and *ptc* revealed mild ectopic induction in the far A compartment of the wing disc consistent with the mild gain-of-function phenotype observed in the adult wings (Figure 3.8H, I). Expression of $Smo^{c1\text{-}4A}$

failed to induce the high threshold target gene *en*, but restored the *ptc* and *dpp* stripe. However, *ptc* levels were slightly reduced compared to wt Smo and no ectopic *ptc* or *en* signal was detected (Figure 3.8J, K). Taken together, $Smo^{c1\text{-}4A}$ affects expression of intermediate to high threshold Hh target genes, which is in line with the *gprk2* mutant phenotype. However, *ptc* expression seems less affected by expression of $Smo^{c1\text{-}4A}$ than it was in *gprk2* mutants. Based on these results and on the phenotypes observed in the adult wings, we conclude that mutating the Gprk2 sites is not sufficient to replicate the loss of the kinase *in vivo*. Therefore, we postulate that Gprk2 also has a second role in the Hh pathway, most likely independent of its function in Smo phosphorylation. I will explore this idea further in Chapter 4.

3.6.2. Turnover of Smo depends on direct Gprk2 phosphorylation.

Interestingly, the $Smo^{c1\text{-}4A}$ mutant was capable of recapitulating one aspect of the *in vivo gprk2* mutant phenotype. Loss of Gprk2 caused an ectopic accumulation of endogenous Smo in the Hh-responsive zone within the A compartment of a wing disc (Figure 3.1J). This region can be identified by visualizing the Ci^{155} protein, which is the transcription factor of the Hh pathway. *ci* was only expressed in the A compartment of the disc and Ci^{155} protein levels were elevated in the presence of Hh (Figure 3.8L, M; bracket). $Smo^{c1\text{-}4A}$ accumulated in the same way as endogenous Smo did in a *gprk2* mutant (compare Figures 3.8G and 3.1J). $Smo^{c1\text{-}4A}$ behaved different than wt Smo, whose levels were low throughout most of the A compartment (Figure 3.8L). This argues that accumulation of $Smo^{c1\text{-}4A}$ is due to loss of Gprk2 phosphorylation. The *in vivo* results are in line with the cell surface biotinylation experiments in S2 cells, demonstrating that $Smo^{c1\text{-}4A}$ accumulates at the plasma membrane (Figure 3.6C). We conclude that Gprk2 phosphorylation promotes internalization and downregulation of active Smo.

It is worth pointing out that the *in vivo* accumulation phenotype of $Smo^{c1\text{-}4A}$ also validates our mapping results. The fact that $Smo^{c1\text{-}4A}$ replicates the trafficking defect of Smo in *gprk2* mutants suggests that we have indeed found all Gprk2 sites within Smo. This also provides indirect evidence for the notion that the additional role Gprk2 plays in the Hh pathway is not linked to Smo phosphorylation.

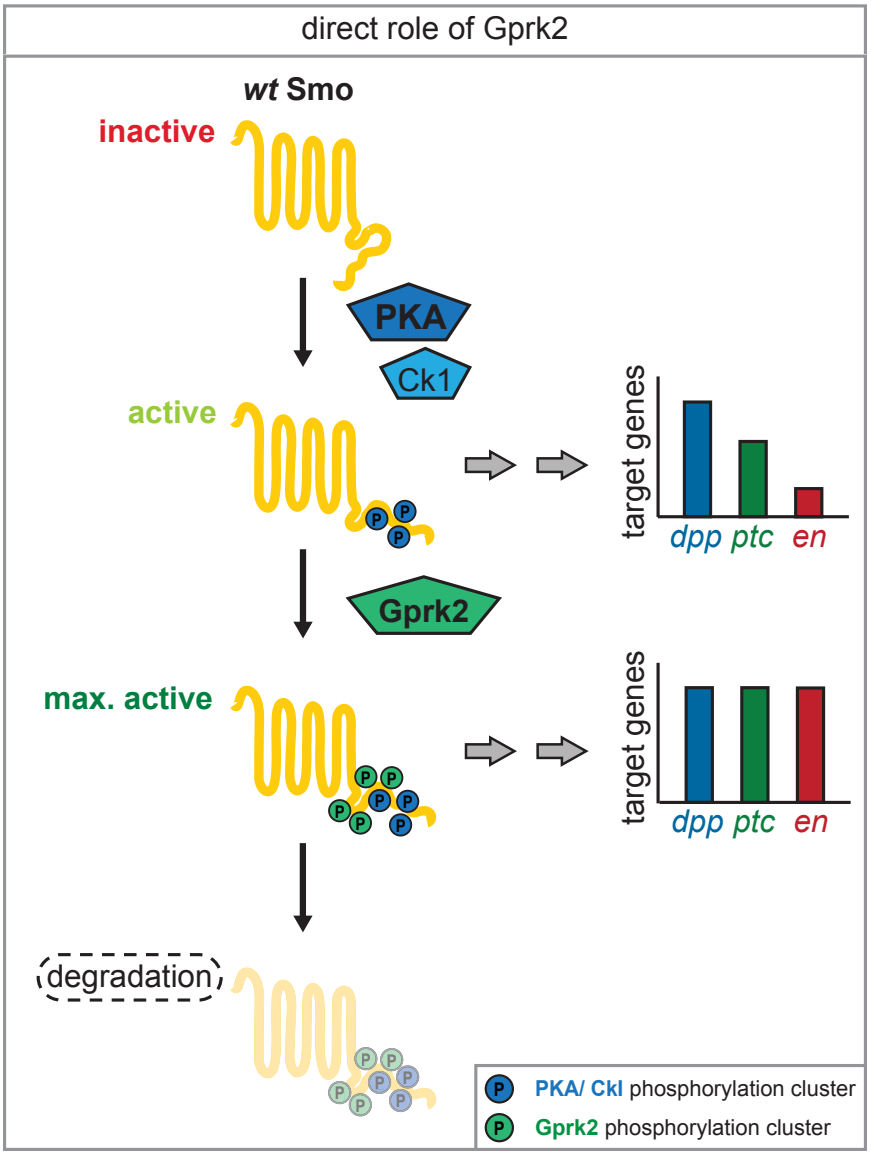

Figure 3.9. Model for the role of direct Gprk2 phosphorylation in Smo activation.

In the presence of Hh, Smo is phosphorylated within the SAID by PKA and then CKI. This leads to Smo accumulation at the plasma membrane, promotes its dimerization (not shown) and shift to an active conformation. In this state, target gene expression is strongly, but not fully, activated. Gprk2 phosphorylates Smo at the plasma membrane, driving Smo into its most active state and promoting full target gene expression. Gprk2 phosphorylation also triggers internalization and degradation of activated Smo in Hh-responding cells, limiting the duration of Smo signaling.

3.7. Summary of Chapter 3 and model for the direct role of Gprk2 in Smo activation.

Loss of Gprk2 in *Drosophila* has two effects: expression of intermediate to high Hh threshold target genes is impaired and Smo accumulates inappropriately at the plasma membrane of Hh receiving cells. We demonstrate that Gprk2 phosphorylates active Smo within four phosphorylation clusters in the membrane-proximal C-terminus and this post-translational modification is required for Smo turnover from the plasma membrane (Figure 3.9). Furthermore, we show that Gprk2 targets active forms of Smo and acts downstream of PKA/Ck1 (Figure 3.9). Gprk2 acts positively in the Hh pathway by promoting maximal Smo activation and dimerization of Smo cytoplasmic tails. However, preventing Gprk2 phosphorylation by mutating the Gprk2 sites in Smo only modestly impacts Hh target gene expression *in vivo*. In terms of Hh signaling responses mutation of Smo phosphorylation sites seems only to partially recapitulate the *gprk2* mutant phenotype. Based on this we hypothesize that Gprk2 plays an additional role in the Hh pathway. The nature and mechanism behind this second function is closely examined in the following chapter.

Chapter 4: Results – part II

Gprk2 modulates Hh signaling indirectly by controlling cellular cAMP levels.

4.1. Bridge between Chapter 3 and 4.

As discussed in the previous chapter, the Hh phenotype in *gprk2* mutants cannot be solely accounted for by the loss of direct Gprk2-dependent Smo phosphorylation. This suggests that Gprk2 plays an additional role in the Hh pathway. But how could Gprk2 affect the Hh pathway independently of its role as a Smo kinase? Is it possible that we have not completely characterized the *gprk2* mutant phenotype? Maybe loss of Gprk2 causes additional abnormalities interfering with Hh signaling.

In an attempt to answer these questions, we focussed on classical GRK biology. As detailed in section 1.5.2., GRKs are involved in the process of GPCR desensitization. In brief, phosphorylation of active GPCRs by GRKs terminates GPCR signaling through heterotrimeric G proteins and further initiates arrestin- and clathrin-dependent receptor internalization. GRKs therefore act as negative regulators of GPCR signaling. Consequently, GRK mutants are often characterized by GPCR hyper-activation, which leads to abnormally prolonged and intense GPCR signaling responses. Heterotrimeric G proteins downstream of GPCRs often control cellular second messengers such as cAMP, phospholipids or calcium, and consequently, the baseline equilibria of these second messengers could be shifted in GRK mutants. Based on this we formulated our first hypothesis: GPCR/G protein signaling and second messenger levels might be misregulated in *gprk2* mutants.

But which of the approximately 100 GPCRs encoded in the *Drosophila* genome is affected in *gprk2* mutants (Brody and Cravchik, 2000)? An obvious candidate is Smo, which we already showed is a target for Gprk2 phosphorylation. Smo is a distant and atypical member of the GPCR superfamily, but evidence from several organisms and tissue culture systems nevertheless suggest that Smo is indeed capable of signaling through heterotrimeric G proteins (see section 1.4.2.). In *Drosophila* tissue culture cells, Hh stimulation leads to a Smo-dependent drop in cellular cAMP concentrations, implying that Smo engages with the $G_{\alpha i}$ subunit of heterotrimeric G proteins. Furthermore, the same study demonstrated through genetic modifications that Smo-$G_{\alpha i}$ signaling is required for Hh pathway activity *in vivo* (Ogden et al., 2008).

But if we find evidence for GPCR misregulation in *gprk2* mutants, how does this affect the Hh pathway? The most direct way involves the second messenger cAMP. Cellular cAMP concentrations directly control the activity of PKA, which plays two crucial roles in the Hh pathway (introduced in section 1.2.5.). First, PKA acts negatively on the Hh pathway by promoting proteasome-dependent processing of Ci into a transcription repressor. Second, PKA has a positive function in Hh signaling by controlling Smo activity. Because of these two opposing roles of PKA in the Hh pathway, it is easy to imagine that cAMP levels and therefore PKA activity must be tightly controlled to ensure proper signaling. We speculated that in *gprk2* mutants, the Hh response is compromised because cAMP levels, and consequently PKA activity, are disturbed. The data presented in this chapter support this hypothesis and demonstrate that Gprk2 keeps cAMP levels and PKA activity within a permissive range for Hh signaling.

4.2. A connection between Gprk2 and baseline concentrations of the second messenger cAMP.

A link between Gprk2 and cAMP regulation has already been established in the literature. Tissue-specific loss of Gprk2 in the fly ovary caused a drop in baseline cAMP levels by about 3-fold compared to wt (Lannutti and Schneider, 2001). Based on this report in the literature and on the rationale outlined above, we decided to investigate a potential connection between Gprk2, cAMP levels and Hh signaling.

4.2.1. cAMP levels are abnormally low in *gprk2* mutants.

To address whether Gprk2 affects cAMP levels in other tissues, we measured cAMP concentrations in whole larval extracts of wt and *gprk2* mutant animals using a commercial immunoassay. To reduce variability between measurements, we carefully age-matched larvae of the indicated genotypes, normalized cAMP concentration to total protein levels and pooled data from three independent experiments. As shown in Figure 4.1A, loss of Gprk2 caused roughly a 60% reduction in baseline cAMP concentrations compared to wt control.

We next wondered if the changes in cAMP concentrations are specific to the loss of Gprk2. To answer this question we turned to a cAMP biosensor allowing us to quantify cAMP

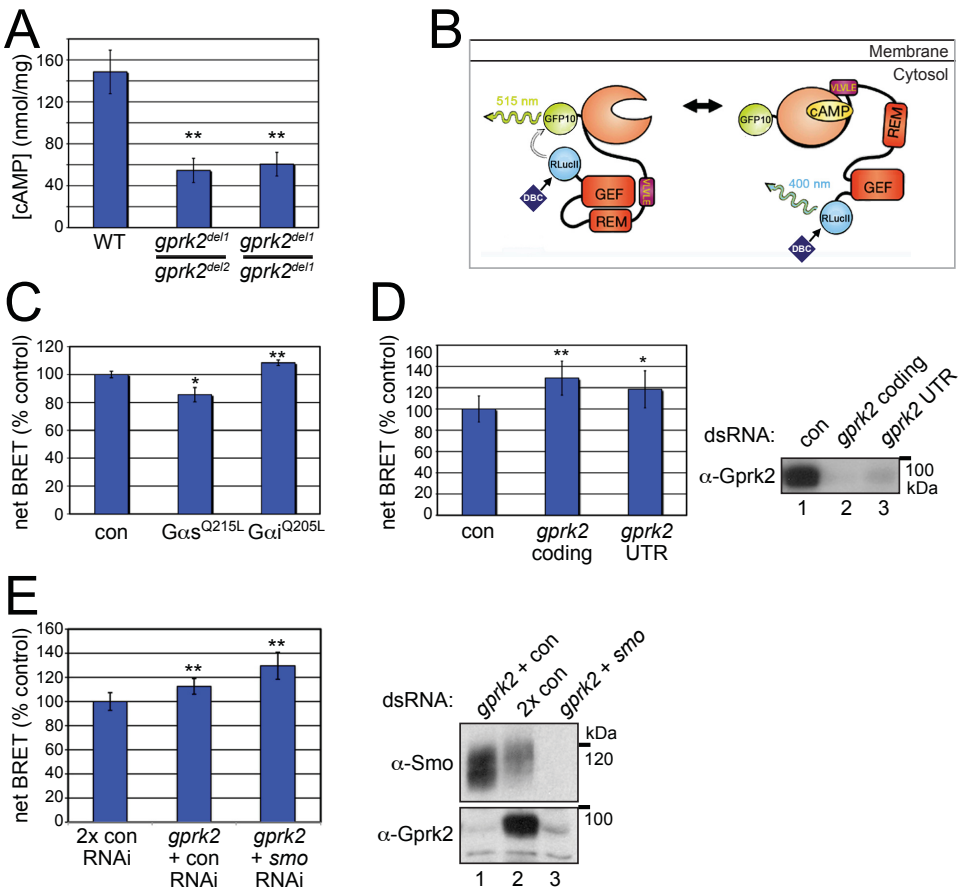

Figure 4.1. Loss of Gprk2 reduces cAMP levels.

(A) cAMP concentrations in whole larva lysates were ~60% lower than normal in two different genotypes of *gprk2* mutant larvae. Larvae were cultured at 29°C and the various genotypes (w^{1118}, $gprk2^{del1}$ / $gprk2^{del1}$ and $gprk2^{del1}/gprk2^{del2}$) were age matched. **, p<.005 vs control, *T*-test. **(B)** Model for the conformational change following binding of cAMP to the regulatory domain of EPAC. BRET efficiency between the RLucII and GFP10 tag inversely correlates with cAMP concentrations. Schematic adapted from (Ponsioen et al., 2004). **(C-E)** Measurement of cellular cAMP levels by BRET in EPAC-BRET-expressing S2 cells. **(C)** S2 cells were transiently transfected with the EPAC-BRET expression plasmid, together with empty vector (Con) or plasmids driving expression of constitutively active forms of $G_{\alpha s}$ ($G_{\alpha s}^{Q215L}$) or $G_{\alpha i}$ ($G\alpha i^{Q205L}$). An increase in net BRET ratio indicates a reduction in cAMP levels, and vice versa. cAMP levels were significantly higher in $G_{\alpha s}$-expressing cells and significantly lower in $G_{\alpha i}$-expressing cells, as expected, indicating that the EPAC-BRET cAMP biosensor is functional in S2 cells. Data pooled from three independent experiments. *, p<.001 **, p<.005, vs control (respectively), *T*-test. **(D)** EPAC-BRET analysis in S2 cells in which Gprk2 was depleted using a dsRNA targeting coding sequences or a mixture of dsRNAs targeting 5' and 3' untranslated regions (UTR). Both treatments efficiently depleted Gprk2 (as revealed by immunoblotting with anti-Gprk2 antibody), and both led to a statistically significant decrease in cAMP levels (*T*-test versus control dsRNA-treated cells: *, p<0.01; **, p<.001). **(E)** Simultaneous depletion of Smo and Gprk2 did not counteract the effects of Gprk2 depletion alone on cAMP levels (*T*-test versus control dsRNA treatment: **, p<.005). Western blot at right demonstrates knockdown efficiency.

levels in living tissue culture cells. The biosensor is based on the human cAMP binding protein EPAC1, which in its wt form acts as a GEF for small GTPases of the Rap family. The EPAC protein undergoes a conformational change in response to cAMP binding, which regulates its GEF activity, but is independent of the GEF domain itself. The conformation of the EPAC protein directly correlates to cellular cAMP concentrations, therefore, the protein was engineered as a cAMP biosensor in mammalian tissue culture cells (Jiang et al., 2007). For this purpose, the GEF activity was destroyed by introducing two point mutations (T781A, F782A). The configuration of the protein can be visualized by intramolecular BRET between a GFP10 and a *Renilla* LucII tag fused at each terminus of the protein. BRET occurs after stimulation of the Luciferase and when cAMP concentrations are low. In this situation, EPAC resides in a closed conformation and the *Renilla* LucII and GFP10 tag are in close proximity. Conversely, if cAMP levels are high, EPAC switches into the open conformation, resulting in low BRET efficiency (Figure 4.1B).

We adapted the EPAC cAMP biosensor for expression in *Drosophila* S2 cells and validated the response of the biosensor to well characterized modulators of cellular cAMP levels as positive controls. As expected, co-expression of a constitutively active form of $G_{\alpha s}$ ($G_{\alpha s}^{Q215L}$), which increases cAMP concentrations, showed a significant decrease in background corrected BRET (net BRET) compared to control treatment (Figure 4.1C). Conversely, net BRET levels significantly increased when a constitutively active $G_{\alpha i}$ variant ($G_{\alpha i}^{Q205L}$) was introduced in cells along with the EPAC biosensor (Figure 4.1C). Taken together, these experiments demonstrate that the EPAC cAMP biosensor is functional in *Drosophila* S2 cells.

We next queried the consequence of Gprk2 depletion in this system. Knockdown of *gprk2* in S2 cells was mediated via dsRNA treatment and we targeted either coding or UTR sequences of *gprk2* mRNA transcript. Both procedures eliminated the bulk of the *gprk2* gene product (Figure 4.1 D). Interestingly, Gprk depletion significantly elevated net BRET efficiency of the EPAC biosensor (Figure 4.1D). This suggests that in S2 cells cAMP levels are lower in the absence of Gprk2, which is also in line with cAMP measurements performed on whole larval extracts. Overall, our results indicate that Gprk2 exerts a positive effect on cAMP levels, and therefore loss of Gprk2 results in abnormally low baseline cAMP concentrations.

4.2.2. Evidence for global misregulation of GPCR signaling in response to Gprk2 depletion.

What could be the mechanism behind the positive role of Gprk2 in regulating cAMP concentrations? As outlined above, Gprk2 could terminate Smo-$G_{\alpha i}$ signaling, which is consistent with canonical GRK biology. Therefore, the low cAMP levels measured in the absence of Gprk2 might reflect inappropriate and hyper-active Smo signaling. If this model is accurate, the misregulation of cAMP concentrations in response to Gprk2 depletion depend on Smo. Consequently, simultaneous elimination of Smo and Gprk2 in cells should rescue cAMP levels back to normal. However, this seemed not to be the case, because double knockdown of *gprk2* and *smo* in S2 cells further elevated net BRET efficiency compared to single *gprk2* knockdown (Figure 4.1E). In contrast with our expectations, the BRET results indicated that cAMP levels are further decreased when both Smo and Gprk2 were depleted. We therefore conclude that the changes in cAMP levels are not Smo-dependent and that the model of Smo-$G_{\alpha i}$ hyper-activation cannot account for this result. We therefore propose a more complex model based on the low specificity of GRKs regarding their GPCR substrates. The fly genome encodes about 100 GPCRs but only two GRKs. Therefore each GRK must be capable of regulating many different GPCRs (section 1.5.3.). Consequently, the GPCR/G protein signaling phenotype present in *gprk2* mutants might be a complex mixture of several GPCR signaling defects. The net outcome of this global GPCR misregulation are abnormally low cAMP concentrations. It should be noted that we only tested for changes in cAMP levels and that we used only two systems, whole larvae lysates and S2 cells. Global GPCR misregulation in *gprk2* mutants most likely also causes other defects e.g. changes in the levels of other second messengers. In summary, we postulate that loss of Gprk2 causes global misregulation of heterotrimeric G protein signaling downstream of GPCRs.

4.3. Abnormally low cAMP levels are limiting for Hh target gene expression in *gprk2* mutants.

In Chapter 3, we demonstrate that direct phosphorylation of Smo by Gprk2 is required for full Smo activation. However, this direct role of Gprk2 in Smo regulation accounts for only a part of the *gprk2* mutant phenotype, suggesting that Gprk2 impacts Hh target gene expression in an

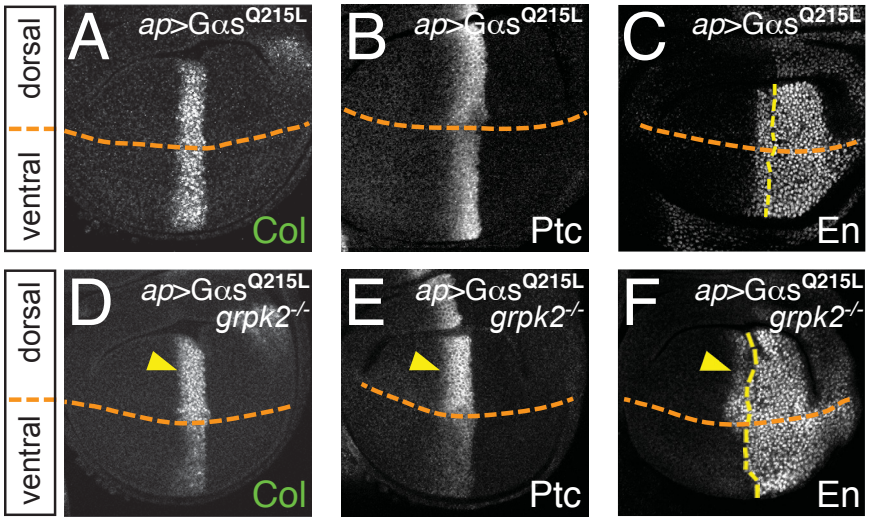

Figure 4.2. cAMP is limiting for Hh target gene expression in the absence of Gprk2.

(A-F) Confocal micrographs of wing discs, oriented with A compartment to left, D compartment up. *Dotted lines*: D/V compartment boundaries. Expression of activated $G_{\alpha s}$ ($G_{\alpha s}^{Q215L}$) in the D compartment of wild-type **(A-C)** and *gprk2* mutant **(D-F)** wing discs (29°C). In *wild-type* discs, expression of Col **(A)**, Ptc **(B)**, and En **(C)** was unaffected by $G\alpha_s^{Q215L}$. In *gprk2* mutant discs, $G_{\alpha s}$ activation restored expression of Col **(D)**, Ptc **(E)**, and En **(F)** specifically in Hh-responding cells (arrowheads).

additional way. As demonstrated above, Gprk2 also affects cellular cAMP levels and *gprk2* mutants are characterized by abnormally low cAMP levels. This prompted us to probe whether the drop of cellular cAMP levels also contributes to the loss of Hh target gene expression. To test this idea, we carried out a series of experiments and genetically manipulated cAMP levels in a *gprk2* mutant background. One example of these kind of studies is presented in Figure 4.2. We reasoned that if cAMP is limiting for Hh target gene expression in a *gprk2* mutant, increasing cAMP levels should rescue transcription of Hh-responsive genes even in the absence of Gprk2. We elevated cAMP concentrations selectively in the dorsal half of the wing disc by expressing the constitutively active $G_{\alpha s}^{Q215L}$ transgene under the control of the *ap*-Gal4 driver. Expression of $G_{\alpha s}^{Q215L}$ in a wt background had no impact on transcription of high threshold Hh target genes such as *col*, *ptc* and A *en* (Figure 4.2A-C, compare dorsal vs ventral). As expected, in a *gprk2* mutant background, protein levels of Col, Ptc and A En were either lost or strongly reduced (Figure 4.2D-F, ventral). Introduction of $G_{\alpha s}^{Q215L}$ in the D compartment restored protein expression of Col, Ptc and A En to normal levels (Figure 4.2D-F, dorsal). These results provide strong evidence that increasing cAMP concentrations is sufficient to overcome the *gprk2* mutant

phenotype. In other words, the loss of high threshold Hh target gene expression in *gprk2* mutants can be in large part attributed to abnormally low cAMP levels which limit Hh target gene expression.

4.4. Gprk2 activates Smo in two ways: through direct phosphorylation and indirectly through controlling PKA activity.

The very strong rescue of the Hh defect in *gprk2* mutants by elevating cAMP levels is surprising and leads to two main questions. First, what is the mechanism behind the rescue? The second question relates to the direct role Gprk2 plays in Smo regulation discussed in the previous chapter. We concluded that Smo phosphorylation by Gprk2 is required for full Smo activation and expression of high threshold target genes. How can we reconcile that boosting cAMP in a *gprk2* mutant seemingly circumvents this direct function of Gprk2?

4.4.1. Gprk2 influences PKA/Ck1-dependent Smo phosphorylation.

We hypothesized that PKA-dependent Smo activation is compromised in *gprk2* mutants because cAMP directly controls the activity of PKA. We speculated that this is a major factor contributing to the Hh signaling defect. If this model is accurate, mimicking complete PKA/Ck1 phosphorylation as in Smo^{SD} should also overcome the loss of Gprk2. To test whether Smo^{SD} can indeed rescue Hh target gene expression in a *gprk2* mutant, we overexpressed it in the D compartment of the wing disc. We focussed on expression of A *en*, the Hh target gene requiring maximal activation of Smo and therefore the most sensitive readout for Smo activation. In a wt background, Smo^{SD} induced Hh-independent *en* expression throughout the A compartment of the disc, consistent with its known constitutive activity (Figure 4.3A, compare dorsal vs ventral). In a *gprk2* mutant background, Smo^{SD} failed to turn on *en* ectopically in the far A of the disc. However, proximal to the A/P border, in the Hh-responsive zone, Smo^{SD} was capable of driving *en* expression (Figure 4.3B), although not quite to wt levels.

To sum up, mimicking complete PKA/Ck1-dependent Smo phosphorylation almost perfectly restores Hh target gene expression in *gprk2* mutants. The result implies that in *gprk2* mutants Smo is not fully phosphorylated by PKA/Ck1 and consequently only partially activated.

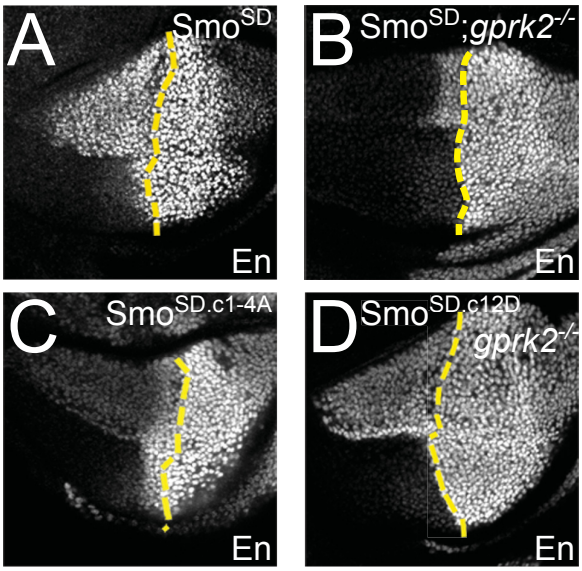

Figure 4.3. Smo requires phosphorylation by PKA and Gprk2 to reach maximal signaling activity.

(A-D) Confocal micrographs of wing discs, oriented with A compartment to left, D com-partment up. *Dotted lines*: A/P compartment boundaries. En expression in wing discs expressing Smo variants in D compartment: Smo^{SD} **(A, B)**, $Smo^{SD.c1-4A}$ **(C)**, or $Smo^{SD.c12D}$ **(D)**. Discs are wild-type **(A, C)** or *gprk2* mutant **(B, D)** background. Ala substitution of all four Gprk2 phosphorylation clusters modestly impairs Smo^{SD} activity *in vivo*, whereas phosphomimetic substitutions restore full Smo^{SD} activity in the absence of Gprk2. **Note:** Images in A, B are the same as in Figure 3.2 F, G. Genotypes in A-D: *ap-GAL4/+;UAS-Smo^{SD}-GFP/tubP::GAL80^{ts}* (A); *ap-GAL4/+;UAS-Smo^{SD}-GFP,gprk2^{del1}/gprk2^{KO}* (B); *ap-GAL4/+;UAS-Smo$^{SD.c1-4A}$-GFP/tubP::GAL80^{ts}* (C); *ap-GAL4/+;UAS-Smo$^{SD.c12D}$-GFP,gprk2^{del1}/gprk2^{KO}* (D).

This PKA-dependent Smo activation defect is caused by abnormally low cAMP levels in *gprk2* mutants. Therefore, increasing cAMP levels in the wing disc or expression of Smo^{SD} both achieve the same thing, full PKA-dependent activation of Smo.

4.4.2. Maximal Smo activity requires phosphorylation by Gprk2 and PKA.

Our rescue experiments using a constitutive active $G_{\alpha s}$ protein or Smo^{SD} argue that the Hh signaling defects in *gprk2* mutant flies are mostly caused by the indirect role Gprk2 plays in the Hh pathway through its effects on cAMP. However, in the previous chapter of this thesis, we concluded that direct phosphorylation of Smo by Gprk2 also contributes to Smo activation and Hh target gene expression. Taken together, Gprk2 exerts two roles in the Hh pathway - a direct and an indirect one (Figure 4.4). But what is is the relationship between these two roles?

We know the mechanisms behind both aspects of Gprk2-dependent Smo regulation. This enables us to functionally test the contribution of each role. To this end, we mutated the Gprk2

sites in the Smo^{SD} background to either non-phosphorylatable Ala ($Smo^{SD.c1-4A}$) or to phospho-mimetic Asp ($Smo^{SD.c12D}$). The mutations were engineered in the Smo^{SD} backbone, therefore, they are not affected by the indirect PKA-dependent role of Gprk2. Therefore, these constructs allowed us to evaluate the role of direct Gprk2-dependent Smo phosphorylation in isolation. We expressed these transgenes in the wing disc using *ap*-Gal4 and again checked for A *en* expression. In contrast to Smo^{SD}, $Smo^{SD.c1-4A}$ failed to induce ectopic *en* expression but led to a subtle but distinct A En protein signal in the Hh-responsive zone proximal to the A/P boundary (Figure 4.3C vs A). Overall, the A *en* expression profile caused by $Smo^{SD.c1-4A}$ expression was similar to the *en* pattern observed when Smo^{SD} was introduced in a *gprk2* mutant background (Figure 4.3B). This suggests that direct phosphorylation of Smo^{SD} by Gprk2 is required for it to drive expression of *en* in the far A of the disc. Furthermore, direct phosphorylation is also necessary to reach wt levels of *en* in the Hh-responsive zone. If this model is true, one would expect that mimicking Gprk2 phosphorylation in a Smo^{SD} backbone ($Smo^{SD.c12D}$) would enable it to drive high *en* expression throughout the disc in the absence of *gprk2*. As shown in Figure 4.3D, this was indeed the case. En protein levels in the A compartment of the disc were evenly high and almost indistinguishable from P compartment levels.

Our assessment of the two roles of Gprk2 in the Hh pathway led to the following conclusions: First, the major function of Gprk2 is to keep cAMP levels and PKA activity within a permissive range for Hh signaling. This is supported by the fact that expression of Smo^{SD} in *gprk2* mutants or introduction of $Smo^{SD.c1-4A}$ in a wt background almost completely rescues the *gprk2*-dependent Hh defects (Figure 4.4). Second, direct phosphorylation of Smo by Gprk2 is required for maximal Smo activation, but this plays a minor role in the Hh pathway. In fact, direct Gprk2 phosphorylation of Smo is only needed to drive expression of A *en*, the target gene requiring the highest Hh threshold (Figure 4.4).

4.5. Summary of Chapter 4.

We have uncovered an additional regulatory mechanism of Gprk2 in the Hh pathway. Gprk2 influences the Hh signaling output by keeping cAMP concentrations, and consequently PKA activity, at permissive levels for PKA-dependent Smo activation. This indirect role of Gprk2 in

the Hh pathway is separate from the function of Gprk2 as a Smo kinase presented in Chapter 3. Functional assessment of the two roles points to the view that disruption of the indirect mechanism is the major cause for the Hh signaling defects in *gprk2* mutants. However, both functions are required for full Smo activation and Hh target gene expression (Figure 4.4).

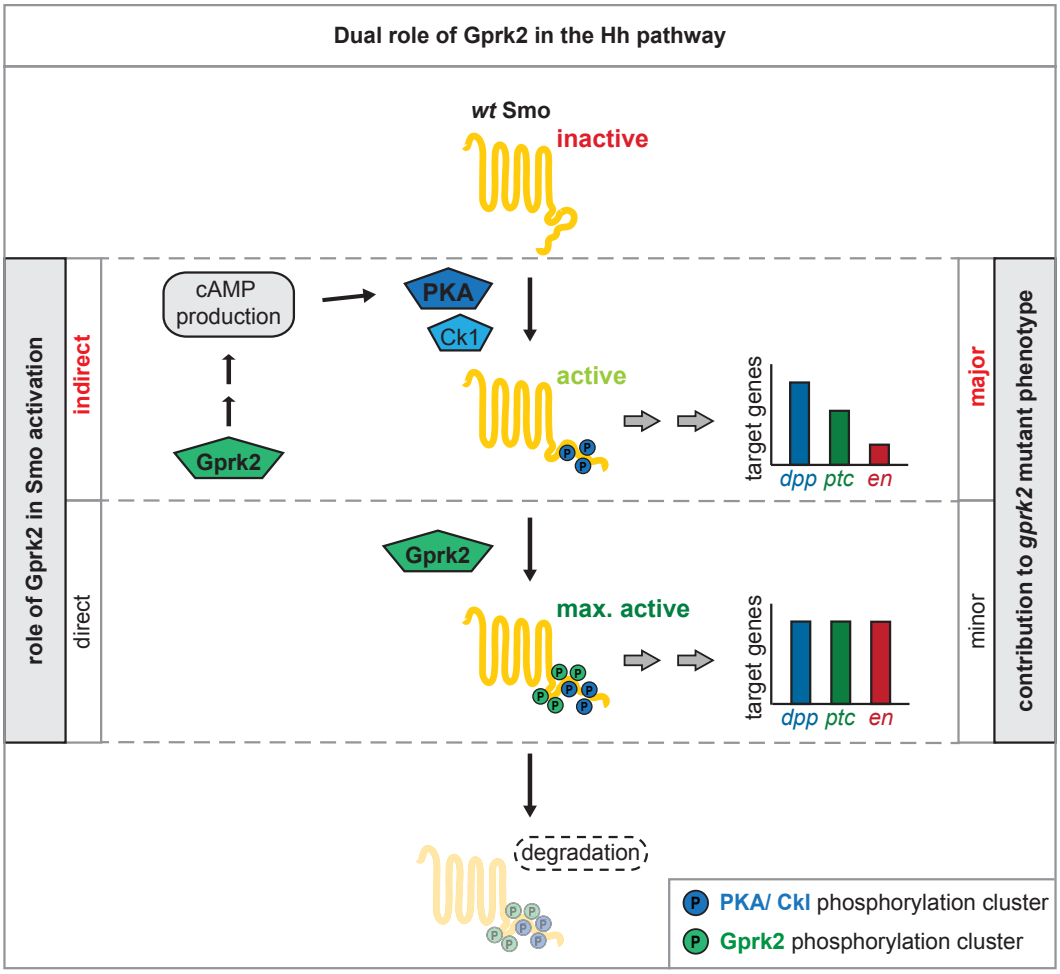

Figure 4.4. Model for a dual role of Gprk2 in Smo activation.

Gprk2 contributes to Smo activation in two ways. Direct Gprk2 phosphorylation is required for maximal activation of Smo signaling and for Smo downregulation. In addition, Gprk2 affects cellular cAMP concentration and therefore PKA-dependent Smo activation. Gprk2 keeps cAMP levels and PKA activity in a permissive range for Hh signaling.

Chapter 5: Results – part III

Gprk2-dependent Smo phosphorylation represents an evolutionarily ancient mechanism of controlling Smo activity.

5.1. Bridge between Chapter 4 and 5.

The work presented so far provides an explanation for the Hh loss-of-function phenotype in *gprk2* mutants. We concluded that in respect to Smo activation in flies, PKA together with Ck1 are absolutely critical, whereas Gprk2 plays only a minor role. The role of PKA in the regulation of Smo highlights one of several significant differences between the mammalian and *Drosophila* Hh pathway (see section 1.3.2). In flies, Hh-dependent Smo activation requires PKA/ Ck1 phosphorylation within the SAID which induces a conformational change and dimerization of Smo C-termini (Zhao et al., 2007). Dimerization of Smo cytoplasmic tails leads to the recruitment and activation of a downstream protein complex, which promotes stabilization and nuclear translocation of Ci (Shi et al., 2011). This protein complex linking Smo signaling to Ci is composed of Cos2, a kinesin-like scaffold protein, and Fu, a Ser/Thr kinase. Both Fu and Cos2 directly bind to Smo through multiple binding sites within the distal Smo C-terminus and this interaction is thought to be essential for Smo signaling in *Drosophila* (Jia et al., 2003; Lum et al., 2003b).

Interestingly, in mammals, Smo regulation and downstream signaling are distinct from the mechanism in flies. In this system, PKA plays no role in controlling Smo activity. However, a recent study focussing on the regulation of murine Smo suggested that GRK2 and Ck1α serve an analogous function to the one of PKA/Ck1 in flies (Chen et al., 2011). By mapping GRK2/Ck1α phosphorylation sites in murine Smo, the authors demonstrated that phosphorylation at these sites is required for Smo activation, ciliary localization and Hh target gene expression. Mechanistically, GRK2/Ck1α-mediated phosphorylation of mouse Smo triggers a conformational change promoting dimerization of Smo cytoplasmic tails, similar to the mechanism of PKA/Ck1-dependent Smo phosphorylation in *Drosophila* (Zhao et al., 2007).

Signaling downstream of mammalian Smo is still poorly understood, but it also ultimately controls stability and nuclear entry of the Hh transcription factor, called Gli in mammals (see section 1.3.3). It is however clear that the mechanism differs substantially from the one in flies. The mammalian ortholog of Fu, STK36, is not involved in Hh signaling (Ingham et al., 2011). The ortholog of Cos2 in mammals, Kif7, participates in Hh signaling, but evidence suggests that it mostly functions at the level of Gli (Cheung et al., 2009). It should be pointed out

that Cos2 in flies also regulates Ci. Direct binding of Kif7 to mouse Smo has not yet been shown, therefore, it is generally thought that only Cos2/Kif7-dependent regulation of Ci/Gli is conserved between the two systems. These and other reasons led to the prevailing view that although Hh signaling in *Drosophila* and mammals ultimately control the same thing, namely Ci/Gli-dependent Hh target gene expression, the signaling downstream of Smo is fundamentally different. This aspect of the Hh pathway might have different evolutionary origins and represent and example of convergent evolution.

A compelling argument for this hypothesis is the fact that the Smo C-terminal tails are vastly different between mammals and insects. Crucial domains in the fly Smo C-terminus, such as the SAID, the PKA phosphorylation clusters and the Fu/Cos2 binding sites, are not present in mammalian Smo orthologs. Therefore, it seems logical that mouse Smo must use a different path towards Gli regulation than fly Smo. However, our work in flies (Chapter 4) and the work by the Jiang/Briscoe labs in mice (Chen et al., 2011) points to the fact that GRK-dependent Smo regulation represents something both systems have in common. We therefore speculated that the molecular function and the underlying mechanism of GRK-dependent Smo activation is evolutionarily conserved. We set out to answer these questions in this chapter.

5.2. The core sequence of Smo is evolutionarily conserved.

To see if the function of GRKs in Smo regulation is conserved, we analyzed multiple sequence alignments of Smo proteins. To appropriately cover the large evolutionary distance between insects and mammals, we included Smo orthologs from all three branches of the bilaterian linage. An excerpt of this alignment is shown in Figure 5.1, focussing on the region within the cytoplasmic C-terminal tail corresponding to the Gprk2 phosphorylation sites in *Drosophila* Smo. We noticed that the first 100 amino acids downstream of the last transmembrane domain, approximately corresponding to residue 651 in *Drosophila* Smo, are broadly conserved within all Smo orthologs. Downstream of this residue the conservation decreases and is diminished even more around amino acid 663 in *Drosophila* Smo (Figure 5.1). The Gprk2 phosphorylation clusters are situated in the junction between conserved and non-conserved sequences. The first two clusters are well conserved throughout all Smo variants. Cluster 3, just downstream of

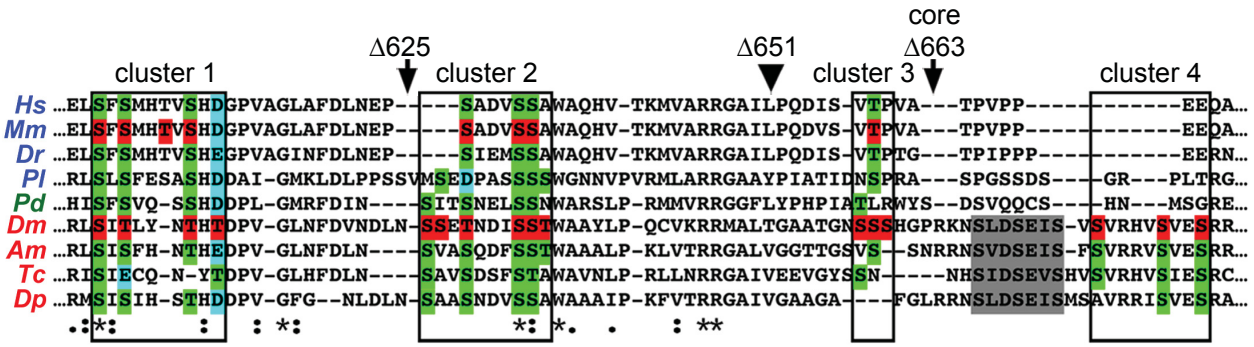

Figure 5.1. Sequence alignment of a portion of the Smo C-terminus.

Orthologues from each of the three main branches of bilaterians are included: deuterostomes - human (Hs), mouse (Mm), zebrafish (Dr), sea urchin (Pl) [*in blue*]; lochotrophozoans - *Platynereis* (Pd) [*in green*]; and ecdysozoans - *Drosophila* (Dm), honey bee (Am), red flour beetle (Tc), and water flea (Dp) [*in red*]. *Boxes*: Gprk2 phosphorylation clusters. *Arrowhead*: approximate end of broad sequence conservation, corresponding to amino acid 651 in *Drosophila* Smo. *Grey shading*: first PKA/CKI phosphorylation cluster. *Red highlighting*: mapped phosphorylation sites in mouse and *Drosophila* Smo. *Green highlighting*: conserved Ser/Thr residues. *Blue highlighting*: Asp/Glu residues where negative charge is conserved.

residue 651, seems moderately preserved whereas cluster 4 is only present in arthropod Smo proteins (Figure 5.1). The extent of conservation of cluster 1-3 is striking, as almost all Ser/Thr residues are either perfectly preserved or align with negatively charged amino acids. This is consistent with the evolution of phospho-sites from negatively charged residues, which is a well accepted model (Pearlman et al., 2011). In addition and more importantly, some of our Gprk2 sites align with phosphorylation sites critical for the activation of murine Smo by GRK2 and Ck1α. The first two Gprk2 cluster correspond to the GRK2/Ck1α cluster PS0 and PS1 in mice (Chen et al., 2011). Strikingly, the study identifying the GRK2/Ck1α sites demonstrated that phosphorylation within PS0 and PS1 is highly relevant for Smo activation and function in mice. This is analogous to our studies showing that cluster 1 and 2 are functionally more significant (Chapter 3). Taken together, this suggests that GRK-dependent Smo phosphorylation and regulation is indeed evolutionarily conserved.

As a model, we propose that all bilaterian Smo species consist of an evolutionarily ancient, functional, GRK-regulated core. The more distal parts of the Smo C-terminus that differ greatly among the bilaterian phyla might have diverged through evolutionary time. In some cases, such as within the arthropod lineage, additional regulatory elements might have been

acquired. This could explain the *Drosophila*-specific function of the SAID, the PKA/Ck1 phosphorylation cluster and the Fu/Cos2 binding sites.

5.3. *Drosophila* Smo^{core} (Smo$^{\Delta 663}$) is functional in tissue culture cells and *in vivo.*

We argue that modern day fly Smo evolved from an evolutionarily ancient, GRK-regulated Smo core protein. If this model is correct, one would expect that a *Drosophila* Smo variant truncated at residue 663 (Smo$^{\Delta 663}$/Smo^{core}; Figures 2.1 and 5.1) should be capable of signaling. Smo^{core} lacks the non-conserved domains of fly Smo, such as the SAID, the PKA/Ck1 clusters and the Fu/Cos2 binding sites, but retains the first three Gprk2 phosphorylation clusters. If Smo^{core} is functional, the signaling activity should be Gprk2-dependent, to prove that GRKs represent the ancient mode of controlling Smo activity.

We first tested the signaling activity of Smo^{core} in a *ptc-luc* reporter assays in S2-R+ cells. We considered it plausible that Smo^{core} forms heterodimers with endogenous Smo, leading to the activation of wt Smo signaling. In this scenario, Smo^{core} would have no intrinsic signaling capability. To rule out any complication arising from the presence of endogenous Smo, we treated the cells with a dsRNA targeting the UTR regions of endogenous *smo* mRNA. Depletion of endogenous Smo was efficient, evident by the almost complete abolition of Hh-driven *ptc-luc* reporter signal (Figure 5.2A). Even in the absence of endogenous Smo, Smo^{core} induced transcription about 7-fold over baseline, but was about about 4-fold less active than Smo^{SD} (Figure 5.2A). It should also be pointed out that Smo^{core} seems to be constitutively active because *ptc-luc* reporter activity was measured without Hh stimulation.

The constitutive signaling activity of Smo^{core} was confirmed *in vivo*. We generated Smo^{core} transgenic flies using the *Φ*C31 recombination system and then analyzed the adult wing phenotype in an endogenous *smo* RNAi background. As I have already shown in Chapter 3, expression of the RNAi construct throughout the developing disc using *nub*-Gal4, resulted in a strong impairment of the Hh pathway, as evident by the absence of the central part of the wing (Figure 5.2D vs C). Co-expression of Smo^{core} completely rescued normal wing patterning and induced ectopic vein formation in the A part of the wing, indicative of a Hh gain-of-function phenotype (Figure 5.2E). This is consistent with the constitutive activity of Smo^{core} in *ptc-luc*

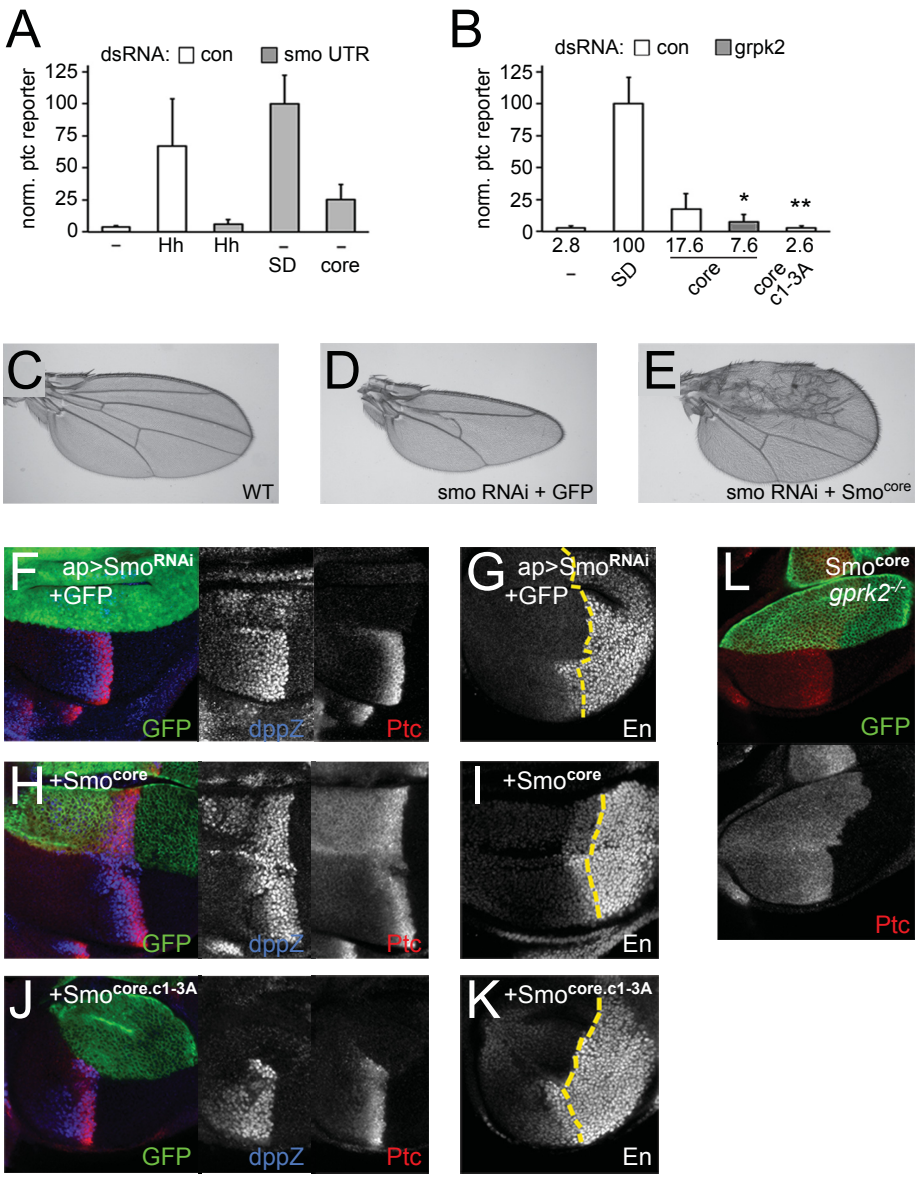

Figure 5.2. The conserved core of Smo is a GRK-regulated, signaling-competent protein.

(A) *ptc-luc* reporter assay of cells treated with control or *smo 3'UTR* dsRNA and transfected with empty vector (-) or expression vectors for Hh^{N}, Smo^{SD}-GFP, or Smo^{core}-GFP. **(B)** *ptc-luc* reporter assay of control (-) or *gprk2* dsRNA and transfected with Smo^{SD}-GFP, Smo^{core}-GFP, or $Smo^{core.c1-3A}$-GFP. * and **, significantly lower than Smo^{core}, $p<.05$ and .001, respectively. **(C)** Wild-type wing. **(D)** Depletion of endogenous Smo from the entire wing by *nub*-GAL4-driven expression of a *smo 3'-UTR* dsRNA transgene (along with GFP as a negative control) led to loss of the central region of the wing patterned by Hh. **(E)** Reintroduction of Smo^{core}-GFP expression rescued the central region of the wing and induced A Hh gain-of-function phenotypes. **Note:** Images in C, D are the same as in Figure 3.8 A, B. Genotypes in C-E: *UAS-Dcr/+;nub-GAL4/+* (C); *UAS-Dcr/UAS-GFP;nub-GAL4/UAS-smo$^{3'UTR}$-dsRNA* (D); *UAS-Dcr/+;nub-GAL4/UAS-smo$^{3'UTR}$-dsRNA;UAS-Smo^{core}/+* (E).

[*continued on next page*]

Figure 5.2. The conserved core of Smo is a GRK-regulated, signaling-competent protein. [*continued*]

(F-K) Wing discs with endogenous Smo depleted from the D compartment by *ap-GAL4*-driven expression of *smo 3'UTR* dsRNA and replaced with GFP **(F, G)**, Smo^{core}-GFP **(H, I)** or $Smo^{core.c1\text{-}3A}$-GFP **(J, K)**. Micrographs show immunostainings for Ptc and *dpp-LacZ* **(F, H, J)** or En **(G, I, K)**. **(L)** *gprk2* mutant wing disc with Smo^{core}-GFP expressed in the D compartment, immunostained for Ptc. **Note:** Images in F, G are the same as in Figure 3.8 F, G. Genotypes in F-L: *UAS-Dcr/UAS-GFP;ap-GAL4,dpp^{10638}/UAS-smo$^{3'UTR}$-dsRNA* (F, G); *UAS-Dcr/+;ap-GAL4,dpp^{10638}/UAS-smo$^{3'UTR}$-dsRNA;UAS-Smo^{core}-GFP/+* (H, I); *UAS-Dcr/+;ap-GAL4,dpp^{10638}/UAS-smo$^{3'UTR}$-dsRNA;UAS-Smo$^{core.c1\text{-}3A}$-GFP/+* (J, K); *ap-GAL4/+;UAS-Smo^{core}-GFP,gprk2^{del1}/gprk2^{KO}* (L).

reporter assays and suggests that Smo^{core} drives ectopic Hh target gene expression in the far A compartment in the wing disc independent of Hh.

Analysis of Hh target gene expression in third instar wing discs confirmed the results seen in the adult wings. As described in Chapter 3, endogenous Smo was depleted in the D compartment of the disc by expression of a *smo* RNAi construct under the control of *ap*-Gal4. The knockdown efficiently eliminated expression of high threshold Hh target genes such as *ptc* and A *en*. Protein levels of the low threshold Hh target gene *dpp* were reduced, suggesting a subtle residual activity of endogenous Smo (Figure 5.2F, G). *ap*-Gal4-driven expression of Smo^{core} in this background restored Hh target gene expression. In the Hh-responsive zone, *dpp* and *ptc* levels were completely rescued and even the expression of *en* was partially recovered (Figure 5.2H, I). This is particularly surprising, given that *en* is the Hh-responsive gene requiring the highest Hh thresholds and maximal Smo activity. The constitutive Hh-independent activity of Smo^{core} was evident in the far A compartment where some expression of *dpp* and *ptc* was detectable (Figure 5.2H, I). Taken together, Smo^{core} is a signaling-competent form of *Drosophila* Smo in tissue culture cells and *in vivo*. Our studies suggest that Smo^{core} is less active than wt Smo, however the difference seems relatively minor *in vivo*.

We next sought to address whether the activity of Smo^{core} is Gprk2-dependent. In *ptc-luc* reporter assays, *gprk2* knockdown or mutation of Gprk2 phosphorylation sites present in Smo^{core} ($Smo^{core.c1\text{-}3A}$; Figure 2.1) drastically reduced or completely blocked the reporter signal, respectively (Figure 5.2B). This observation was also validated *in vivo*. In a *gprk2* mutant background, Smo^{core} failed to restore *ptc* expression in the D compartment (Figure 5.2L). The Gprk2 dependence of Smo^{core} signaling was even more apparent when we tested $Smo^{core.c1\text{-}3A}$.

Expression of $Smo^{core.c1\text{-}3A}$ in the D compartment of a wt wing disc did not induce any detectable expression of *en*, *ptc* or *dpp* (Figure 5.2J, K).

We conclude that Gprk2 phosphorylation is absolutely required for Smo^{core} signaling. This stands in contrast to Gprk2 phosphorylation of wt Smo, which is not absolutely required for signaling but enhances it to its maximal level.

5.4. Smo^{core} recruits Cos2 to a novel binding site in the membrane-proximal Smo C-terminus.

Signaling of wt Smo in *Drosophila* requires direct association of Fu and Cos2 to the cytoplasmic C-terminal tail of Smo. The respective binding sites have been roughly mapped and located between between amino acids 651–686 and 818–1035 for Cos2 (Jia et al., 2003; Lum et al., 2003b). The Fu binding domain falls between amino acids 976–1035 or within the last 59 residues of the Smo protein (Claret et al., 2007). $Smo^{core}/Smo^{\Delta 663}$ lacks most of these binding sites. However, about half the sequence of one Cos2 interaction domain is still present in $Smo^{core}/Smo^{\Delta 663}$. To provide a signaling mechanism for Smo^{core}, we speculated that Smo^{core} recruits Cos2 to the remaining interaction domain. Cos2 binding to Smo^{core}, and therefore its signaling activity, might be dependent on Gprk2 phosphorylation.

To examine Cos2 recruitment to Smo^{core}, we adopted a method established by the Jiang group (Shi et al., 2011). They tagged variants of Smo and Cos2 C-terminally with FRET-compatible fluorophores. FRET between Cos2 and Smo was high in the presence of Hh, indicating binding of Cos2 to Smo under this condition (Shi et al., 2011). We modified this method for BRET-based experiments in living cells by cloning C-terminal fusion of Smo^{core} with GFP10 and Cos2 with *Renilla* LucII (Figure 5.3A). The fusion proteins were co-expressed in S2R+ cells and background-subtracted net BRET levels were measured. Co-expression of Smo^{core} and Cos2 yielded a net BRET signal, suggesting that Smo^{core} is capable of binding to Cos2 (Figure 5.3A). Cos2 recruitment to Smo^{core} depended on the presence of Gprk2 because knockdown of endogenous *gprk2* mRNA significantly reduced net BRET levels, whereas re-expression of the kinase in this background restored net BRET levels and therefore Cos2 binding (Figure 5.3A).

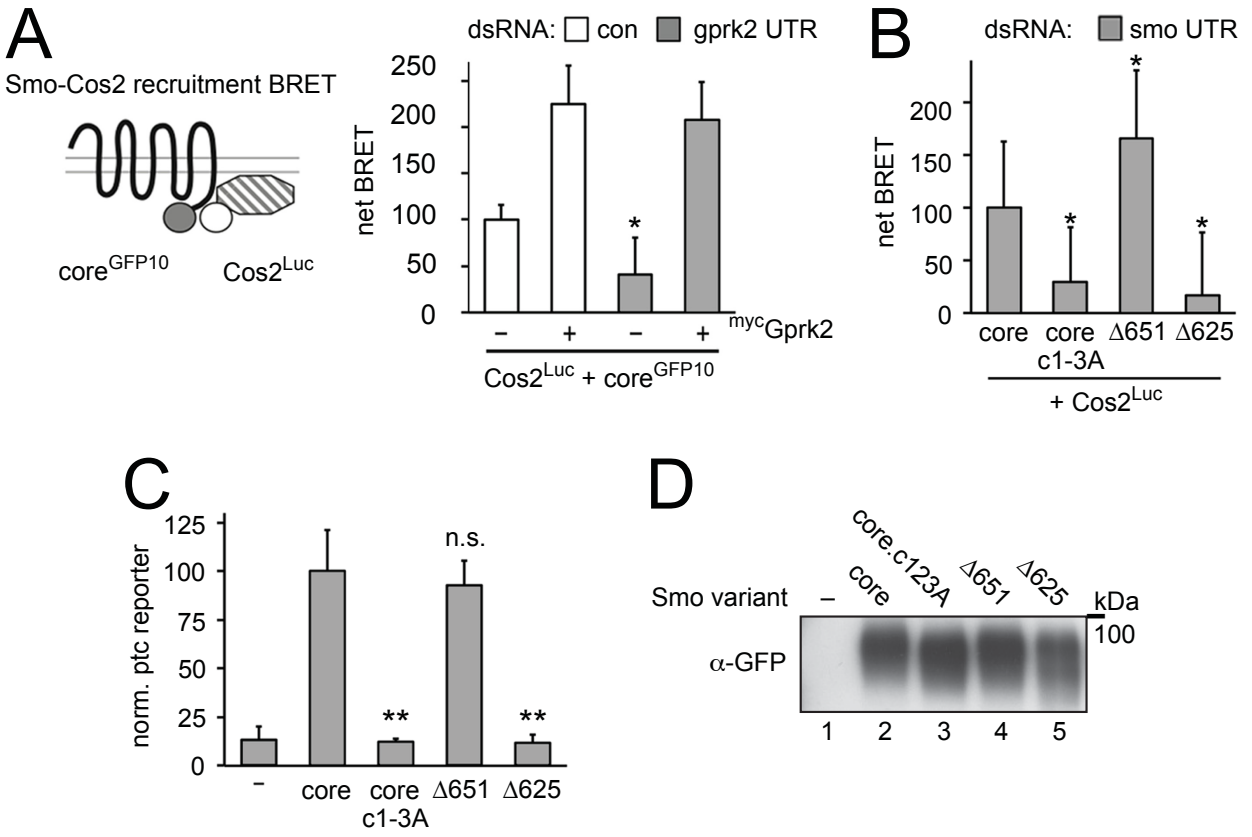

Figure 5.3. Smo^{core} recruits Cos2.

(A) BRET efficiency between C-terminally GFP10-tagged Smo^{core} and C-terminally RLucII-tagged Cos2 in S2 cells. Cells were treated with *β-gal* (control) or *gprk2* dsRNA and transfected without (-) or with (+) myc-tagged Gprk2 in addition to Smo^{core}. Data are expressed as mean net BRET ± standard deviation. Gprk2 promotes interaction between Smo^{core}-GFP10 and Cos2-Luc . *, significantly lower than *β-gal* dsRNA-treated control cells, p<.01. **(B)** BRET efficiency between C-terminally GFP10-tagged truncated Smo variants and RLucII-tagged Cos2 in S2 cells treated with *smo 3'UTR* dsRNA to deplete endogenous Smo. Interaction with Cos2 depended upon Gprk2 phosphorylation and Smo sequences between amino acids 625-651. *, significantly different than Smo^{core}-GFP10, p<.01. **(C)** *ptc-luc* reporter assay of cells expressing truncated Smo variants. The ability to stimulate reporter expression depended upon Gprk2 phosphorylation and Smo sequences between amino acids 625-651. **, significantly lower than Smo^{core}-GFP, p<.001. **(D)** Expression analysis of C-terminally truncated Smo variants. Immunoblot analysis of the indicated C-terminally truncated Smo-GFP proteins. Proteins were expressed at similar levels.

Although unlikely, the determined recruitment of Cos2 to Smo^{core} could in fact reflect Cos2 binding to wt Smo in a Smo/Smo^{core} dimer. To rule out this possibility, we depleted endogenous Smo in S2R+ cells via dsRNA treatment (Figure 5.3B). Under this condition, we still measured a robust net BRET signal of Smo^{core}. More importantly, mutating the Gprk2 phosphorylation sites significantly decreased net BRET levels (Figure 5.3B). We therefore conclude that Gprk2 phosphorylation of Smo^{core} promotes Cos2 recruitment.

We expected that Cos2 associates with Smo^{core} through the remaining Cos2 binding domain downstream of residue 651. To formally test this hypothesis, we truncated Smo at amino acid 651 ($Smo^{\Delta 651}$; Figure 2.1), expecting to eliminate Cos2 recruitment. To our surprise, net BRET levels between $Smo^{\Delta 651}$ and Cos2 were similar to the ones between Smo^{core} and Cos2, suggesting that $Smo^{\Delta 651}$ binds as efficiently to Cos2 as Smo^{core} (Figure 5.3B). We therefore conclude that a novel Cos2 binding site must exist in Smo. We place this novel binding site between amino acids 625–651, because a Smo mutant truncated at residue 625 ($Smo^{\Delta 625}$; Figure 2.1) failed to recruit Cos2 in the BRET assay (Figure 5.3B). The absence or presence of Cos2 association with the various Smo truncations correlated directly with the ability of these mutants to drive *ptc-luc* reporter gene expression. Smo^{core} and $Smo^{\Delta 651}$ promoted reporter activity, whereas $Smo^{core.c1\text{-}3A}$ and $Smo^{\Delta 625}$ failed to do so (Figure 5.3C). All Smo variants were expressed at similar levels (Figure 5.3D), hence, we are confident that the observed changes reflect true differences in the signaling capabilities of the tested mutants. In conclusion, we propose that Cos2 binding to Smo^{core} and $Smo^{\Delta 651}$ is Gprk2-dependent and required for downstream signaling.

5.5. Summary of Chapter 5.

We discovered that the core sequence and the membrane-proximal GRK phosphorylation sites in the C-terminal domain of Smo are well conserved throughout the evolution of bilaterian animals. We demonstrate that the conserved part of *Drosophila* Smo (Smo^{core}) promotes Hh signaling in a Gprk2-dependent manner but without relying on any known domains relevant for wt Smo signaling such as the SAID, the PKA/Ck1 phosphorylation clusters and Fu/Cos2 binding sites. Instead, Gprk2 phosphorylation controls the recruitment of Cos2 to a novel binding site in the membrane-proximal C-terminus of Smo^{core} (Figure 5.4).

The essential role of Gprk2 in controlling Smo^{core} activity differs from the relatively minor role Gprk2 plays in the activation of wt Smo (Chapter 3). Interestingly, the Gprk2-dependent regulation of Smo^{core} is reminiscent of Smo activation in mammals. We speculate that through the functional characterization of Smo^{core} signaling we have unmasked an evolutionarily ancient and universal GRK-dependent mechanism of Smo regulation.

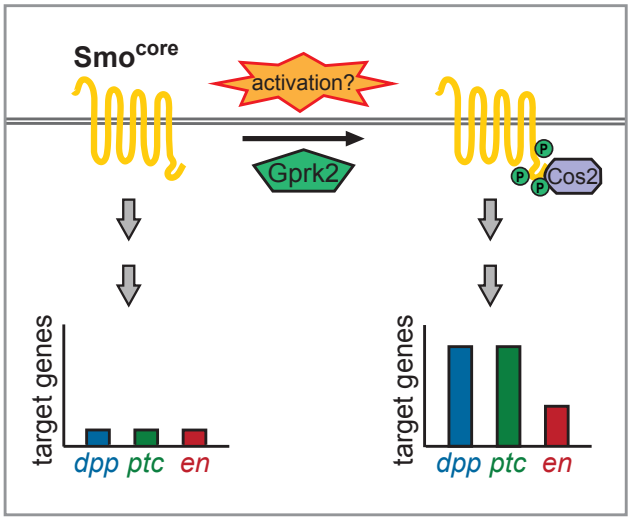

Figure 5.4. Model for Gprk2 function in Smo^{core} activation.

Smo^{core} signals even in the absence of Hh, leading to some constitutive expression of low and intermediate threshold target genes. The activation of Smo^{core} depends on Gprk2 phosphorylation and to some extend on Hh. In the presence of Hh, Gprk2-phosphorylated Smo^{core} promotes strong expression of low and intermediate threshold targets and weak expression of high threshold targets. Mechanistically, Smo^{core} recruits Cos2 to a novel binding site in the membrane-proximal Smo C-terminus.

Chapter 6: Discussion

6.1. Overall summary of results presented in this study.

In this thesis I present a thorough analysis of the developmental defects caused by the loss of Gprk2 in *Drosophila*. *gprk2* mutants are characterized by an impairment of Hh signaling, which manifests itself by the loss of high threshold Hh target gene expression in the wing disc. Gprk2 influences the Hh pathway at the level of Smo, the central signal transducer of Hh signaling. In the absence of Gprk2, Smo resides in a hypo-phosphorylated state and accumulates ectopically at the plasma membrane of fly wing discs and in tissue culture cells.

GRKs are known to primarily phosphorylate GPCRs in the context of GPCR desensitization. Smo is a member of the GPCR superfamily, therefore, we speculate that Smo is a target for Gprk2 phosphorylation resulting in turnover of membrane Smo. By combining the use of site-directed mutagenesis, Smo phospho-proteomics and phospho-specific antisera, I map and validate four clusters of Gprk2 phosphorylation sites in Smo. These clusters are located in the membrane-proximal cytoplasmic tail of Smo and mutating these sites is sufficient to replicate the Smo accumulation phenotype observed in *gprk2* mutants. We conclude that Gprk2 drives Smo internalization and degradation, most likely in an arrestin-dependent manner.

The reality appears to be more complicated with respect to the *gprk2*-dependent Hh signaling phenotype. Direct phosphorylation of Smo by Gprk2 is apparently required for Smo to reach its maximal signaling activity (Figure 6.1A). However, the exchange of Gprk2 phosphorylation sites to non-phosphorylatable residues fails to mimic the full severity of the *gprk2* mutant phenotype *in vivo*. Taken together, my results suggest that direct phosphorylation of Smo by Gprk2 plays a relatively minor role in Smo activation and consequently contributes little to the *gprk2*-dependent Hh signaling defects.

In *Drosophila*, the conversion of Smo from inactive to active states depends on PKA phosphorylation of the SAID. The activity of PKA directly correlates with cellular cAMP concentrations. I demonstrate that loss of Gprk2 causes a substantial drop of basal cAMP levels and that this is the main contributing factor for the loss of high threshold Hh target gene expression in *gprk2* mutants (Figure 6.1A). Furthermore, we show through genetic means that the abnormally low cAMP levels cause an impairment of PKA-dependent Smo activation (Figure 6.1A). Interestingly, the cAMP phenotype of *gprk2* mutants seems not to depend on the presence

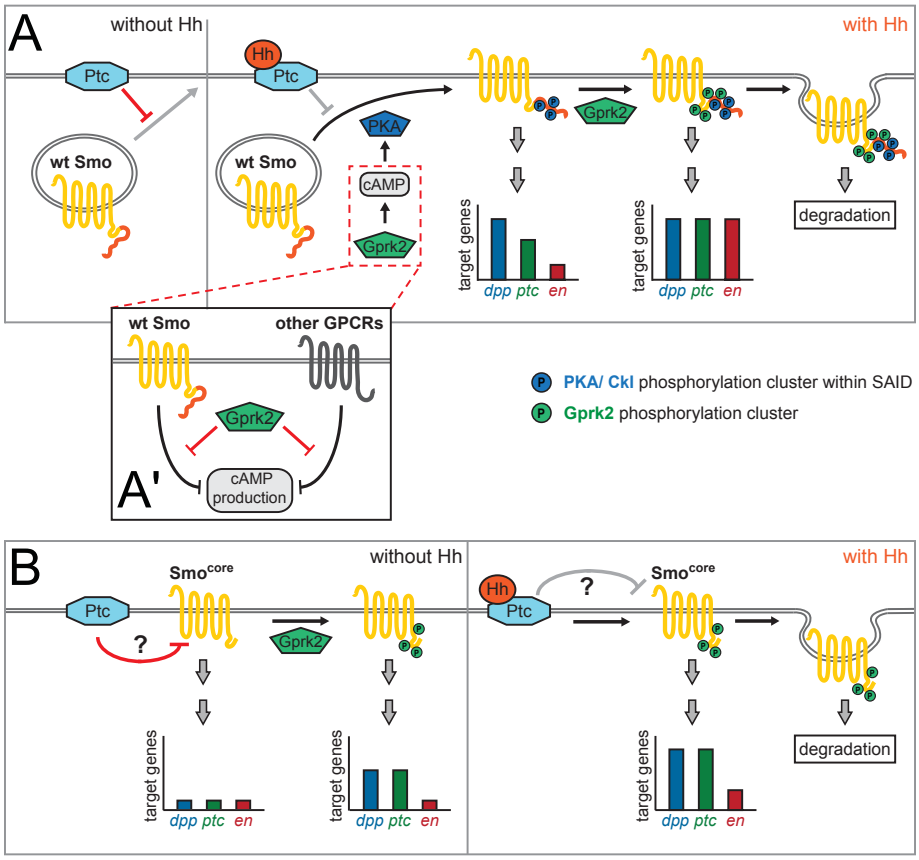

Figure 6.1. Model for the multiple roles of Gprk2 in the regulation of Smo/Smo^{core} in *Drosophila.*

(A) Roles of Gprk2 in the wt Hh pathway. In the absence of Hh, Ptc inhibits Smo by promoting its ubiquitin-dependent degradation and preventing it from accumulating at the plasma membrane. Binding of Hh inhibits Ptc. Phosphorylation of the SAID by PKA and then CKI (not shown) leads to Smo accumulation at the plasma membrane, and promotes its dimerization and shift to an active conformation. In this state, target gene expression is strongly, but not fully, activated. Gprk2 contributes to Smo activation by phosphorylating Smo at the plasma membrane, driving Smo into its most active state and promoting full target gene expression. Gprk2 phosphorylation also promotes internalization and degradation of activated Smo in Hh-responding cells, limiting the duration of Smo signaling. **(A')** Gprk2 affects PKA-dependent Smo activation by controlling cellular cAMP concentrations. In the two systems we studied, *Drosophila* S2 cells and embryonic wing discs, the signaling of other GPCRs seems to promote a decrease in cAMP levels. Gprk2 antagonizes signaling of these other GPCRs through homologous desensitization. By doing so, Gprk2 keeps cAMP levels and PKA activity in a permissive range for Hh signaling.

(B) Function of Gprk2 in Smo^{core} activation. Smo^{core} is partially resistant to downregulation by Ptc, likely because it lacks the inhibitory SAID. Nonetheless, Ptc does inhibit Smo^{core} activity. GRK phosphorylation partially activates Smo^{core} even in the absence of Hh, leading to some constitutive expression of low and intermediate threshold target genes. Binding of Hh inactivates Ptc, relieving it inhibition of Smo^{core}. Gprk2-phosphorylated Smo^{core} promotes strong expression of low and intermediate threshold targets and weak expression of high threshold targets. As with full-length Smo, Gprk2 phosphorylation promotes internalization and degradation of Smo^{core} in Hh-responding cells.

of Smo. Instead, we hypothesize that it is the result of global GPCR misregulation caused by the lack of GRK-dependent receptor desensitization (Figure 6.1A′).

In the last data chapter of my thesis, I show that the core sequence of Smo and most of the GRK phosphorylation sites are evolutionarily well-conserved, whereas most of the domains critical for signaling of *Drosophila* Smo seem specific to the arthropod linage. Reduction of *Drosophila* Smo to its common core (Smo^{core}) results in a Hh signaling competent, strictly GRK-regulated protein. We identify a novel binding site of Cos2 in the membrane-proximal C-terminal tail of Smo^{core}. Recruitment of Cos2 to this site depends on Gprk2 phosphorylation and is required for Smo^{core}-driven Hh target gene expression. (Figure 6.1B). We hypothesize that GRK-dependent Smo phosphorylation constitutes a part of a broadly conserved Smo signaling mechanism.

6.2. Significance of this thesis and key points of the discussion.

Overall our work made three significant contributions to the current understanding of Hh signaling. First, we provide clear evidence that misregulation of cAMP levels, potentially through global GPCR misregulation, influences the outcome of Hh signaling. Second, the fact that Smo^{core} is capable of propagating Hh signaling in flies has profound consequences for how we describe the Hh pathway in *Drosophila*. Smo^{core} induces Hh target gene expression without relying on known Smo signaling domains such as the SAID and previously published Fu/Cos2 binding sites. This implies that Smo^{core} activates the transcriptional response of the Hh pathway through a novel signaling mechanism. The third contribution relates to the evolutionary origin of Smo signaling. Specifically, my work suggests that all bilataran Smo proteins originated from a common ancestor that used a GRK-regulated signaling mode similar to the one of Smo^{core} and present day mammalian Smo proteins. At some time in history, the arthropod lineage acquired the long C-terminal tail and with it novel signaling domains.

6.3. The relationship between GPCR signaling and the Hh pathway.

The role of G protein signaling in the Hh pathway has been somewhat controversial due to contradictory experimental evidence (see section 1.4.3). Our work provides a new angle on this

topic by evaluating the role of cAMP-dependent Hh regulation in the context of global GPCR signaling.

The Hh signaling defect of *gprk2* mutants is in large part caused by abnormally low cAMP levels (Chapter 4). We suspect that misregulation of global GPCR signaling is the root cause for this *gprk2* mutant phenotype. With respect to the *gprk2*-dependent Hh signaling defect, we argue that low cAMP concentrations in the wing disc lead to insufficient activation of PKA and consequently reduced PKA-dependent Smo activation. cAMP levels in cells are in large part regulated by GPCR signaling through heterotrimeric G proteins. Therefore, we hypothesize that GPCR signaling influences the Hh pathway via signaling cross-talk through the regulation of cAMP levels. In short, our work on the role of Gprk2 in the Hh pathway has led us to propose three key concepts. First, cellular cAMP concentrations set a threshold for Hh signaling. Second, GPCR signaling can modulate the outcome of the Hh pathway. And third, global GPCR misregulation is the root cause for the abnormally low cAMP levels in *gprk2* mutants. In the following sections I will review our data and the literature in support for these outlined concepts.

6.3.1. Cellular cAMP levels constitute a threshold for Hh signaling.

How the Hh pathway reacts to changes in cAMP concentrations depends on the context in which the pathway is studied. We argue that cAMP is only limiting for the Hh response in wing discs derived from *gprk2* mutants but not from wt animals. We reached this conclusion after conducting a series of genetic manipulations affecting cAMP metabolism in both *gprk2* mutants and wt animals. This work was done by Shuofei Cheng, a former PhD student of the lab and I included only an excerpt of it in my thesis. As shown in Figure 4.2. increasing cAMP concentrations via overexpression of constitutively active $G_{\alpha s}$ ($G_{\alpha s}^{Q215L}$) in the wing disc rescued the Hh target gene expression in *gprk2* mutants but had no effect on Hh signaling in a wt background. Conversely, lowering cAMP levels by introducing the unregulated and active $G_{\alpha i}$ variant ($G_{\alpha i}^{Q205L}$) resulted in a more pronounced Hh signaling defect in *gprk2* mutants but again had no effect in wt background (Cheng et al., 2012). Our interpretation is that in a wt wing disc, cAMP levels are permissive and not limiting for Hh signaling. This explains why further increases in cAMP levels in this background had no effect. We hypothesize that overexpression

of $G_{\alpha i}^{Q205L}$ only modestly decreased cAMP levels, consistent with the modest effect of this transgene in the EPAC-BRET assay (Figure 4.1 C). This could be the reason why it did not impair Hh target gene expression in a wt disc.

Is this envisioned cAMP threshold specific to Hh signaling in *gprk2* mutant wing discs or a common element in the *Drosophila* Hh pathway? We argue that the latter is true. An interesting case for this can be made by focussing on Hh signaling in the epidermis of wt fly embryos. Hh signaling in the embryonic epidermis seems to behave in the same way as in a *gprk2* mutant wing disc (Maier et al., 2012). In both tissues, Hh target gene expression can be strongly enhanced by expressing a constitutive active form of PKA (mC*) (Cheng et al., 2012; Zhou et al., 2006). This stands in contrast to the effects of mC* overexpression in a wt wing disc. Here, the constitutively active form of PKA has only minor effects on the transcriptional response of the Hh pathway (Jia et al., 2004). These observations can be explained in the context of cAMP thresholds. In the embryonic epidermis and in a *gprk2* mutant wing disc, cAMP may be limiting for Hh pathway activity, therefore changes in cAMP concentrations or PKA activity hasve dramatic effects on Hh signaling responses. In a wt wing disc this would not be the case. Here, baseline cAMP levels are high and always in the permissive range for Hh signaling. Overall, we argue that the effect of cAMP regulation in the *Drosophila* Hh pathway depend on the cellular context and cannot be generalized.

Our tissue-specific and differential approach could explain the differences between Hh signaling in the embryonic epidermis and in the wing disc of *Drosophila* larvae. It will be interesting to see if our model could also be applicable to vertebrate Hh signaling. For instance, overexpression of $G_{\alpha i}$ had no effect on neural tube patterning (Low et al., 2008). Maybe, Hh signaling in this tissue is not susceptible to changes in cAMP, similar to the situation in a wt *Drosophila* wing disc. Future studies might shed some light on this issue.

6.3.2. The Hh pathway response and GPCR signaling are linked via regulation of cAMP levels through signaling cross-talk.

If tissue specific cAMP baselines can set a threshold for Hh target gene expression, then pathway activity in any given tissue depends in large part on the subset of GPCRs which are expressed

and active in that tissue. We hypothesize that GPCR signaling influences the Hh pathway via signaling cross-talk through the regulation of cAMP levels. If this is accurate, specific GPCRs, coupling either to $G_{\alpha s}$ or $G_{\alpha i}$, should modulate the Hh signaling response.

As it turns out, there are several studies on the Hh pathway in vertebrates describing GPCR-dependent modulation of Hh signaling responses. The fact that these discoveries were made in the vertebrate system might not be too surprising. With respect to regulation of cAMP levels and PKA activity, the vertebrate pathway has a simpler setup than its *Drosophila* counterpart. In vertebrates, PKA has only one function in the Hh pathway, promoting degradation of the Hh transcription factor, called Gli in vertebrates (Briscoe and Therond, 2013). Consequently, activation of PKA via increases in cAMP levels blocks Hh signaling. Conversely, reduction of cAMP concentrations promotes Hh target gene expression. Several examples in the literature demonstrate that this regulatory mechanism is applied *in vivo*. A recent publication found that GRP161, a $G_{\alpha s}$-coupled GPCR expressed in the primary cilium of mice plays an inhibitory role in Hh-dependent neural tube development. The proposed model for the role of GRP161 in the Hh pathway states that it functions parallel to Ptc in the absence of Hh. Hh deactivates both Ptc and GRP161 by triggering removal of the two proteins from the ciliary membrane (Mukhopadhyay et al., 2013). Another example is the GPCR PAC_1, which activates adenylyl cyclase most likely by coupling to $G_{\alpha s}$ in response to its ligand, the PACAP peptide. Active PAC_1 increases cAMP levels and this has an inhibitory role on the formation of medulloblastoma in *ptc1* mutant mice. Medulloblastoma is a brain cancer caused by excessive proliferation of cerebellar granular cells. Shh signaling promotes proliferation of these cells and the *ptc1* mutant mice is a common model for medulloblastoma. PAC_1 demonstrates again that increasing cAMP levels in vertebrates has inhibitory effects on Hh signaling (Lelievre et al., 2008; Nicot et al., 2002). Interestingly, a positive influence of $G_{\alpha i}$-coupled GPCRs on Hh target gene expression on proliferation of cerebellar granular cells in mice has also been demonstrated. The GPCR Cxcr4 signals through $G_{\alpha i}$, promotes Shh signaling and induces cell proliferation (Klein et al., 2001). These two receptors, PAC1 and Cxcr4 nicely illustrate that the Hh signaling outcomes can be positively and negatively influenced depending on the cAMP response of the respective GPCRs.

So far, these GPCRs have always been interpreted as novel members of the Hh pathway, regulating the signaling outcome in specific tissues. We argue against this notion and propose that GPCR are not members of the Hh signaling cascade but that they manipulate the Hh pathway indirectly via signaling cross talk. Therefore, any GPCR regulating cAMP levels is in principle capable of adjusting the Hh output. This model could have potential medical implications. Several forms of cancers, medulloblastoma and basal cell carcinoma for instance, are caused by inappropriate activation of the Hh pathway. If GPCR signaling can dampen the Hh response it might be exploitable as a therapeutic approach. GPCRs are pharmacologically highly accessible and about 40% of medicinal drugs are directed against GPCRs. Blocking cancerous Hh pathway activity by manipulating GPCR signaling might be a valuable addition to the limited number of therapies combating these cancers.

6.3.2. Are *gprk2* mutants characterized by global GPCR misregulation?

We hypothesize that the inappropriately low cAMP levels in *gprk2* mutants are caused by global GPCR misregulation (Figure 6.1A′). We infer this model from the canonical function of GRKs as negative regulators of GPCR signaling and from precedent in the literature. A typical feature of GRKs is their capability of regulating multiple GPCR substrates (section 1.5.3.). This feature is a necessity given that the human genome encodes approximately 800 GPCRs but only seven GRKs. Consequently, loss of GRK function affects signaling of several GPCRs. This view was developed based on GRK knockout mice and depletion of GRKs in mammalian tissue culture systems. Particularly interesting are the phenotypes observed by loss of GRK2. Analogous to Gprk2 in *Drosophila*, GRK2 regulates Smo, and GRK2 knockout mice are characterized by a Hh signaling defect (Chen et al., 2011; Philipp et al., 2008). In addition to Smo, GRK2 controls the signaling response of other GPCRs. Depletion of GRK2 in tissue culture cells leads to elevated cAMP production downstream of the activated V2 Vasopressin receptor (Ren et al., 2005). Signaling of Angiotensin II Type 1A receptor was also hyper-activated causing increased diacylglycerol levels (Violin et al., 2006). However, signaling of some other GPCRs was unaffected by loss of GRK2 (Violin et al., 2008). The situation appears similar for loss of GRK6 function which also altered signaling responses of some, but not all, GPCRs examined

(Kavelaars et al., 2003; Ren et al., 2005; Vroon et al., 2004). Taken together, loss of GRK activity causes inappropriate signaling responses of multiple GPCRs. It should, however, be pointed out that functional redundancy might mask some of the GPCR signaling defects caused by loss of a single GRK. In mammals, there are four ubiquitously expressed GRKs. Based on structural features, these four GRKs are separated in two groups (GRK2/3 vs GRK5/6). Although this division suggests some functional differences, the four GRKs assume compensatory roles to a certain extent (Gurevich et al., 2012).

The situation is very likely similar in flies. Here about 100 GPCRs are controlled by two GRKs, Gprk1 and Gprk2 (see section 1.5.7). There are only two GRKs in *Drosophila*, which makes overlapping functions less likely. Therefore global GPCR misregulation might be more pronounced in a fly GRK mutant than in a GRK knockout mouse. Furthermore, Gprk1 and 2 are structurally distinct based on the respective presence or absence of a Pleckstrin homology (PH) domain (Figure 1.6). PH domains are known mediators of membrane recruitment and protein-protein interactions. This implies that Gprk1 and Gprk2 locate to different areas in the cell and assume distinct functions in GPCR regulation. However, little is known about GRK localization, structure and function in *Drosophila*. More insight into these aspects of GRK biology in flies are needed to back up this claim. Nevertheless, the cited examples in the literature and the very limited number of GRKs in flies make global GPCR misregulation in *gprk2* mutants quite likely.

The above arguments are all circumstantial and our experimental data can only provide indirect evidence for this model. We show in S2 cells that Gprk2 plays a positive role in regulating cAMP levels but this function does not require the presence of Smo, which itself might signal through $G_{\alpha i}$ and lower cAMP concentrations. This is evident by the fact that double knockdown of *smo* and *gprk2* does not restore normal cAMP levels in S2 cells compared to knockdown of *gprk2* alone (Figure 4.1.). How could we gather more evidence for GPCR signaling defects caused by the loss of Gprk2? We could quantify the basal levels of other second messengers such as phospholipids, diacylglycerol and calcium ions in S2 cells. Our model would predict that these other second messengers are also affected by Gprk2 depletion. Furthermore, through the means of expression profiling, we could identify which GPCR are transcribed in S2 cells. This would allow us to selectively activate these GPCRs and evaluate their signaling

response in the absence or presence of Gprk2. These approaches should allow us to evaluate whether loss of Gprk2 causes inappropriate signaling responses of multiple GPCRs.

6.4. Evolution of Smo proteins.

We demonstrate that the evolutionarily conserved core of Smo in flies (Smo^{core}) is phosphorylated by Gprk2 at conserved regulatory sites and this is crucial for the signaling activity of Smo^{core}. This is remarkable, because the prevailing view states that signaling downstream of mammalian and arthropod Smo orthologs is fundamentally different. In flies, Smo signaling strictly depends on non-conserved domains such as the SAID and Fu/Cos2 binding sites in the distal C-terminus of the Smo sequence. However, none of these domains are present in mammalian Smo proteins or in Smo^{core}. Based on the robust signaling activity of Smo^{core}, we argue that Smo^{core} and mammalian Smo variants promote Hh target gene expression in a similar manner. In other words, all bilaterian Smo proteins are capable of signaling through a universal and ancient mechanism. In flies, however, this ancient mechanism appears to have been in large part replaced by a non-conserved signaling mode. This model has several implications for Smo signaling in *Drosophila*, some of which I will address in the following section. But first, how can we rationalize our model of a universal Smo signaling mechanism?

Two lines of thought favor this view. First, there are striking parallels between the regulation of Smo^{core} and mammalian Smo. Both Smo variants strictly dependent on GRK phosphorylation for Hh target gene expression. As the GRK phosphorylation sites are highly conserved, it is tempting to assume that GRK phosphorylation has the same functional consequence in both systems. We show that Gprk2 phosphorylation triggers Cos2 recruitment to a novel binding site in Smo^{core}. Kif7 is the ortholog of Cos2 in mammals and assumes positive and negative roles in the Hh pathway like its fly counterpart (Cheung et al., 2009; Endoh-Yamagami et al., 2009; Liem et al., 2009). The negative role of Kif7/Cos2 involves regulation of the the Hh transcription factor Gli/Ci, respectively (Cheung et al., 2009; Zhang et al., 2005). The positive role of Kif7 in the mammalian Hh pathway is so far not well understood. However, one report suggests that Kif7 engages with Smo through a complex with the cilia-specific proteins

Evc and Evc2 (Yang et al., 2012). It would be interesting to test whether Kif7 recruitment to mammalian Smo is dependent on GRK2 phosphorylation.

The second argument for the existence of a common Smo ancestor and signaling mode is that our model provides a compelling explanation for the possible evolution of Smo proteins and the origin of the *Drosophila*-specific features of the Hh pathway. The conserved core sequence of Smo encodes the signaling competence of Smo. What is not conserved is the distal C-terminus of Smo proteins. However, our data and supporting literature suggests that this region limits Smo activity and prevents inappropriate Smo signaling in all bilaterian Smo proteins. For instance, mutation of critical residues in this domain in murine Smo (Zhao et al., 2007) or removal of the region altogether in *Drosophila* (Smo^{core}; Chapter 5) results in constitutive, Hh-independent expression of target genes. We propose that evolution has created multiple ways to block improper Smo activity. In mammals, the non-conserved part of the cytoplasmic Smo tail is relatively short (~100 amino acids) and encodes multiple positive charged arginine clusters. These clusters are thought to engage with the membrane proximal part of the Smo cytoplasmic tail through electrostatic interactions. In this condition, Smo adopts a closed inactive conformation. Phosphorylation at the Ck1α and GRK2 sites breaks the electrostatic bonds and activates Smo (Chen et al., 2011). In addition, mammals have a second safeguard mechanism for Smo - translocation of active Smo into the primary cilium, which is a prerequisite for Smo signaling (Briscoe and Therond, 2013).

The activity of fly Smo is controlled through two different mechanisms both involving the SAID. First, phosphorylation by PKA/Ck1 at three Ser clusters within the SAID activates Smo by inducing a conformational change (Zhao et al., 2007). Parallels exist in the way phosphorylation stimulates Smo signaling in mammalian and fly Smo variants. Nevertheless the mechanisms are distinct as phosphorylation at the conserved Gprk2 sites in *Drosophila* Smo only marginally contributes to Smo signaling (Chapter 3). The second safeguard mechanism for Smo in flies relies on Ptc-mediated ubiquitination in the SAID. Ubiquitinated Smo is rapidly degraded and this mechanism ensures that Smo protein levels are low in the absence of Hh (Li et al., 2012; Xia et al., 2012).

In a nutshell, we argue that a universal and evolutionary ancient Smo signaling mechanism exists in all bilaterians. In opposition to the current literature, we hypothesize that the downstream signaling mechanism of Smo is not fundamentally different between the arthropod and vertebrate lineages. Instead, we propose that the inhibitory mechanisms, which contain the activity of Smo, have diverged between arthropod and mammalian Smo orthologs. What could have been the selection pressure for this divergence? We can only speculate about this, but an interesting correlation is that fly cells − with very few exceptions − lack the primary cilium as cell compartment. It seems plausible that with the disappearance of the cilium in the arthropod lineage, an important inhibitory mechanism for Smo was lost as well. This generated selection pressure to find new ways to block Smo and ultimately favored Smo variants which contained the SAID.

6.5. Mechanism of Smo^{core} signaling.

What is the mechanism of Smo^{core} signaling? We are not yet in the position to answer this question but several clues can be deduced from our results. In the following sections I will focus on two aspects. I will first address whether Smo^{core} is still antagonized by Ptc and activated by Hh. Later, I elaborate on possible scenarios for downstream signaling mechanisms of Smo^{core}.

6.5.1. Smo^{core} is blocked by Ptc and activated by Hh.

As already mentioned in the previous section, Smo^{core} is constitutively active and promotes target gene expression in that absence of Hh. But is Smo^{core} completely uncoupled from Hh- and Ptc-dependent regulation? We argue against this and propose that Smo^{core} is still positively influenced by Hh and negatively by Ptc. Smo^{core} induces *ptc-luc* reporter gene activity in the absence of Hh, but the response can be completely abolished by co-expression of Ptc (data not shown). This suggests that Ptc still controls Smo^{core}, but endogenous expression levels of Ptc are not sufficient to counteract its signaling activity entirely. In other words, in the absence of Hh, endogenous Ptc is only capable of antagonizing Smo^{core} partially. If this model is accurate, one would expect that Smo^{core} signaling is Hh-stimulatable, because Hh deactivates Ptc. Indeed, Smo^{core}-driven reporter gene expression in S2 cells was further elevated by co-expression of Hh,

even when endogenous Smo was depleted via dsRNA treatment (data not shown). We conclude that in S2 cells Smo^{core} is still regulated by Hh and Ptc (Figure 6.1B).

The partial Hh dependence of Smo^{core} signaling is also reflected *in vivo*. Smo^{core} has constitutive activity, evident in the presence of ectopic veins in the the adult wing and in the expression of Hh target genes in the far A compartment of the wing disc (Figure 5.2E, H). But the expression levels of ectopic Hh targets was substantially weaker than in the Hh responsive zone of the wing disc (Figure 5.2H). This suggest that Hh stimulates Smo^{core} signaling *in vivo*, most likely by blocking Ptc (Figure 6.1B).

The fact that Ptc impairs Smo^{core} signaling is particularly interesting. The inhibitory function of Ptc is thought to be mediated in large part by promoting Smo degradation. Specifically, Ptc enables ubiquitination of Smo at several lysine residues within the SAID (Li et al., 2012). However, Smo^{core} lacks the SAID and therefore this mechanism cannot apply. How does Ptc block Smo^{core}? One possibility is that Ptc triggers the attachment of ubiquitin to other lysine residues outside the SAID.

An alternative and more exciting explanation is that Ptc controls the availability of a small molecule acting either as Smo^{core} agonist or antagonist (see section 1.2.2). Ptc shows structural homology to bacterial membrane transporter proteins. It has been a long standing hypothesis in the Hh field that Ptc controls the availability of an endogenous Smo ligand. In the most simple model, Ptc would limit the presence of a Smo agonist through its function as membrane transporter. Hh stops the transporter activity of Ptc and the Smo agonist accumulates and shifts Smo^{core} in an active state. Analogous to other GPCRs, the active state of Smo^{core} is recognized by Gprk2 which phosphorylates Smo^{core}. This in turn triggers Cos2 binding and initiates Smo^{core}-dependent Hh target gene expression. This vision of Smo^{core} activation and signaling is in many ways analogous to typical GPCR-GRK biology and I will address some of these parallels in the following section. Although this model is attractive, the nature of this ligand is still elusive (see section 1.2.2).

Research on Ptc function in more recent years focussed on its role in directing trafficking of endosomal Smo vesicles. This function of Ptc seems to affect Smo indirectly by controlling the lipid composition of Smo vesicles (Callejo et al., 2008). The lipid structure of Smo vesicles

in turn determines whether Smo accumulates at the plasma membrane or is degraded via lysosomes (Khaliullina et al., 2009). We hypothesize that this function of Ptc depends on the presence of the SAID and might be linked to Smo ubiquitination. Therefore it does not apply for Smo^{core}. This explains the fundamentally different post-translationally-controlled accumulation patterns of full-length, wt Smo and Smo^{core}. Wt Smo levels are high in the P compartment of the fly wing disc, peak to maximal levels in the very first rows of A cells and decay rapidly to low levels throughout the rest of the A compartment (Figure 3.8L). Loss of Gprk2 phosphorylation leads to the accumulation of Smo protein in the Hh responsive zone of the disc, consistent with the role of Gprk2 in activity-dependent turnover of Smo (Figure 3.8M). However, the low levels of Smo in the far A compartment of the disc are caused by Ptc, which promotes tonic Smo turnover (Cheng et al., 2010). This stands in contrast to the localization pattern of Smo^{core}. Protein levels of Smo^{core} are low everywhere where Hh is present, specifically in the P compartment and in the Hh diffusion zone within the A compartment of the wing disc. The far A compartment of the disc is characterized by high amounts of Smo^{core} protein. Loss of Gprk2 phosphorylation leads to uniformly high Smo^{core} levels throughout the disc (Maier et al., 2014). Thus, in terms of protein stability, Smo^{core} behaves opposite to wt Smo. The pattern of Smo^{core} is explainable if we assume that only Gprk2 and not Ptc controls Smo^{core} turnover.

In conclusion, we argue that Smo^{core} is activated by Hh through the inhibition of Ptc. Ptc seems to directly influence the activity of Smo^{core} rather than its subcellular localization, possibly by controlling the availability of an endogenous Smo ligand.

6.5.2. Two models for signaling downstream of Smo^{core}.

How does Smo^{core} promote Hh target gene expression? We have uncovered one piece of the puzzle - Smo^{core} recruits Cos2 to a novel binding site in its C-terminus. But how does this contribute to inducing Hh target gene expression?

We hypothesize two possible scenarios. In the first one, Smo^{core} essentially signals analogously to wt Smo. Gprk2 phosphorylation shifts Smo^{core} in an open conformation and promotes dimerization of the short C-terminal tails. Cos2 binds and recruits Fu, leading to Fu dimerization and activation via trans-auto-phosphorylation. Fu phosphorylates Cos2 which in

turn releases full length Ci to promote target gene expression. Further studies focussing on Smo^{core} dimerization and on the phosphorylation states of Fu and Cos2 could validate this model.

Although this first scenario of Smo^{core} signaling is plausible, we also consider a second scenario. In section 6.4. we introduced the concept of a common Smo ancestor and of a conserved and universal signaling mechanism. We propose that the *Drosophila*-specific features of Hh signaling were acquired later in evolution and argue that Smo^{core} relays the Hh signal in a similar way as mammalian Smo orthologs. Signaling downstream of mammalian Smo is still poorly understood, but some characteristics are established. For instance, the ortholog of Fu, STK36, plays no role in the mammalian Hh pathway (Ingham et al., 2011). In addition, Hh signaling in mammals is strongly inhibited by SuFu, an aspect that in flies has only marginal relevance (Cooper et al., 2005; Preat, 1992; Svard et al., 2006). If Smo^{core} functions analogous to mammalian Smo orthologues, the outlined signaling characteristics should also apply for Smo^{core}. Functional assessments of the role of Fu and Sufu in Smo^{core} signaling could address this possibility.

6.5.3. Possible parallels between Smo^{core} and non-canonical GPCR signaling.

As already briefly mentioned in section 6.5.1., we make the argument that the signaling of the common Smo ancestor follows the typical GPCR signaling architecture. We propose that the signaling of ancient Smo and Smo^{core} is divided in these steps: Smo gets activated through an endogenous ligand controlled by Ptc and Hh. Active Smo is recognized by GRKs and phosphorylated. This leads to Cos2 recruitment to Smo and release of full-length Ci. SuFu prevents translocation of full-length Ci into the nucleus, however, this inhibition is overcome in the presence of Hh through an unknown mechanism.

This setup of Smo signaling shows striking parallels to arrestin-dependent, non-canonical GPCR signaling (Lefkowitz and Shenoy, 2005). Arrestins act as scaffold proteins and their binding to active, GRK phosphorylated GPCRs leads to conformational changes opening up interacting domains for downstream effectors. This enables arrestins for instance to initialize clathrin-dependent endocytosis via the interaction with the clathrin adaptor protein AP-2. In

addition, active, GPCR-bound arrestin can also recruit and activate some members of the Mitogen-Activated Protein Kinase (MAPK) cascade and promote MAPK signaling in this way.

Our proposed model of the Hh pathway follows a similar architecture. However, instead of arrestin, Cos2 is recruited to GRK phosphorylated Smo and this induces Hh target genes expression. In the absence of Hh, Ci is in complex with Cos2 and full-length Ci (Ci^{155}) is released in the presence of Hh. It is tempting to speculate that Cos2 undergoes a conformational change in response to Smo binding and that this causes the release of Ci^{155}. It would be interesting to asses whether binding of Cos2 to Smo^{core} triggers conformational changes in Cos2. Structural studies of Cos2 could yield insights into this questions. The parallels between arrestins and Cos2 are intriguing. However, we note that the two proteins are not related. Therefore, it is plausible that Cos2 recruitment to Smo^{core} depends on the presence of arrestins. The precise roles of arrestins and Cos2 in Smo^{core} signaling need to be defined. The results might further highlight the similarities between Smo and arrestin-dependent GPCR signaling.

Our model implies that Smo signaling evolved as a variation of non-canonical GPCR signaling. But what about canonical GPCR signaling activity of Smo? In *Drosophila* S2 cells, Hh stimulation leads to a drop in cellular cAMP levels suggesting that Smo couples to and signals through $G_{\alpha i}$. However, direct recruitment of $G_{\alpha i}$ to wt Smo was not shown (Ogden et al., 2008). This is in contrast to mammalian Smo which has been proven to be a potent activator of $G_{\alpha i}$ signaling (Riobo et al., 2006; Shen et al., 2013). It is tempting to speculate that Smo-G protein signaling was a feature of the conserved Smo ancestor. It seems to be preserved in the mammalian orthologs but might have lost significance in the arthropod lineage including *Drosophila*. This explanation makes sense, first because fly Smo has the long C-terminal tail possibly hindering G protein access to Smo. Second, wt Smo in *Drosophila* is activated by PKA (Jia et al., 2004) and strong $G_{\alpha i}$ signaling would block Smo activation. As already pointed out, mammalian Smo proteins and Smo^{core} lack the long C-terminus and are not activated by PKA. Furthermore, as mentioned in section 6.3.2, several examples are documented in the mammalian/ vertebrate system showing that lowering cAMP levels promotes Hh signaling. It would be interesting to re-evaluate the role of G protein signaling in the *Drosophila* Hh pathway in context

of Smo^{core}-driven Hh responses. These studies could reveal further similarities in the signaling mechanisms of mammalian Smo and *Drosophila* Smo^{core}.

6.6. Concluding remarks.

In the last few years I focussed on the multi-facetted roles of Gprk2 in the *Drosophila* Hh pathway. I approached this topic less from the typical Hh signaling point of view but more from a GPCR-GRK biology angle. My thesis work has shown that Gprk2 regulates Smo much in the same mechanism as it controls any other GPCR in the context of homologous GPCR desensitization. I have also uncovered an universal mechanism of Smo signaling, through the discovery and initial characterization of Smo^{core} in *Drosophila*. I speculate that we can employ Smo^{core} as a simplified model for mammalian Smo signaling. If this is indeed the case we can take advantage of fly genetics which enable us to manipulate virtually every aspect of Hh signaling in a well established setting. Unraveling the mechanism of Smo^{core} activity in flies might provide much needed insight into the signaling events of the mammalian Hh pathway.

Although we are at the very beginning of understanding how Smo^{core} works, I notice striking parallels between Smo^{core} and arrestin-dependent non-canonical GPCR signaling. Arrestin binding to active, GRK phosphorylated GPCRs often triggers G protein-independent signaling events for instance through the MAPK pathway. Smo^{core} recruits Cos2 in a Gprk2 phosphorylation-dependent manner and this leads to Hh target gene expression. I envision that Smo signaling evolved as a variation of non-canocical GPCR signaling. The reinterpretation of the Hh pathway in this context might give new motivations for Hh research in coming years.

THE END.

References

Alcedo, J., Ayzenzon, M., Von Ohlen, T., Noll, M., Hooper, J.E., 1996. The Drosophila smoothened gene encodes a seven-pass membrane protein, a putative receptor for the hedgehog signal. Cell 86, 221-232.

Apionishev, S., Katanayeva, N.M., Marks, S.A., Kalderon, D., Tomlinson, A., 2005. Drosophila Smoothened phosphorylation sites essential for Hedgehog signal transduction. Nat Cell Biol 7, 86-92.

Bai, C.B., Stephen, D., Joyner, A.L., 2004. All mouse ventral spinal cord patterning by hedgehog is Gli dependent and involves an activator function of Gli3. Developmental cell 6, 103-115.

Barthet, G., Carrat, G., Cassier, E., Barker, B., Gaven, F., Pillot, M., Framery, B., Pellissier, L.P., Augier, J., Kang, D.S., Claeysen, S., Reiter, E., Baneres, J.L., Benovic, J.L., Marin, P., Bockaert, J., Dumuis, A., 2009. Beta-arrestin1 phosphorylation by GRK5 regulates G protein-independent 5-HT4 receptor signalling. The EMBO journal 28, 2706-2718.

Barzi, M., Berenguer, J., Menendez, A., Alvarez-Rodriguez, R., Pons, S., 2010. Sonic-hedgehog-mediated proliferation requires the localization of PKA to the cilium base. Journal of cell science 123, 62-69.

Barzi, M., Kostrz, D., Menendez, A., Pons, S., 2011. Sonic Hedgehog-induced proliferation requires specific Galpha inhibitory proteins. The Journal of biological chemistry 286, 8067-8074.

Beachy, P.A., Hymowitz, S.G., Lazarus, R.A., Leahy, D.J., Siebold, C., 2010. Interactions between Hedgehog proteins and their binding partners come into view. Genes & development 24, 2001-2012.

Beachy, P.A., Karhadkar, S.S., Berman, D.M., 2004. Tissue repair and stem cell renewal in carcinogenesis. Nature 432, 324-331.

Benovic, J.L., Gomez, J., 1993. Molecular cloning and expression of GRK6. A new member of the G protein-coupled receptor kinase family. The Journal of biological chemistry 268, 19521-19527.

Benovic, J.L., Mayor, F., Jr., Somers, R.L., Caron, M.G., Lefkowitz, R.J., 1986. Light-dependent phosphorylation of rhodopsin by beta-adrenergic receptor kinase. Nature 321, 869-872.

Bier, E., 2005. Drosophila, the golden bug, emerges as a tool for human genetics. Nature reviews. Genetics 6, 9-23.

Bijlsma, M.F., Spek, C.A., Zivkovic, D., van de Water, S., Rezaee, F., Peppelenbosch, M.P., 2006. Repression of smoothened by patched-dependent (pro-)vitamin D3 secretion. PLoS biology 4, e232.

Bischof, J., Maeda, R.K., Hediger, M., Karch, F., Basler, K., 2007. An optimized transgenesis system for Drosophila using germ-line-specific phiC31 integrases. Proceedings of the National Academy of Sciences of the United States of America 104, 3312-3317.

Bjarnadottir, T.K., Gloriam, D.E., Hellstrand, S.H., Kristiansson, H., Fredriksson, R., Schioth, H.B., 2006. Comprehensive repertoire and phylogenetic analysis of the G protein-coupled receptors in human and mouse. Genomics 88, 263-273.

Blair, S.S., 1995. Compartments and appendage development in Drosophila. BioEssays : news and reviews in molecular, cellular and developmental biology 17, 299-309.

Briscoe, J., Therond, P.P., 2013. The mechanisms of Hedgehog signalling and its roles in development and disease. Nature reviews. Molecular cell biology 14, 416-429.

Brody, T., Cravchik, A., 2000. Drosophila melanogaster G protein-coupled receptors. The Journal of cell biology 150, F83-88.

Callejo, A., Culi, J., Guerrero, I., 2008. Patched, the receptor of Hedgehog, is a lipoprotein receptor. Proceedings of the National Academy of Sciences of the United States of America 105, 912-917.

Cant, S.H., Pitcher, J.A., 2005. G protein-coupled receptor kinase 2-mediated phosphorylation of ezrin is required for G protein-coupled receptor-dependent reorganization of the actin cytoskeleton. Molecular biology of the cell 16, 3088-3099.

Capdevila, J., Guerrero, I., 1994. Targeted expression of the signaling molecule decapentaplegic induces pattern duplications and growth alterations in Drosophila wings. The EMBO journal 13, 4459-4468.

Carman, C.V., Parent, J.L., Day, P.W., Pronin, A.N., Sternweis, P.M., Wedegaertner, P.B., Gilman, A.G., Benovic, J.L., Kozasa, T., 1999. Selective regulation of Galpha(q/11) by an RGS domain in the G protein-coupled receptor kinase, GRK2. The Journal of biological chemistry 274, 34483-34492.

Cassill, J.A., Whitney, M., Joazeiro, C.A., Becker, A., Zuker, C.S., 1991. Isolation of Drosophila genes encoding G protein-coupled receptor kinases. Proceedings of the National Academy of Sciences of the United States of America 88, 11067-11070.

Chatterjee, A., Tanoue, S., Houl, J.H., Hardin, P.E., 2010. Regulation of gustatory physiology and appetitive behavior by the Drosophila circadian clock. Current biology : CB 20, 300-309.

Chelius, D., Bondarenko, P.V., 2002. Quantitative profiling of proteins in complex mixtures using liquid chromatography and mass spectrometry. Journal of proteome research 1, 317-323.

Chen, C.H., von Kessler, D.P., Park, W., Wang, B., Ma, Y., Beachy, P.A., 1999a. Nuclear trafficking of Cubitus interruptus in the transcriptional regulation of Hedgehog target gene expression. Cell 98, 305-316.

Chen, C.K., Burns, M.E., Spencer, M., Niemi, G.A., Chen, J., Hurley, J.B., Baylor, D.A., Simon, M.I., 1999b. Abnormal photoresponses and light-induced apoptosis in rods lacking rhodopsin kinase. Proceedings of the National Academy of Sciences of the United States of America 96, 3718-3722.

Chen, J., Makino, C.L., Peachey, N.S., Baylor, D.A., Simon, M.I., 1995. Mechanisms of rhodopsin inactivation in vivo as revealed by a COOH-terminal truncation mutant. Science 267, 374-377.

Chen, L., Feany, M.B., 2005. Alpha-synuclein phosphorylation controls neurotoxicity and inclusion formation in a Drosophila model of Parkinson disease. Nature neuroscience 8, 657-663.

Chen, W., Ren, X.R., Nelson, C.D., Barak, L.S., Chen, J.K., Beachy, P.A., de Sauvage, F., Lefkowitz, R.J., 2004. Activity-dependent internalization of smoothened mediated by beta-arrestin 2 and GRK2. Science 306, 2257-2260.

Chen, Y., Gallaher, N., Goodman, R.H., Smolik, S.M., 1998. Protein kinase A directly regulates the activity and proteolysis of cubitus interruptus. Proceedings of the National Academy of Sciences of the United States of America 95, 2349-2354.

Chen, Y., Jiang, J., 2013. Decoding the phosphorylation code in Hedgehog signal transduction. Cell research 23, 186-200.

Chen, Y., Li, S., Tong, C., Zhao, Y., Wang, B., Liu, Y., Jia, J., Jiang, J., 2010. G protein-coupled receptor kinase 2 promotes high-level Hedgehog signaling by regulating the active state of Smo through kinase-dependent and kinase-independent mechanisms in Drosophila. Genes & development 24, 2054-2067.

Chen, Y., Sasai, N., Ma, G., Yue, T., Jia, J., Briscoe, J., Jiang, J., 2011. Sonic Hedgehog dependent phosphorylation by CK1alpha and GRK2 is required for ciliary accumulation and activation of smoothened. PLoS biology 9, e1001083.

Chen, Y., Struhl, G., 1996. Dual roles for patched in sequestering and transducing Hedgehog. Cell 87, 553-563.

Cheng, S., Maier, D., Hipfner, D.R., 2012. Drosophila G-protein-coupled receptor kinase 2 regulates cAMP-dependent Hedgehog signaling. Development 139, 85-94.

Cheng, S., Maier, D., Neubueser, D., Hipfner, D.R., 2010. Regulation of Smoothened by Drosophila G-protein-coupled receptor kinases. Developmental biology 337, 99-109.

Cheung, H.O., Zhang, X., Ribeiro, A., Mo, R., Makino, S., Puviindran, V., Law, K.K., Briscoe, J., Hui, C.C., 2009. The kinesin protein Kif7 is a critical regulator of Gli transcription factors in mammalian hedgehog signaling. Science signaling 2, ra29.

Claing, A., Laporte, S.A., Caron, M.G., Lefkowitz, R.J., 2002. Endocytosis of G protein-coupled receptors: roles of G protein-coupled receptor kinases and beta-arrestin proteins. Prog Neurobiol 66, 61-79.

Claret, S., Sanial, M., Plessis, A., 2007. Evidence for a novel feedback loop in the Hedgehog pathway involving Smoothened and Fused. Current biology : CB 17, 1326-1333.

Connolly, J.B., Roberts, I.J., Armstrong, J.D., Kaiser, K., Forte, M., Tully, T., O'Kane, C.J., 1996. Associative learning disrupted by impaired Gs signaling in Drosophila mushroom bodies. Science 274, 2104-2107.

Cooper, A.F., Yu, K.P., Brueckner, M., Brailey, L.L., Johnson, L., McGrath, J.M., Bale, A.E., 2005. Cardiac and CNS defects in a mouse with targeted disruption of suppressor of fused. Development 132, 4407-4417.

Corcoran, R.B., Scott, M.P., 2006. Oxysterols stimulate Sonic hedgehog signal transduction and proliferation of medulloblastoma cells. Proceedings of the National Academy of Sciences of the United States of America 103, 8408-8413.

Debburman, S.K., Kunapuli, P., Benovic, J.L., Hosey, M.M., 1995. Agonist-dependent phosphorylation of human muscarinic receptors in Spodoptera frugiperda insect cell membranes by G protein-coupled receptor kinases. Molecular pharmacology 47, 224-233.

DeCamp, D.L., Thompson, T.M., de Sauvage, F.J., Lerner, M.R., 2000. Smoothened activates Galphai-mediated signaling in frog melanophores. The Journal of biological chemistry 275, 26322-26327.

Denef, N., Neubuser, D., Perez, L., Cohen, S.M., 2000. Hedgehog induces opposite changes in turnover and subcellular localization of patched and smoothened. Cell 102, 521-531.

Dixon, R.A., Kobilka, B.K., Strader, D.J., Benovic, J.L., Dohlman, H.G., Frielle, T., Bolanowski, M.A., Bennett, C.D., Rands, E., Diehl, R.E., Mumford, R.A., Slater, E.E., Sigal, I.S., Caron, M.G., Lefkowitz, R.J., Strader, C.D., 1986. Cloning of the gene and cDNA for mammalian beta-adrenergic receptor and homology with rhodopsin. Nature 321, 75-79.

Dominguez, M., Brunner, M., Hafen, E., Basler, K., 1996. Sending and receiving the hedgehog signal: control by the Drosophila Gli protein Cubitus interruptus. Science 272, 1621-1625.

Dorn, K.V., Hughes, C.E., Rohatgi, R., 2012. A Smoothened-Evc2 complex transduces the Hedgehog signal at primary cilia. Developmental cell 23, 823-835.

Dwyer, J.R., Sever, N., Carlson, M., Nelson, S.F., Beachy, P.A., Parhami, F., 2007. Oxysterols are novel activators of the hedgehog signaling pathway in pluripotent mesenchymal cells. The Journal of biological chemistry 282, 8959-8968.

Echelard, Y., Epstein, D.J., St-Jacques, B., Shen, L., Mohler, J., McMahon, J.A., McMahon, A.P., 1993. Sonic hedgehog, a member of a family of putative signaling molecules, is implicated in the regulation of CNS polarity. Cell 75, 1417-1430.

Endoh-Yamagami, S., Evangelista, M., Wilson, D., Wen, X., Theunissen, J.W., Phamluong, K., Davis, M., Scales, S.J., Solloway, M.J., de Sauvage, F.J., Peterson, A.S., 2009. The mammalian Cos2 homolog Kif7 plays an essential role in modulating Hh signal transduction during development. Current biology : CB 19, 1320-1326.

Fan, J., Liu, Y., Jia, J., 2012. Hh-induced Smoothened conformational switch is mediated by differential phosphorylation at its C-terminal tail in a dose- and position-dependent manner. Developmental biology 366, 172-184.

Farzan, S.F., Ascano, M., Jr., Ogden, S.K., Sanial, M., Brigui, A., Plessis, A., Robbins, D.J., 2008. Costal2 functions as a kinesin-like protein in the hedgehog signal transduction pathway. Current biology : CB 18, 1215-1220.

Forbes, A.J., Nakano, Y., Taylor, A.M., Ingham, P.W., 1993. Genetic analysis of hedgehog signalling in the Drosophila embryo. Dev Suppl, 115-124.

Freedman, N.J., Kim, L.K., Murray, J.P., Exum, S.T., Brian, L., Wu, J.H., Peppel, K., 2002. Phosphorylation of the platelet-derived growth factor receptor-beta and epidermal growth factor receptor by G protein-coupled receptor kinase-2. Mechanisms for selectivity of desensitization. The Journal of biological chemistry 277, 48261-48269.

Fumoto, K., Hoogenraad, C.C., Kikuchi, A., 2006. GSK-3beta-regulated interaction of BICD with dynein is involved in microtubule anchorage at centrosome. The EMBO journal 25, 5670-5682.

Gainetdinov, R.R., Bohn, L.M., Walker, J.K., Laporte, S.A., Macrae, A.D., Caron, M.G., Lefkowitz, R.J., Premont, R.T., 1999. Muscarinic supersensitivity and impaired receptor desensitization in G protein-coupled receptor kinase 5-deficient mice. Neuron 24, 1029-1036.

Goetz, S.C., Anderson, K.V., 2010. The primary cilium: a signalling centre during vertebrate development. Nature reviews. Genetics 11, 331-344.

Gong, W.J., Golic, K.G., 2003. Ends-out, or replacement, gene targeting in Drosophila. Proceedings of the National Academy of Sciences of the United States of America 100, 2556-2561.

Grau, Y., Simpson, P., 1987. The segment polarity gene costal-2 in Drosophila. I. The organization of both primary and secondary embryonic fields may be affected. Developmental biology 122, 186-200.

Gurevich, E.V., Tesmer, J.J., Mushegian, A., Gurevich, V.V., 2012. G protein-coupled receptor kinases: more than just kinases and not only for GPCRs. Pharmacology & therapeutics 133, 40-69.

Hamm, H.E., 1998. The many faces of G protein signaling. The Journal of biological chemistry 273, 669-672.

Hammerschmidt, M., McMahon, A.P., 1998. The effect of pertussis toxin on zebrafish development: a possible role for inhibitory G-proteins in hedgehog signaling. Developmental biology 194, 166-171.

Hargrave, P.A., McDowell, J.H., Curtis, D.R., Wang, J.K., Juszczak, E., Fong, S.L., Rao, J.K., Argos, P., 1983. The structure of bovine rhodopsin. Biophysics of structure and mechanism 9, 235-244.

Heng, B.C., Aubel, D., Fussenegger, M., 2013. An overview of the diverse roles of G-protein coupled receptors (GPCRs) in the pathophysiology of various human diseases. Biotechnology advances 31, 1676-1694.

Ho, K.S., Suyama, K., Fish, M., Scott, M.P., 2005. Differential regulation of Hedgehog target gene transcription by Costal2 and Suppressor of Fused. Development 132, 1401-1412.

Hollinger, S., Hepler, J.R., 2002. Cellular regulation of RGS proteins: modulators and integrators of G protein signaling. Pharmacological reviews 54, 527-559.

Hooper, J.E., Scott, M.P., 1989. The Drosophila patched gene encodes a putative membrane protein required for segmental patterning. Cell 59, 751-765.

Hooper, J.E., Scott, M.P., 2005. Communicating with Hedgehogs. Nature reviews. Molecular cell biology 6, 306-317.

Huangfu, D., Liu, A., Rakeman, A.S., Murcia, N.S., Niswander, L., Anderson, K.V., 2003. Hedgehog signalling in the mouse requires intraflagellar transport proteins. Nature 426, 83-87.

Hui, C.C., Angers, S., 2011. Gli proteins in development and disease. Annual review of cell and developmental biology 27, 513-537.

Humke, E.W., Dorn, K.V., Milenkovic, L., Scott, M.P., Rohatgi, R., 2010. The output of Hedgehog signaling is controlled by the dynamic association between Suppressor of Fused and the Gli proteins. Genes & development 24, 670-682.

Infante, R.E., Abi-Mosleh, L., Radhakrishnan, A., Dale, J.D., Brown, M.S., Goldstein, J.L., 2008. Purified NPC1 protein. I. Binding of cholesterol and oxysterols to a 1278-amino acid membrane protein. The Journal of biological chemistry 283, 1052-1063.

Ingham, P.W., McMahon, A.P., 2001. Hedgehog signaling in animal development: paradigms and principles. Genes & development 15, 3059-3087.

Ingham, P.W., Nakano, Y., Seger, C., 2011. Mechanisms and functions of Hedgehog signalling across the metazoa. Nature reviews. Genetics 12, 393-406.

Ingham, P.W., Nystedt, S., Nakano, Y., Brown, W., Stark, D., van den Heuvel, M., Taylor, A.M., 2000. Patched represses the Hedgehog signalling pathway by promoting modification of the Smoothened protein. Current biology : CB 10, 1315-1318.

Jaber, M., Koch, W.J., Rockman, H., Smith, B., Bond, R.A., Sulik, K.K., Ross, J., Jr., Lefkowitz, R.J., Caron, M.G., Giros, B., 1996. Essential role of beta-adrenergic receptor kinase 1 in cardiac development and function. Proceedings of the National Academy of Sciences of the United States of America 93, 12974-12979.

Jia, H., Liu, Y., Xia, R., Tong, C., Yue, T., Jiang, J., Jia, J., 2010. Casein kinase 2 promotes Hedgehog signaling by regulating both smoothened and Cubitus interruptus. The Journal of biological chemistry 285, 37218-37226.

Jia, H., Liu, Y., Yan, W., Jia, J., 2009. PP4 and PP2A regulate Hedgehog signaling by controlling Smo and Ci phosphorylation. Development 136, 307-316.

Jia, J., Tong, C., Jiang, J., 2003. Smoothened transduces Hedgehog signal by physically interacting with Costal2/Fused complex through its C-terminal tail. Genes & development 17, 2709-2720.

Jia, J., Tong, C., Wang, B., Luo, L., Jiang, J., 2004. Hedgehog signalling activity of Smoothened requires phosphorylation by protein kinase A and casein kinase I. Nature 432, 1045-1050.

Jia, J., Zhang, L., Zhang, Q., Tong, C., Wang, B., Hou, F., Amanai, K., Jiang, J., 2005. Phosphorylation by double-time/CKIepsilon and CKIalpha targets cubitus interruptus for Slimb/beta-TRCP-mediated proteolytic processing. Developmental cell 9, 819-830.

Jiang, L.I., Collins, J., Davis, R., Lin, K.M., DeCamp, D., Roach, T., Hsueh, R., Rebres, R.A., Ross, E.M., Taussig, R., Fraser, I., Sternweis, P.C., 2007. Use of a cAMP BRET sensor to characterize a novel regulation of

cAMP by the sphingosine 1-phosphate/G13 pathway. The Journal of biological chemistry 282, 10576-10584.

Johnson, L.R., Scott, M.G., Pitcher, J.A., 2004. G protein-coupled receptor kinase 5 contains a DNA-binding nuclear localization sequence. Molecular and cellular biology 24, 10169-10179.

Kasai, K., Takahashi, M., Osumi, N., Sinnarajah, S., Takeo, T., Ikeda, H., Kehrl, J.H., Itoh, G., Arnheiter, H., 2004. The G12 family of heterotrimeric G proteins and Rho GTPase mediate Sonic hedgehog signalling. Genes to cells : devoted to molecular & cellular mechanisms 9, 49-58.

Kavelaars, A., Vroon, A., Raatgever, R.P., Fong, A.M., Premont, R.T., Patel, D.D., Lefkowitz, R.J., Heijnen, C.J., 2003. Increased acute inflammation, leukotriene B4-induced chemotaxis, and signaling in mice deficient for G protein-coupled receptor kinase 6. Journal of immunology 171, 6128-6134.

Kent, D., Bush, E.W., Hooper, J.E., 2006. Roadkill attenuates Hedgehog responses through degradation of Cubitus interruptus. Development 133, 2001-2010.

Khaliullina, H., Panakova, D., Eugster, C., Riedel, F., Carvalho, M., Eaton, S., 2009. Patched regulates Smoothened trafficking using lipoprotein-derived lipids. Development 136, 4111-4121.

Kim, J., Kato, M., Beachy, P.A., 2009. Gli2 trafficking links Hedgehog-dependent activation of Smoothened in the primary cilium to transcriptional activation in the nucleus. Proceedings of the National Academy of Sciences of the United States of America 106, 21666-21671.

Kinoshita, E., Kinoshita-Kikuta, E., Takiyama, K., Koike, T., 2006. Phosphate-binding tag, a new tool to visualize phosphorylated proteins. Molecular & cellular proteomics : MCP 5, 749-757.

Klein, R.S., Rubin, J.B., Gibson, H.D., DeHaan, E.N., Alvarez-Hernandez, X., Segal, R.A., Luster, A.D., 2001. SDF-1 alpha induces chemotaxis and enhances Sonic hedgehog-induced proliferation of cerebellar granule cells. Development 128, 1971-1981.

Kovacs, J.J., Whalen, E.J., Liu, R., Xiao, K., Kim, J., Chen, M., Wang, J., Chen, W., Lefkowitz, R.J., 2008. Beta-arrestin-mediated localization of smoothened to the primary cilium. Science 320, 1777-1781.

Kuhn, H., Dreyer, W.J., 1972. Light dependent phosphorylation of rhodopsin by ATP. FEBS letters 20, 1-6.

Kunapuli, P., Onorato, J.J., Hosey, M.M., Benovic, J.L., 1994. Expression, purification, and characterization of the G protein-coupled receptor kinase GRK5. The Journal of biological chemistry 269, 1099-1105.

Lam, C.W., Xie, J., To, K.F., Ng, H.K., Lee, K.C., Yuen, N.W., Lim, P.L., Chan, L.Y., Tong, S.F., McCormick, F., 1999. A frequent activated smoothened mutation in sporadic basal cell carcinomas. Oncogene 18, 833-836.

Lannutti, B.J., Schneider, L.E., 2001. Gprk2 controls cAMP levels in Drosophila development. Developmental biology 233, 174-185.

Lee, S.J., Xu, H., Montell, C., 2004. Rhodopsin kinase activity modulates the amplitude of the visual response in Drosophila. Proceedings of the National Academy of Sciences of the United States of America 101, 11874-11879.

Lefkowitz, R.J., Shenoy, S.K., 2005. Transduction of receptor signals by beta-arrestins. Science 308, 512-517.

Lelievre, V., Seksenyan, A., Nobuta, H., Yong, W.H., Chhith, S., Niewiadomski, P., Cohen, J.R., Dong, H., Flores, A., Liau, L.M., Kornblum, H.I., Scott, M.P., Waschek, J.A., 2008. Disruption of the PACAP gene promotes medulloblastoma in ptc1 mutant mice. Developmental biology 313, 359-370.

Li, S., Chen, Y., Shi, Q., Yue, T., Wang, B., Jiang, J., 2012. Hedgehog-regulated ubiquitination controls smoothened trafficking and cell surface expression in Drosophila. PLoS biology 10, e1001239.

Li, S., Ma, G., Wang, B., Jiang, J., 2014. Hedgehog induces formation of PKA-Smoothened complexes to promote Smoothened phosphorylation and pathway activation. Science signaling 7, ra62.

Liem, K.F., Jr., He, M., Ocbina, P.J., Anderson, K.V., 2009. Mouse Kif7/Costal2 is a cilia-associated protein that regulates Sonic hedgehog signaling. Proceedings of the National Academy of Sciences of the United States of America 106, 13377-13382.

Liggett, S.B., 2011. Phosphorylation barcoding as a mechanism of directing GPCR signaling. Science signaling 4, pe36.

Liu, R., Lu, P., Chu, J.W., Sharom, F.J., 2009. Characterization of fluorescent sterol binding to purified human NPC1. The Journal of biological chemistry 284, 1840-1852.

Logan, C.Y., Nusse, R., 2004. The Wnt signaling pathway in development and disease. Annual review of cell and developmental biology 20, 781-810.

Lorenz, W., Inglese, J., Palczewski, K., Onorato, J.J., Caron, M.G., Lefkowitz, R.J., 1991. The receptor kinase family: primary structure of rhodopsin kinase reveals similarities to the beta-adrenergic receptor kinase. Proceedings of the National Academy of Sciences of the United States of America 88, 8715-8719.

Low, W.C., Wang, C., Pan, Y., Huang, X.Y., Chen, J.K., Wang, B., 2008. The decoupling of Smoothened from Galphai proteins has little effect on Gli3 protein processing and Hedgehog-regulated chick neural tube patterning. Developmental biology 321, 188-196.

Lum, L., Yao, S., Mozer, B., Rovescalli, A., Von Kessler, D., Nirenberg, M., Beachy, P.A., 2003a. Identification of Hedgehog pathway components by RNAi in Drosophila cultured cells. Science 299, 2039-2045.

Lum, L., Zhang, C., Oh, S., Mann, R.K., von Kessler, D.P., Taipale, J., Weis-Garcia, F., Gong, R., Wang, B., Beachy, P.A., 2003b. Hedgehog signal transduction via Smoothened association with a cytoplasmic complex scaffolded by the atypical kinesin, Costal-2. Molecular cell 12, 1261-1274.

Luo, J., Busillo, J.M., Benovic, J.L., 2008. M3 muscarinic acetylcholine receptor-mediated signaling is regulated by distinct mechanisms. Molecular pharmacology 74, 338-347.

Maier, D., Cheng, S., Faubert, D., Hipfner, D.R., 2014. A broadly conserved g-protein-coupled receptor kinase phosphorylation mechanism controls Drosophila smoothened activity. PLoS genetics 10, e1004399.

Maier, D., Cheng, S., Hipfner, D.R., 2012. The complexities of G-protein-coupled receptor kinase function in Hedgehog signaling. Fly 6, 135-141.

Martin, V., Carrillo, G., Torroja, C., Guerrero, I., 2001. The sterol-sensing domain of Patched protein seems to control Smoothened activity through Patched vesicular trafficking. Current biology : CB 11, 601-607.

Martini, J.S., Raake, P., Vinge, L.E., DeGeorge, B.R., Jr., Chuprun, J.K., Harris, D.M., Gao, E., Eckhart, A.D., Pitcher, J.A., Koch, W.J., 2008. Uncovering G protein-coupled receptor kinase-5 as a histone deacetylase kinase in the nucleus of cardiomyocytes. Proceedings of the National Academy of Sciences of the United States of America 105, 12457-12462.

Mas, C., Ruiz i Altaba, A., 2010. Small molecule modulation of HH-GLI signaling: current leads, trials and tribulations. Biochemical pharmacology 80, 712-723.

Matkovich, S.J., Diwan, A., Klanke, J.L., Hammer, D.J., Marreez, Y., Odley, A.M., Brunskill, E.W., Koch, W.J., Schwartz, R.J., Dorn, G.W., 2nd, 2006. Cardiac-specific ablation of G-protein receptor kinase 2 redefines its roles in heart development and beta-adrenergic signaling. Circulation research 99, 996-1003.

McMahon, A.P., Ingham, P.W., Tabin, C.J., 2003. Developmental roles and clinical significance of hedgehog signaling. Current topics in developmental biology 53, 1-114.

Meloni, A.R., Fralish, G.B., Kelly, P., Salahpour, A., Chen, J.K., Wechsler-Reya, R.J., Lefkowitz, R.J., Caron, M.G., 2006. Smoothened signal transduction is promoted by G protein-coupled receptor kinase 2. Molecular and cellular biology 26, 7550-7560.

Methot, N., Basler, K., 2000. Suppressor of fused opposes hedgehog signal transduction by impeding nuclear accumulation of the activator form of Cubitus interruptus. Development 127, 4001-4010.

Milenkovic, L., Scott, M.P., Rohatgi, R., 2009. Lateral transport of Smoothened from the plasma membrane to the membrane of the cilium. The Journal of cell biology 187, 365-374.

Molnar, C., Holguin, H., Mayor, F., Jr., Ruiz-Gomez, A., de Celis, J.F., 2007. The G protein-coupled receptor regulatory kinase GPRK2 participates in Hedgehog signaling in Drosophila. Proceedings of the National Academy of Sciences of the United States of America 104, 7963-7968.

Molnar, C., Ruiz-Gomez, A., Martin, M., Rojo-Berciano, S., Mayor, F., de Celis, J.F., 2011. Role of the Drosophila non-visual ss-arrestin kurtz in hedgehog signalling. PLoS genetics 7, e1001335.

Moore, C.A., Milano, S.K., Benovic, J.L., 2007. Regulation of receptor trafficking by GRKs and arrestins. Annu Rev Physiol 69, 451-482.

Mukhopadhyay, S., Wen, X., Ratti, N., Loktev, A., Rangell, L., Scales, S.J., Jackson, P.K., 2013. The ciliary G-protein-coupled receptor Gpr161 negatively regulates the Sonic hedgehog pathway via cAMP signaling. Cell 152, 210-223.

Nachtergaele, S., Mydock, L.K., Krishnan, K., Rammohan, J., Schlesinger, P.H., Covey, D.F., Rohatgi, R., 2012. Oxysterols are allosteric activators of the oncoprotein Smoothened. Nature chemical biology 8, 211-220.

Nakano, Y., Guerrero, I., Hidalgo, A., Taylor, A., Whittle, J.R., Ingham, P.W., 1989. A protein with several possible membrane-spanning domains encoded by the Drosophila segment polarity gene patched. Nature 341, 508-513.

Nakano, Y., Nystedt, S., Shivdasani, A.A., Strutt, H., Thomas, C., Ingham, P.W., 2004. Functional domains and sub-cellular distribution of the Hedgehog transducing protein Smoothened in Drosophila. Mechanisms of development 121, 507-518.

Neilson, K.A., Ali, N.A., Muralidharan, S., Mirzaei, M., Mariani, M., Assadourian, G., Lee, A., van Sluyter, S.C., Haynes, P.A., 2011. Less label, more free: approaches in label-free quantitative mass spectrometry. Proteomics 11, 535-553.

Neves, S.R., Ram, P.T., Iyengar, R., 2002. G protein pathways. Science 296, 1636-1639.

Nicot, A., Lelievre, V., Tam, J., Waschek, J.A., DiCicco-Bloom, E., 2002. Pituitary adenylate cyclase-activating polypeptide and sonic hedgehog interact to control cerebellar granule precursor cell proliferation. The Journal of neuroscience : the official journal of the Society for Neuroscience 22, 9244-9254.

Nobles, K.N., Xiao, K., Ahn, S., Shukla, A.K., Lam, C.M., Rajagopal, S., Strachan, R.T., Huang, T.Y., Bressler, E.A., Hara, M.R., Shenoy, S.K., Gygi, S.P., Lefkowitz, R.J., 2011. Distinct phosphorylation sites on the beta(2)-adrenergic receptor establish a barcode that encodes differential functions of beta-arrestin. Science signaling 4, ra51.

Nusslein-Volhard, C., Wieschaus, E., 1980. Mutations affecting segment number and polarity in Drosophila. Nature 287, 795-801.

Ogden, S.K., Fei, D.L., Schilling, N.S., Ahmed, Y.F., Hwa, J., Robbins, D.J., 2008. G protein Galphai functions immediately downstream of Smoothened in Hedgehog signalling. Nature 456, 967-970.

Ohlmeyer, J.T., Kalderon, D., 1997. Dual pathways for induction of wingless expression by protein kinase A and Hedgehog in Drosophila embryos. Genes & development 11, 2250-2258.

Ohlmeyer, J.T., Kalderon, D., 1998. Hedgehog stimulates maturation of Cubitus interruptus into a labile transcriptional activator. Nature 396, 749-753.

Parameswaran, N., Pao, C.S., Leonhard, K.S., Kang, D.S., Kratz, M., Ley, S.C., Benovic, J.L., 2006. Arrestin-2 and G protein-coupled receptor kinase 5 interact with NFkappaB1 p105 and negatively regulate lipopolysaccharide-stimulated ERK1/2 activation in macrophages. The Journal of biological chemistry 281, 34159-34170.

Parks, A.L., Cook, K.R., Belvin, M., Dompe, N.A., Fawcett, R., Huppert, K., Tan, L.R., Winter, C.G., Bogart, K.P., Deal, J.E., Deal-Herr, M.E., Grant, D., Marcinko, M., Miyazaki, W.Y., Robertson, S., Shaw, K.J., Tabios, M., Vysotskaia, V., Zhao, L., Andrade, R.S., Edgar, K.A., Howie, E., Killpack, K., Milash, B., Norton, A., Thao, D., Whittaker, K., Winner, M.A., Friedman, L., Margolis, J., Singer, M.A., Kopczynski, C., Curtis, D., Kaufman, T.C., Plowman, G.D., Duyk, G., Francis-Lang, H.L., 2004. Systematic generation of high-resolution deletion coverage of the Drosophila melanogaster genome. Nat Genet 36, 288-292.

Peake, K.B., Vance, J.E., 2010. Defective cholesterol trafficking in Niemann-Pick C-deficient cells. FEBS letters 584, 2731-2739.

Pearce, L.R., Komander, D., Alessi, D.R., 2010. The nuts and bolts of AGC protein kinases. Nature reviews. Molecular cell biology 11, 9-22.

Pearlman, S.M., Serber, Z., Ferrell, J.E., Jr., 2011. A mechanism for the evolution of phosphorylation sites. Cell 147, 934-946.

Peppel, K., Boekhoff, I., McDonald, P., Breer, H., Caron, M.G., Lefkowitz, R.J., 1997. G protein-coupled receptor kinase 3 (GRK3) gene disruption leads to loss of odorant receptor desensitization. The Journal of biological chemistry 272, 25425-25428.

Philipp, M., Fralish, G.B., Meloni, A.R., Chen, W., MacInnes, A.W., Barak, L.S., Caron, M.G., 2008. Smoothened signaling in vertebrates is facilitated by a G protein-coupled receptor kinase. Molecular biology of the cell 19, 5478-5489.

Phillips, R.G., Roberts, I.J., Ingham, P.W., Whittle, J.R., 1990. The Drosophila segment polarity gene patched is involved in a position-signalling mechanism in imaginal discs. Development 110, 105-114.

Pitcher, J.A., Freedman, N.J., Lefkowitz, R.J., 1998a. G protein-coupled receptor kinases. Annual review of biochemistry 67, 653-692.

Pitcher, J.A., Hall, R.A., Daaka, Y., Zhang, J., Ferguson, S.S., Hester, S., Miller, S., Caron, M.G., Lefkowitz, R.J., Barak, L.S., 1998b. The G protein-coupled receptor kinase 2 is a microtubule-associated protein kinase that phosphorylates tubulin. The Journal of biological chemistry 273, 12316-12324.

Polizio, A.H., Chinchilla, P., Chen, X., Kim, S., Manning, D.R., Riobo, N.A., 2011. Heterotrimeric Gi proteins link Hedgehog signaling to activation of Rho small GTPases to promote fibroblast migration. The Journal of biological chemistry 286, 19589-19596.

Ponsioen, B., Zhao, J., Riedl, J., Zwartkruis, F., van der Krogt, G., Zaccolo, M., Moolenaar, W.H., Bos, J.L., Jalink, K., 2004. Detecting cAMP-induced Epac activation by fluorescence resonance energy transfer: Epac as a novel cAMP indicator. EMBO reports 5, 1176-1180.

Preat, T., 1992. Characterization of Suppressor of fused, a complete suppressor of the fused segment polarity gene of Drosophila melanogaster. Genetics 132, 725-736.

Premont, R.T., Claing, A., Vitale, N., Freeman, J.L., Pitcher, J.A., Patton, W.A., Moss, J., Vaughan, M., Lefkowitz, R.J., 1998. beta2-Adrenergic receptor regulation by GIT1, a G protein-coupled receptor kinase-associated ADP ribosylation factor GTPase-activating protein. Proceedings of the National Academy of Sciences of the United States of America 95, 14082-14087.

Premont, R.T., Gainetdinov, R.R., 2007. Physiological roles of G protein-coupled receptor kinases and arrestins. Annu Rev Physiol 69, 511-534.

Price, M.A., Kalderon, D., 2002. Proteolysis of the Hedgehog signaling effector Cubitus interruptus requires phosphorylation by Glycogen Synthase Kinase 3 and Casein Kinase 1. Cell 108, 823-835.

Rahnama, F., Toftgard, R., Zaphiropoulos, P.G., 2004. Distinct roles of PTCH2 splice variants in Hedgehog signalling. The Biochemical journal 378, 325-334.

Raju, T.N., 2000. The Nobel chronicles. 1995: Edward B Lewis (b 1918), Christiane Nusslein-Volhard (b 1942), and Eric Francis Wieschaus (b 1947). Lancet 356, 81.

Ranieri, N., Ruel, L., Gallet, A., Raisin, S., Therond, P.P., 2012. Distinct phosphorylations on kinesin costal-2 mediate differential hedgehog signaling strength. Developmental cell 22, 279-294.

Reifenberger, J., Wolter, M., Weber, R.G., Megahed, M., Ruzicka, T., Lichter, P., Reifenberger, G., 1998. Missense mutations in SMOH in sporadic basal cell carcinomas of the skin and primitive neuroectodermal tumors of the central nervous system. Cancer research 58, 1798-1803.

Ren, X.R., Reiter, E., Ahn, S., Kim, J., Chen, W., Lefkowitz, R.J., 2005. Different G protein-coupled receptor kinases govern G protein and beta-arrestin-mediated signaling of V2 vasopressin receptor. Proceedings of the National Academy of Sciences of the United States of America 102, 1448-1453.

Riobo, N.A., Saucy, B., Dilizio, C., Manning, D.R., 2006. Activation of heterotrimeric G proteins by Smoothened. Proceedings of the National Academy of Sciences of the United States of America 103, 12607-12612.

Robbins, D.J., Nybakken, K.E., Kobayashi, R., Sisson, J.C., Bishop, J.M., Therond, P.P., 1997. Hedgehog elicits signal transduction by means of a large complex containing the kinesin-related protein costal2. Cell 90, 225-234.

Rohatgi, R., Milenkovic, L., Scott, M.P., 2007. Patched1 regulates hedgehog signaling at the primary cilium. Science 317, 372-376.

Rosenbaum, D.M., Rasmussen, S.G., Kobilka, B.K., 2009. The structure and function of G-protein-coupled receptors. Nature 459, 356-363.

Ruel, L., Rodriguez, R., Gallet, A., Lavenant-Staccini, L., Therond, P.P., 2003. Stability and association of Smoothened, Costal2 and Fused with Cubitus interruptus are regulated by Hedgehog. Nat Cell Biol 5, 907-913.

Schaefer, M., Petronczki, M., Dorner, D., Forte, M., Knoblich, J.A., 2001. Heterotrimeric G proteins direct two modes of asymmetric cell division in the Drosophila nervous system. Cell 107, 183-194.

Schioth, H.B., Fredriksson, R., 2005. The GRAFS classification system of G-protein coupled receptors in comparative perspective. General and comparative endocrinology 142, 94-101.

Schneider, L.E., Spradling, A.C., 1997. The Drosophila G-protein-coupled receptor kinase homologue Gprk2 is required for egg morphogenesis. Development 124, 2591-2602.

Shen, F., Cheng, L., Douglas, A.E., Riobo, N.A., Manning, D.R., 2013. Smoothened is a fully competent activator of the heterotrimeric G protein G(i). Molecular pharmacology 83, 691-697.

Shi, Q., Li, S., Jia, J., Jiang, J., 2011. The Hedgehog-induced Smoothened conformational switch assembles a signaling complex that activates Fused by promoting its dimerization and phosphorylation. Development 138, 4219-4231.

Sillibourne, J.E., Milne, D.M., Takahashi, M., Ono, Y., Meek, D.W., 2002. Centrosomal anchoring of the protein kinase CK1delta mediated by attachment to the large, coiled-coil scaffolding protein CG-NAP/AKAP450. Journal of molecular biology 322, 785-797.

Slusarski, D.C., Motzny, C.K., Holmgren, R., 1995. Mutations that alter the timing and pattern of cubitus interruptus gene expression in Drosophila melanogaster. Genetics 139, 229-240.

Smelkinson, M.G., Zhou, Q., Kalderon, D., 2007. Regulation of Ci-SCFSlimb binding, Ci proteolysis, and hedgehog pathway activity by Ci phosphorylation. Dev Cell 13, 481-495.

Strigini, M., Cohen, S.M., 1997. A Hedgehog activity gradient contributes to AP axial patterning of the Drosophila wing. Development 124, 4697-4705.

Strutt, H., Thomas, C., Nakano, Y., Stark, D., Neave, B., Taylor, A.M., Ingham, P.W., 2001. Mutations in the sterol-sensing domain of Patched suggest a role for vesicular trafficking in Smoothened regulation. Current biology : CB 11, 608-613.

Su, Y., Ospina, J.K., Zhang, J., Michelson, A.P., Schoen, A.M., Zhu, A.J., 2011. Sequential phosphorylation of smoothened transduces graded hedgehog signaling. Science signaling 4, ra43.

Svard, J., Heby-Henricson, K., Persson-Lek, M., Rozell, B., Lauth, M., Bergstrom, A., Ericson, J., Toftgard, R., Teglund, S., 2006. Genetic elimination of Suppressor of fused reveals an essential repressor function in the mammalian Hedgehog signaling pathway. Developmental cell 10, 187-197.

Tabata, T., Kornberg, T.B., 1994. Hedgehog is a signaling protein with a key role in patterning Drosophila imaginal discs. Cell 76, 89-102.

Taipale, J., Cooper, M.K., Maiti, T., Beachy, P.A., 2002. Patched acts catalytically to suppress the activity of Smoothened. Nature 418, 892-897.

Tanoue, S., Krishnan, P., Chatterjee, A., Hardin, P.E., 2008. G protein-coupled receptor kinase 2 is required for rhythmic olfactory responses in Drosophila. Current biology : CB 18, 787-794.

Taylor, S.S., Buechler, J.A., Yonemoto, W., 1990. cAMP-dependent protein kinase: framework for a diverse family of regulatory enzymes. Annual review of biochemistry 59, 971-1005.

Thibault, S.T., Singer, M.A., Miyazaki, W.Y., Milash, B., Dompe, N.A., Singh, C.M., Buchholz, R., Demsky, M., Fawcett, R., Francis-Lang, H.L., Ryner, L., Cheung, L.M., Chong, A., Erickson, C., Fisher, W.W., Greer, K., Hartouni, S.R., Howie, E., Jakkula, L., Joo, D., Killpack, K., Laufer, A., Mazzotta, J., Smith, R.D., Stevens, L.M., Stuber, C., Tan, L.R., Ventura, R., Woo, A., Zakrajsek, I., Zhao, L., Chen, F., Swimmer, C., Kopczynski, C., Duyk, G., Winberg, M.L., Margolis, J., 2004. A complementary transposon tool kit for Drosophila melanogaster using P and piggyBac. Nat Genet 36, 283-287.

Tiecke, E., Turner, R., Sanz-Ezquerro, J.J., Warner, A., Tickle, C., 2007. Manipulations of PKA in chick limb development reveal roles in digit patterning including a positive role in Sonic Hedgehog signaling. Developmental biology 305, 312-324.

Tseng, T.T., Gratwick, K.S., Kollman, J., Park, D., Nies, D.H., Goffeau, A., Saier, M.H., Jr., 1999. The RND permease superfamily: an ancient, ubiquitous and diverse family that includes human disease and development proteins. Journal of molecular microbiology and biotechnology 1, 107-125.

Tukachinsky, H., Lopez, L.V., Salic, A., 2010. A mechanism for vertebrate Hedgehog signaling: recruitment to cilia and dissociation of SuFu-Gli protein complexes. The Journal of cell biology 191, 415-428.

van den Heuvel, M., Ingham, P.W., 1996. smoothened encodes a receptor-like serpentine protein required for hedgehog signalling. Nature 382, 547-551.

Violin, J.D., Dewire, S.M., Barnes, W.G., Lefkowitz, R.J., 2006. G protein-coupled receptor kinase and beta-arrestin-mediated desensitization of the angiotensin II type 1A receptor elucidated by diacylglycerol dynamics. The Journal of biological chemistry 281, 36411-36419.

Violin, J.D., DiPilato, L.M., Yildirim, N., Elston, T.C., Zhang, J., Lefkowitz, R.J., 2008. beta2-adrenergic receptor signaling and desensitization elucidated by quantitative modeling of real time cAMP dynamics. The Journal of biological chemistry 283, 2949-2961.

Vroon, A., Heijnen, C.J., Raatgever, R., Touw, I.P., Ploemacher, R.E., Premont, R.T., Kavelaars, A., 2004. GRK6 deficiency is associated with enhanced CXCR4-mediated neutrophil chemotaxis in vitro and impaired responsiveness to G-CSF in vivo. Journal of leukocyte biology 75, 698-704.

Wang, B., Fallon, J.F., Beachy, P.A., 2000. Hedgehog-regulated processing of Gli3 produces an anterior/posterior repressor gradient in the developing vertebrate limb. Cell 100, 423-434.

Weiss, E.R., Ducceschi, M.H., Horner, T.J., Li, A., Craft, C.M., Osawa, S., 2001. Species-specific differences in expression of G-protein-coupled receptor kinase (GRK) 7 and GRK1 in mammalian cone photoreceptor cells: implications for cone cell phototransduction. The Journal of neuroscience : the official journal of the Society for Neuroscience 21, 9175-9184.

Weller, M., Virmaux, N., Mandel, P., 1975. Light-stimulated phosphorylation of rhodopsin in the retina: the presence of a protein kinase that is specific for photobleached rhodopsin. Proceedings of the National Academy of Sciences of the United States of America 72, 381-385.

Wilbanks, A.M., Fralish, G.B., Kirby, M.L., Barak, L.S., Li, Y.X., Caron, M.G., 2004. Beta-arrestin 2 regulates zebrafish development through the hedgehog signaling pathway. Science 306, 2264-2267.

Xia, R., Jia, H., Fan, J., Liu, Y., Jia, J., 2012. USP8 promotes smoothened signaling by preventing its ubiquitination and changing its subcellular localization. PLoS biology 10, e1001238.

Xie, J., Murone, M., Luoh, S.M., Ryan, A., Gu, Q., Zhang, C., Bonifas, J.M., Lam, C.W., Hynes, M., Goddard, A., Rosenthal, A., Epstein, E.H., Jr., de Sauvage, F.J., 1998. Activating Smoothened mutations in sporadic basal-cell carcinoma. Nature 391, 90-92.

Yam, P.T., Langlois, S.D., Morin, S., Charron, F., 2009. Sonic hedgehog guides axons through a noncanonical, Src-family-kinase-dependent signaling pathway. Neuron 62, 349-362.

Yang, C., Chen, W., Chen, Y., Jiang, J., 2012. Smoothened transduces Hedgehog signal by forming a complex with Evc/Evc2. Cell research 22, 1593-1604.

Zhang, C., Williams, E.H., Guo, Y., Lum, L., Beachy, P.A., 2004. Extensive phosphorylation of Smoothened in Hedgehog pathway activation. Proceedings of the National Academy of Sciences of the United States of America 101, 17900-17907.

Zhang, W., Zhao, Y., Tong, C., Wang, G., Wang, B., Jia, J., Jiang, J., 2005. Hedgehog-regulated Costal2-kinase complexes control phosphorylation and proteolytic processing of Cubitus interruptus. Developmental cell 8, 267-278.

Zhang, Y., Mao, F., Lu, Y., Wu, W., Zhang, L., Zhao, Y., 2011. Transduction of the Hedgehog signal through the dimerization of Fused and the nuclear translocation of Cubitus interruptus. Cell research 21, 1436-1451.

Zhao, Y., Tong, C., Jiang, J., 2007. Hedgehog regulates smoothened activity by inducing a conformational switch. Nature 450, 252-258.

Zhou, Q., Apionishev, S., Kalderon, D., 2006. The contributions of protein kinase A and smoothened phosphorylation to hedgehog signal transduction in Drosophila melanogaster. Genetics 173, 2049-2062.

Zhou, Q., Kalderon, D., 2011. Hedgehog activates fused through phosphorylation to elicit a full spectrum of pathway responses. Developmental cell 20, 802-814.

Supplemental Material

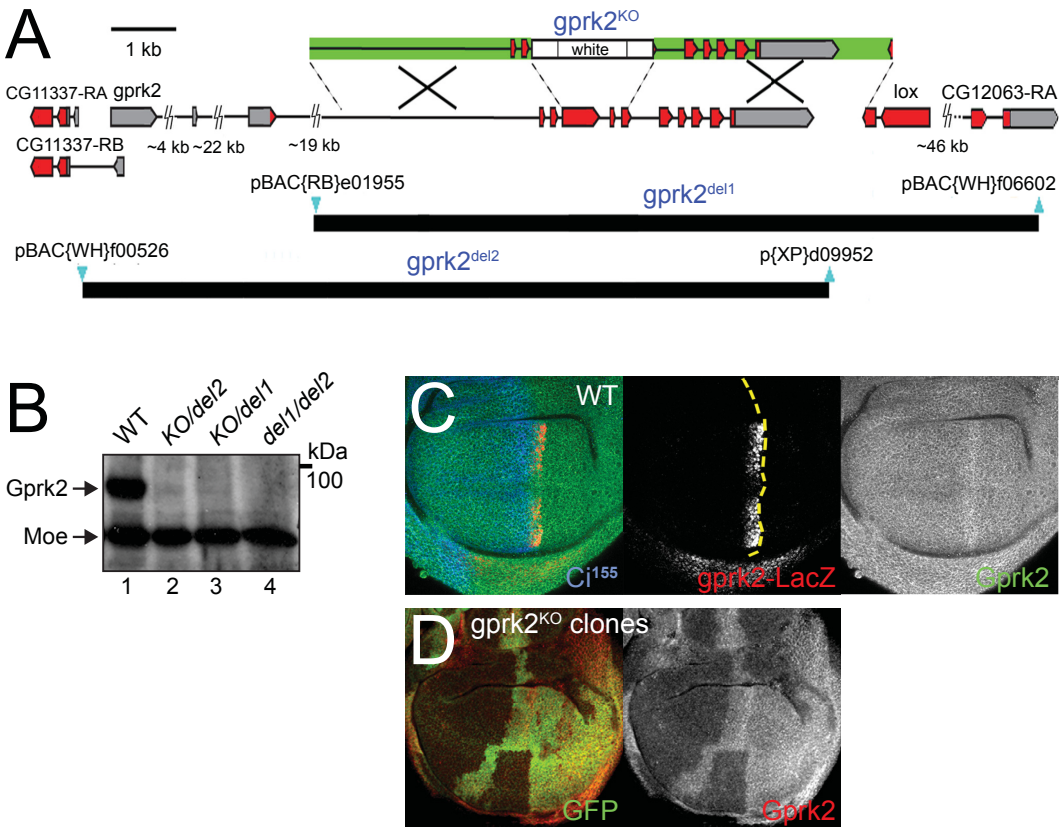

Supplemental Figure 1. Generation and characterization of *gprk2* null alleles.

(A) Map of the *gprk2* locus and defined deletions. The relative positions of non-coding (grey) and coding (red) exons of *gprk2*, the upstream neighbouring gene *CG11337,* and two downstream genes (*lox* and *CG12063*) are indicated. Two additional genes (*CG11333* and *CG11334*) situated between *lox* and *CG12063* are not shown. A schematic of the targeting construct used to generate the $gprk2^{KO}$ allele is shown above the map (arms of homology in green). The positions of the *piggyBac* insertions (blue) used to make the $gprk2^{del1}$ and $gprk2^{del2}$ alleles and extents of the resulting deletions (black) are shown below. **(B)** Western blot analysis of wing disc lysates prepared from wild-type, $gprk2^{KO}/gprk2^{del2}$, $gprk2^{KO}/gprk2^{del1}$, and $gprk2^{del1}/gprk2^{del2}$ third-instar larvae. Gprk2 protein is absent from the mutants. The blot was also probed with an anti-Moesin antibody as a loading control. **(C)** Immunofluorescence staining of a wild-type wing disc to detect Gprk2 (green), nuclear β-galactosidase expressed from a *gprk2-LacZ* enhancer trap (red), and Ci^{155} (blue). In this and all subsequent figures, discs are oriented with dorsal up and posterior to the right. Gprk2 protein is detected throughout the disc. The levels of both *gprk2* enhancer trap activity and Gprk2 protein are upregulated in A cells abutting the A/P compartment boundary (yellow dotted line, as determined by the boundary of Ci immunostaining). **(D)** Immunofluorescence staining of a wing disc with homozygous $gprk2^{KO}$ clones, marked by the absence of GFP (green). Gprk2 staining (red) is strongly reduced in the clones.

Supplemental Table 1. Quantification of Smo^{SD} unmodified and phosphopeptides by LC-MS/MS.

	Phosphosite	CONTROL dsRNA		Gprk2 dsRNA		RATIO CON:Gprk2
		Peptide quantity	phos/un-mod peptide	Peptide quantity	phos/un-mod peptide	
CHYMOTRYPSIN						
cluster 1	none	5.96E+05		3.07E+06		
	pS604	1.70E+06	2.852	8.76E+05	0.285	**10.0**
	pS604, **p**T606	2.31E+05	0.388	1.99E+05	0.065	**6.0**
cluster 1	none	7.91E+07		1.09E+08		
	pT610	3.52E+06	0.045	5.50E+04	0.001	**88.2**
	pT612	8.54E+06	0.108	4.92E+05	0.005	**23.9**
	pT610, **p**T612	1.89E+07	0.239	5.02E+05	0.005	**51.9**
GPS1	none	1.62E+07		1.99E+07		
	pS740 **p**T741	7.96E+06	0.492	4.92E+06	0.248	**2.0**
	pS740, **p**T741	3.46E+06	0.214	8.98E+05	0.045	**4.7**
TRYPSIN						
cluster 3	none	1.14E+09		1.32E+09		
	pS658 **p**S659 **p**S660	1.36E+08	0.120	1.35E+07	0.010	**11.7**
	pS658, **p**S659 **p**S658, **p**S660 **p**S659, **p**S660	1.13E+06	0.001	1.01E+05	0.000	**13.0**
cluster 4	none	7.31E+08		8.25E+08		
	pS675	1.73E+08	0.236	4.14E+07	0.050	**4.7**
	pS675, **p**S680	6.08E+07	0.083	2.55E+06	0.003	**26.9**
	pS675, **p**S680, **p**S683	3.31E+07	0.045	1.33E+06	0.002	**28.0**
cluster 4	none	1.87E+08		2.36E+08		
	pS680	7.07E+06	0.038	7.61E+05	0.003	**11.7**
	pS680, **p**S683	2.07E+08	1.107	2.13E+07	0.090	**12.2**
GPS1	none	2.53E+08		2.52E+08		
	pS740	1.86E+07	0.074	9.80E+06	0.039	**1.9**
	pT741	1.40E+08	0.555	1.11E+08	0.441	**1.3**
	pS740, **p**T741	6.72E+07	0.266	2.06E+07	0.082	**3.2**

[*continued on next page*]

Supplemental Table 1. Quantification of Smo^{SD} unmodified and phospho-peptides by LC-MS/MS [*continued*]

	Phosphosite	CONTROL dsRNA		Gprk2 dsRNA		RATIO CON:Gprk2
		Peptide quantity	phos/un-mod peptide	Peptide quantity	phos/un-mod peptide	
TRYPSIN + ASPN A						
cluster 3	none	2.28E+06		1.39E+06		
	pS658 **p**S659 **p**S660	3.03E+05	0.133	2.70E+04	0.019	**6.8**
	pS658, **p**S659 **p**S658, **p**S660 **p**S659, **p**S660	1.81E+05	0.079	1.00E+04	0.007	**11.0**
	pS658, **p**S659, **p**S660	2.00E+05	0.088	1.00E+04	0.007	**12.2**
cluster 4	**p**S675, **p**S680	1.74E+06		ND		*
cluster 4	none	1.50E+08		7.35E+07		
	pS680	2.28E+07	0.152	1.50E+06	0.020	**7.4**
	pS680, **p**S683	5.30E+06	0.035	7.60E+04	0.001	**34.2**
GPS1	none	4.61E+06		1.26E+06		
	pS740	8.71E+06	0.189	2.59E+05	0.206	**0.9**
	pT741	1.27E+06	0.275	1.47E+05	0.117	**2.4**
	pS740, **p**T741	2.67E+06	0.579	1.47E+05	0.117	**5.0**
TRYPSIN + ASPN B						
cluster 3	none	1.09E+06		2.10E+06		
	pS658 **p**S659 **p**S660	2.41E+05	0.221	5.20E+04	0.025	**8.9**
	pS658, **p**S659 **p**S658, **p**S660 **p**S659, **p**S660	8.51E+04	0.078	1.00E+04	0.005	**16.4**
	pS658, **p**S659, **p**S660	4.58E+04	0.042	1.00E+04	0.005	**8.8**
cluster 4	**p**S675, **p**S680	4.46E+05		ND		*
cluster 4	none	8.23E+07		1.10E+08		
	pS680	3.58E+06	0.043	1.51E+06	0.014	**3.2**
	pS680, **p**S683	4.10E+06	0.050	7.77E+05	0.007	**7.1**
GPS1	none	1.45E+06		4.74E+05		
	pS740	2.33E+05	0.161	3.64E+05	0.131	**1.2**
	pT741	2.65E+06	1.828	3.24E+06	1.165	**1.6**
	pS740, **p**T741	1.50E+06	1.034	1.99E+05	0.420	**2.4**